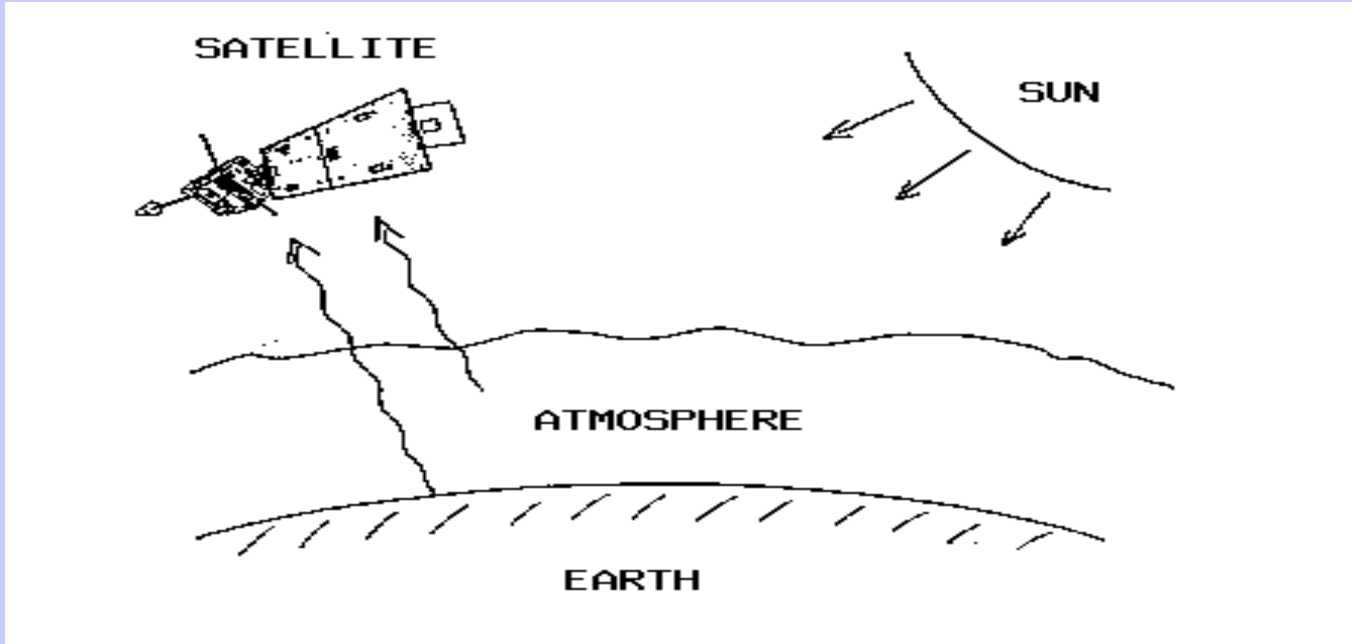


Summary of Satellite Remote Sensing Concepts

Lectures in Monteponi
September 2008

Paul Menzel
UW/CIMSS/AOS

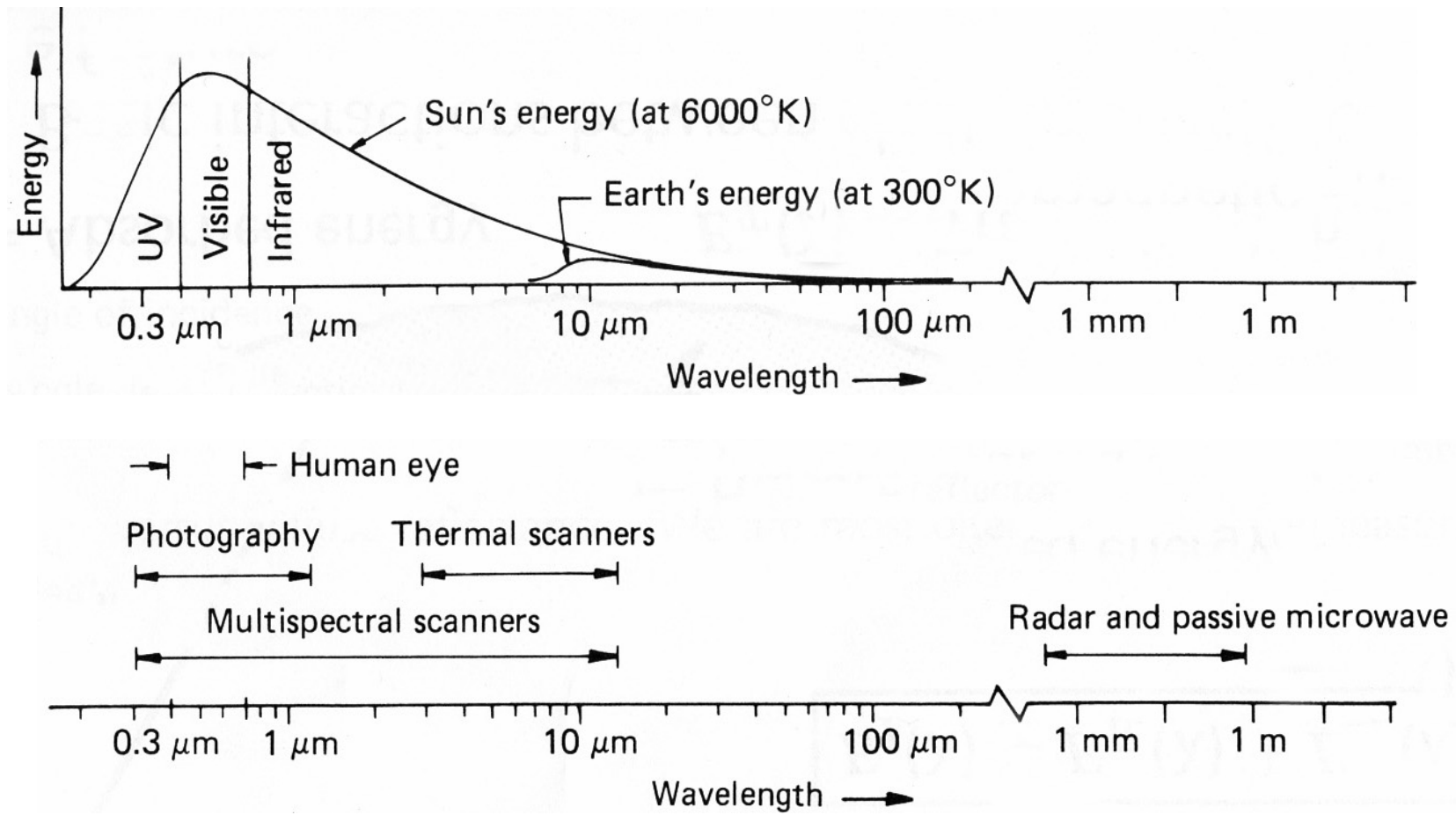
Satellite remote sensing of the Earth-atmosphere



Observations depend on

- telescope characteristics (resolving power, diffraction)
- detector characteristics (signal to noise)
- communications bandwidth (bit depth)
- spectral intervals (window, absorption band)
- time of day (daylight visible)
- atmospheric state (T, Q, clouds)
- earth surface (Ts, vegetation cover)

Spectral Characteristics of Energy Sources and Sensing Systems



Terminology of radiant energy

Energy from
the Earth Atmosphere

over time is

Flux

which strikes the detector area

Irradiance

at a given wavelength interval

**Monochromatic
Irradiance**

over a solid angle on the Earth

**Radiance observed by
satellite radiometer**

is described by

The Planck function

can be inverted to

Brightness temperature

Definitions of Radiation

| QUANTITY | SYMBOL | UNITS |
|-----------------------------|--|---|
| Energy | dQ | Joules |
| Flux | dQ/dt | Joules/sec = Watts |
| Irradiance | $dQ/dt/dA$ | Watts/meter ² |
| Monochromatic Irradiance | $dQ/dt/dA/d\lambda$ or $dQ/dt/dA/d\nu$ | W/m ² /micron W/m ² /cm ⁻¹ |
| Radiance | $dQ/dt/dA/d\lambda/d\Omega$ or $dQ/dt/dA/d\nu/d\Omega$ | W/m ² /micron/ster W/m ² /cm ⁻¹ /ster |

Using wavenumbers

$$c_2 v/T$$

$$B(v, T) = c_1 v^3 / [e^{-v/T} - 1]$$

(mW/m²/ster/cm⁻¹)

$$v(\text{max in cm}^{-1}) = 1.95T$$

$$B(v_{\text{max}}, T) \sim T^{**3}.$$

$$E = \pi \int_0^{\infty} B(v, T) dv = \sigma T^4,$$

$$T = c_2 v / [\ln(\frac{c_1 v^3}{B_v} + 1)]$$

Using wavelengths

$$c_2 / \lambda T$$

$$B(\lambda, T) = c_1 / \{ \lambda^5 [e^{-\lambda/T} - 1] \}$$

(mW/m²/ster/μm)

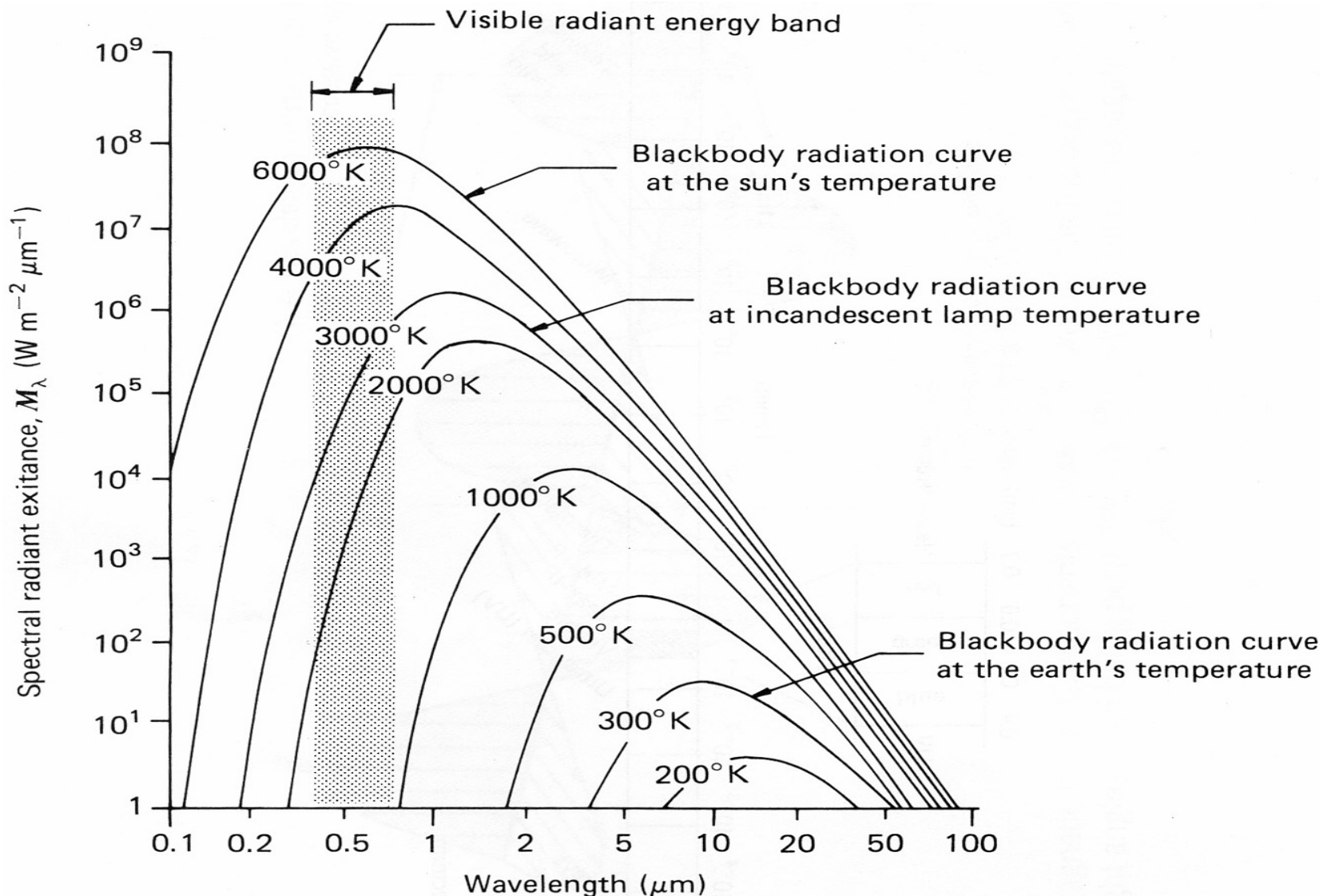
$$\lambda(\text{max in cm})T = 0.2897$$

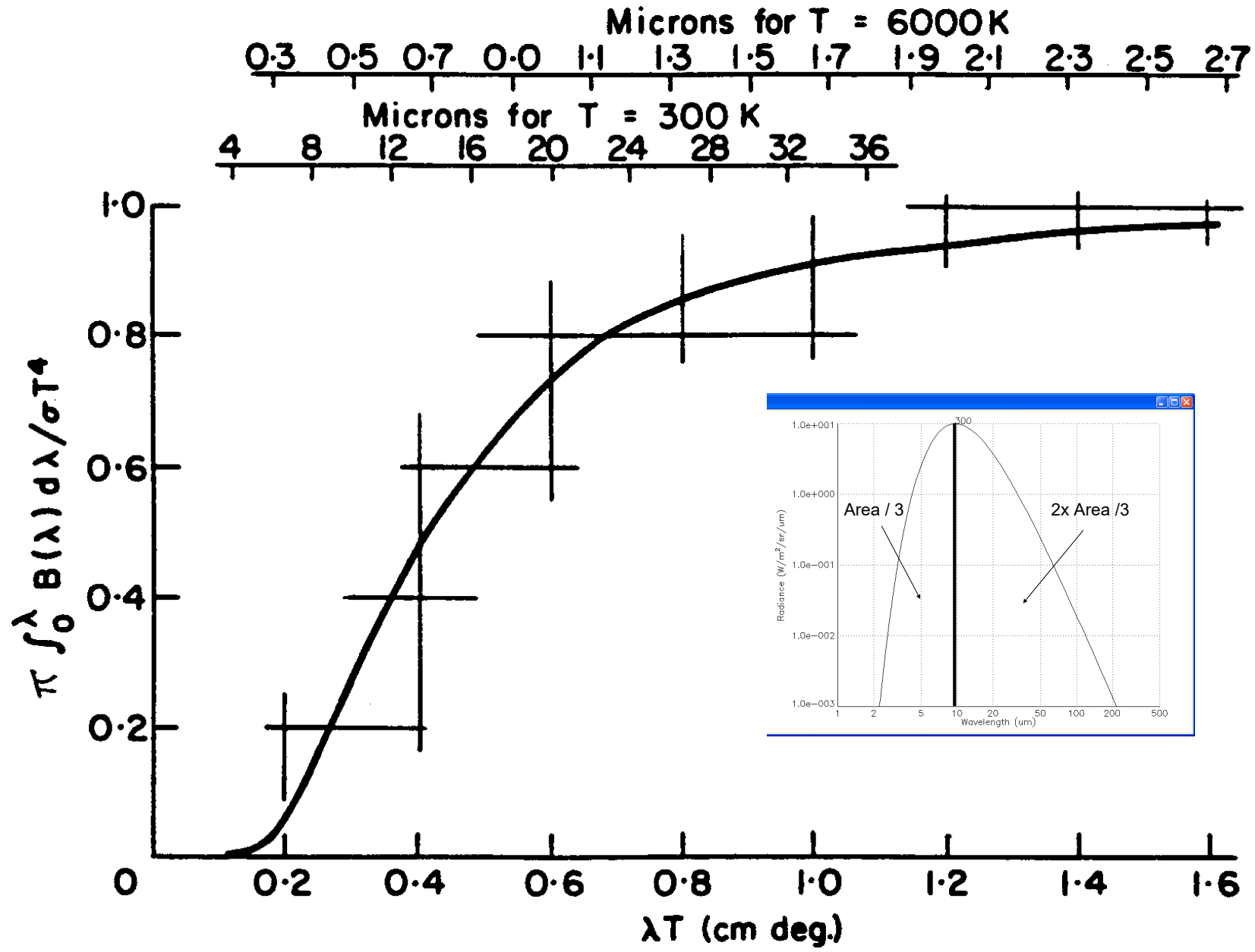
$$B(\lambda_{\text{max}}, T) \sim T^{**5}.$$

$$E = \pi \int_0^{\infty} B(\lambda, T) d\lambda = \sigma T^4,$$

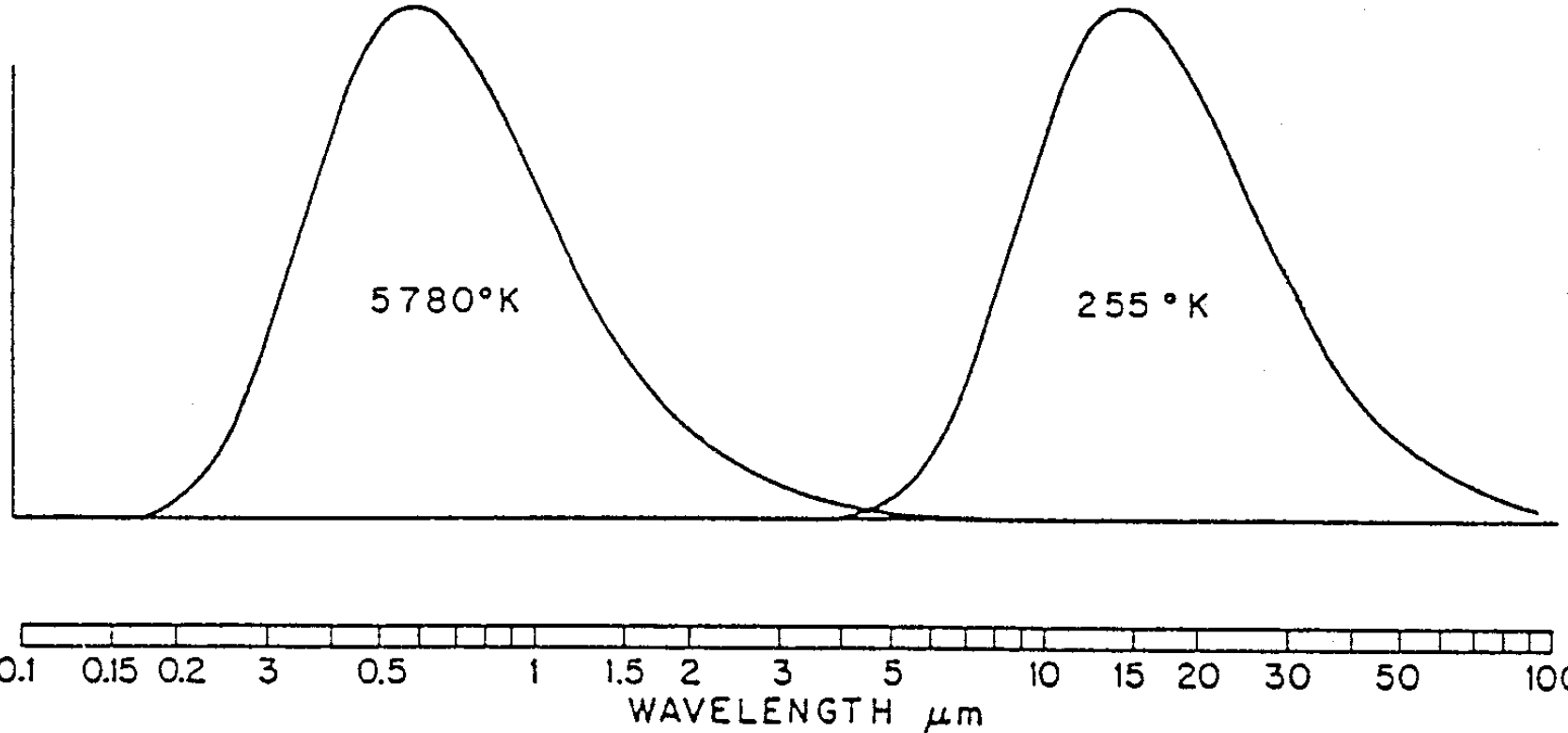
$$T = c_2 / [\lambda \ln(\frac{c_1}{\lambda^5 B_\lambda} + 1)]$$

Spectral Distribution of Energy Radiated from Blackbodies at Various Temperatures

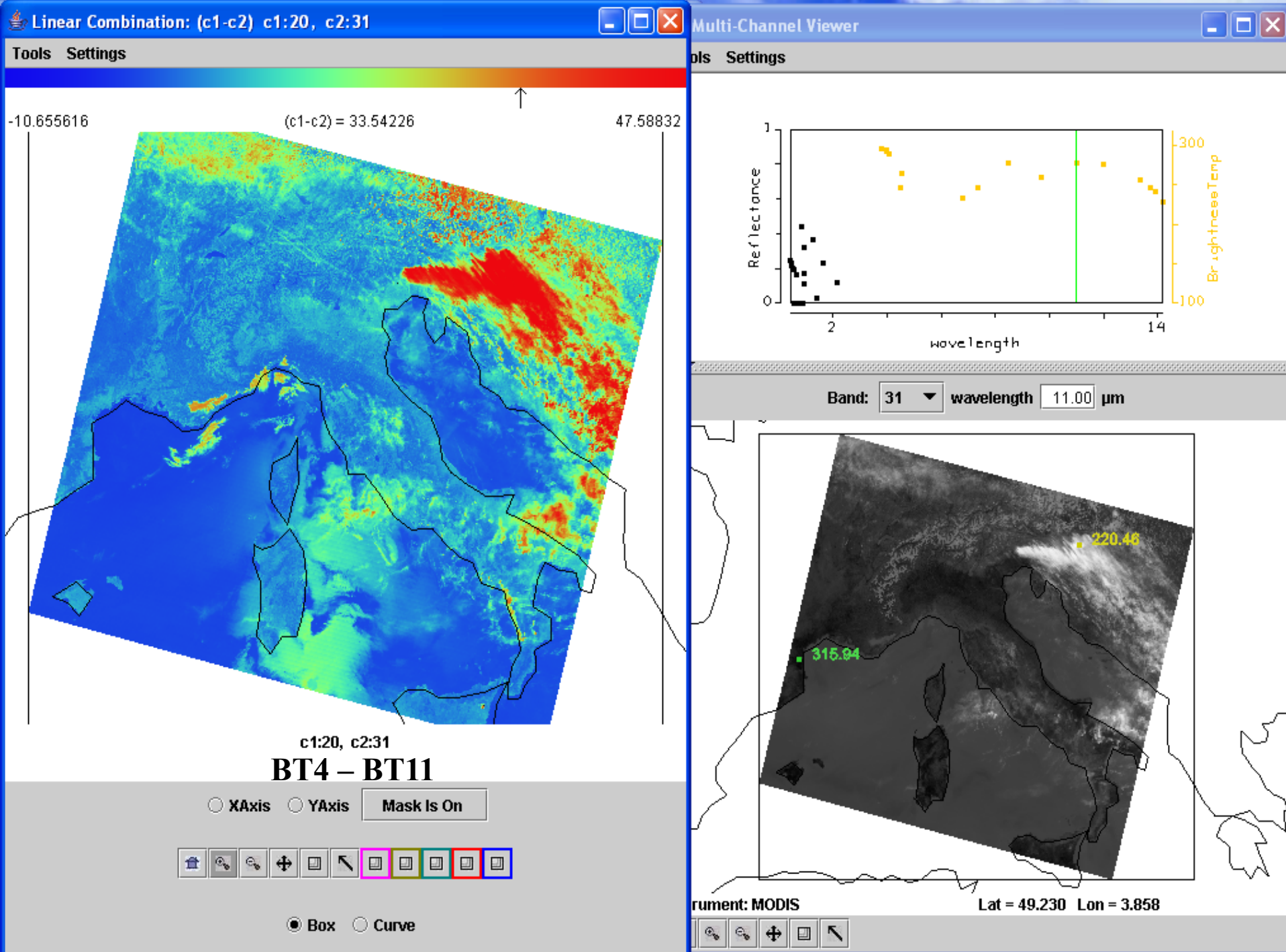




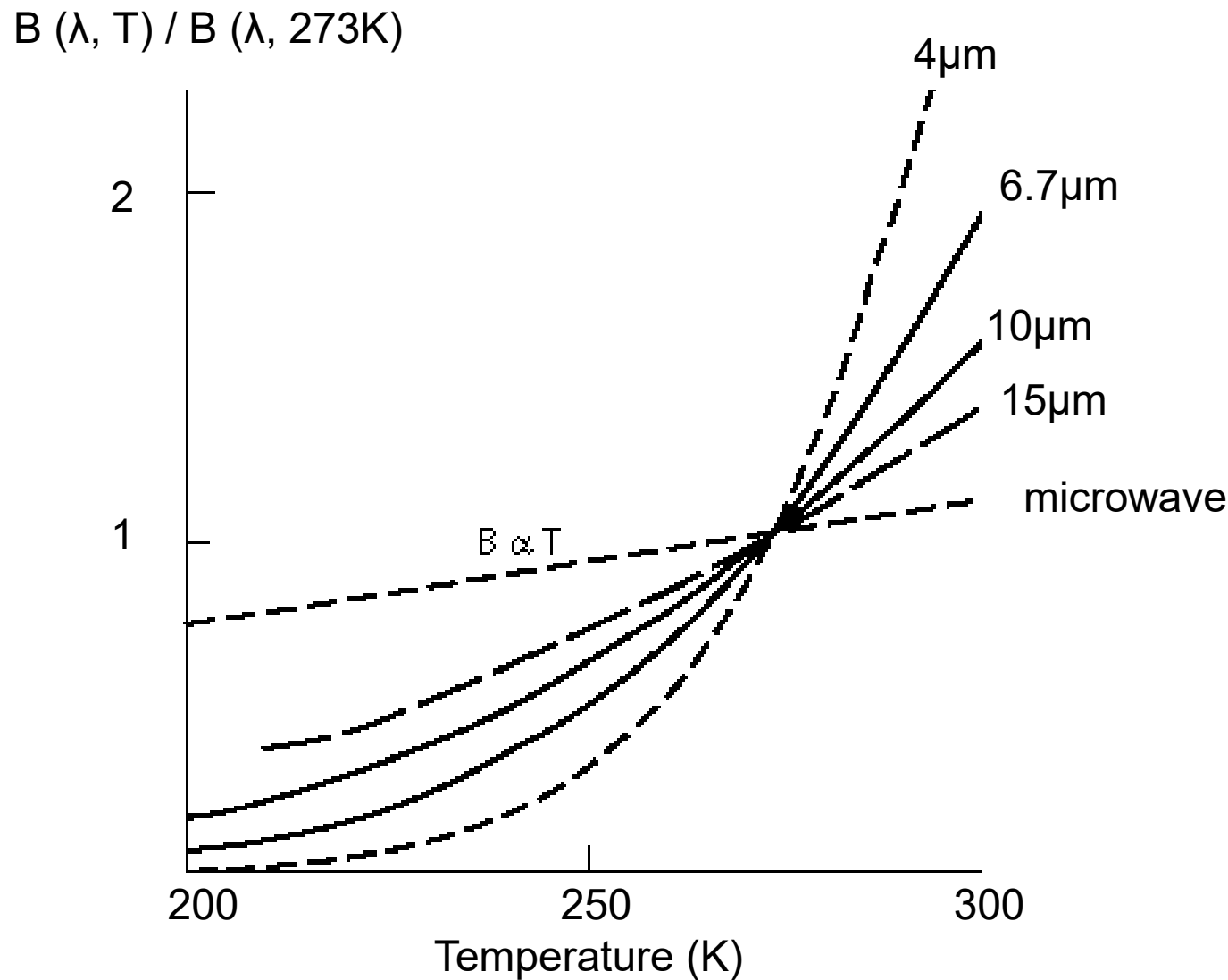
λE_λ (NORMALIZED)



Normalized black body spectra representative of the sun (left) and earth (right), plotted on a logarithmic wavelength scale. The ordinate is multiplied by wavelength so that the area under the curves is proportional to irradiance.



Temperature Sensitivity of $B(\lambda, T)$ for typical earth temperatures



Observed BT at 4 micron

Window Channel:

- little atmospheric absorption
- surface features clearly visible

Range BT[250, 335]

Range R[0.2, 1.7]

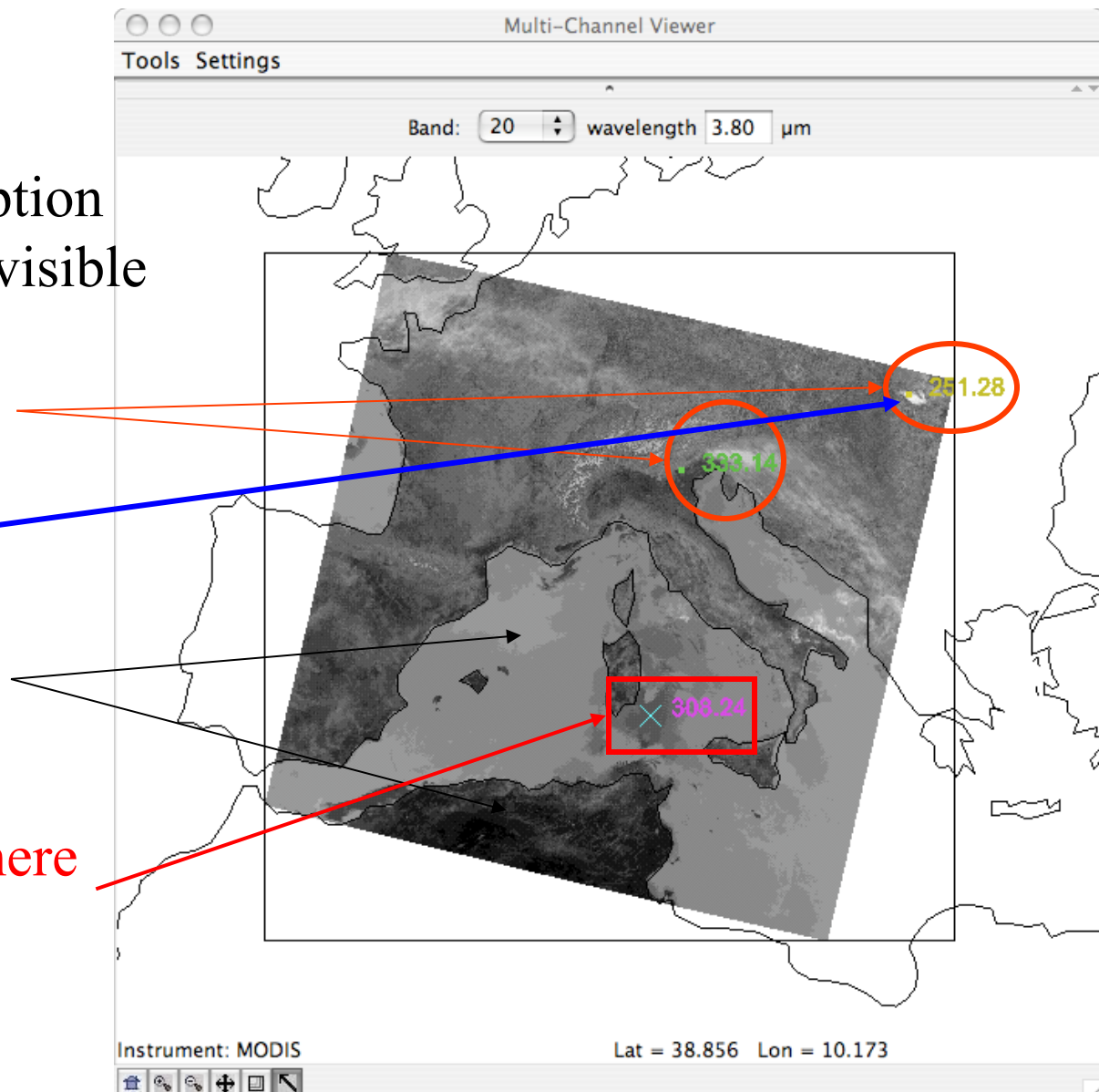
Clouds are cold

Values over land

Larger than over water

Reflected Solar everywhere

Stronger over Sunglint



Observed BT at 11 micron

Window Channel:

- little atmospheric absorption
- surface features clearly visible

Range BT [220, 320]

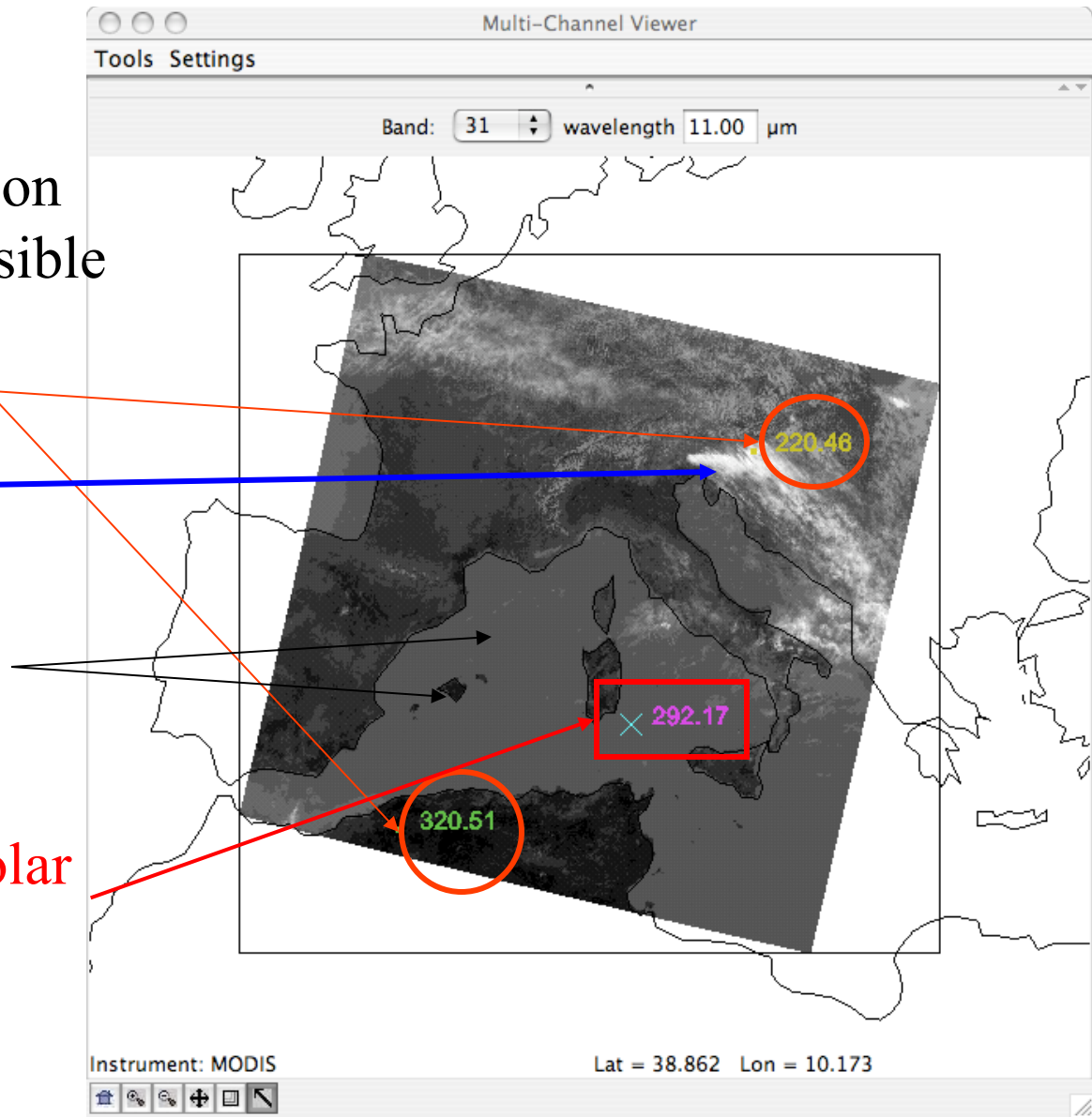
Range R [2.1, 12.4]

Clouds are cold

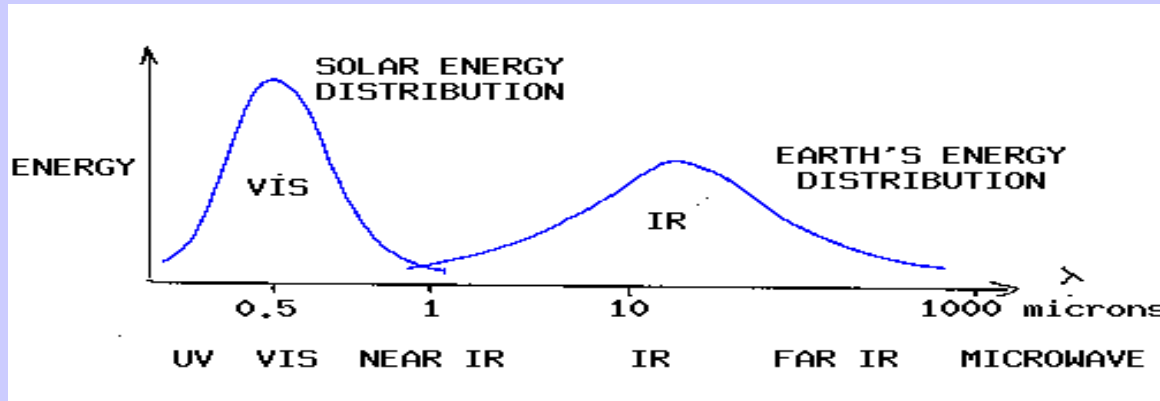
Values over land

Larger than over water

Undetectable Reflected Solar
Even over Sunglint



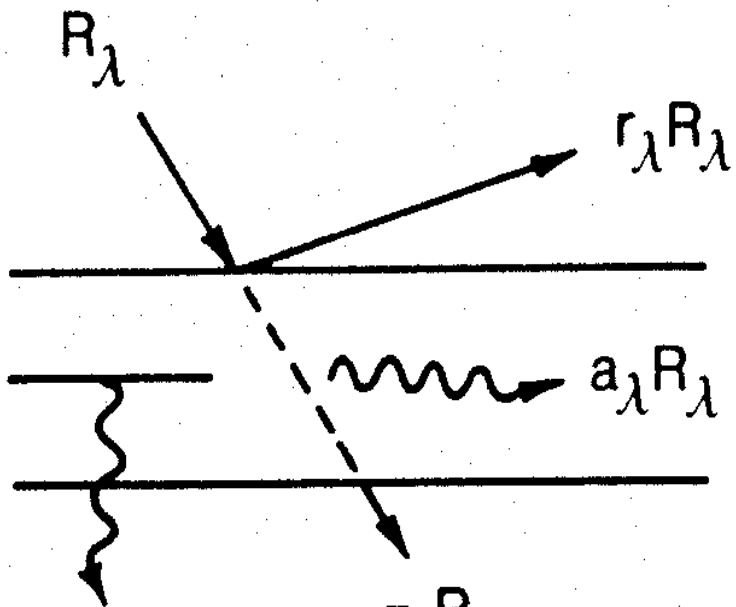
Solar (visible) and Earth emitted (infrared) energy



Incoming solar radiation (mostly visible) drives the earth-atmosphere (which emits infrared).

Over the annual cycle, the incoming solar energy that makes it to the earth surface (about 50 %) is balanced by the outgoing thermal infrared energy emitted through the atmosphere.

The atmosphere transmits, absorbs (by H₂O, O₂, O₃, dust) reflects (by clouds), and scatters (by aerosols) incoming visible; the earth surface absorbs and reflects the transmitted visible. Atmospheric H₂O, CO₂, and O₃ selectively transmit or absorb the outgoing infrared radiation. The outgoing microwave is primarily affected by H₂O and O₂.



$$\epsilon_\lambda B_\lambda(T)$$

$$a_\lambda R_\lambda = R_\lambda - r_\lambda R_\lambda - \tau_\lambda R_\lambda$$

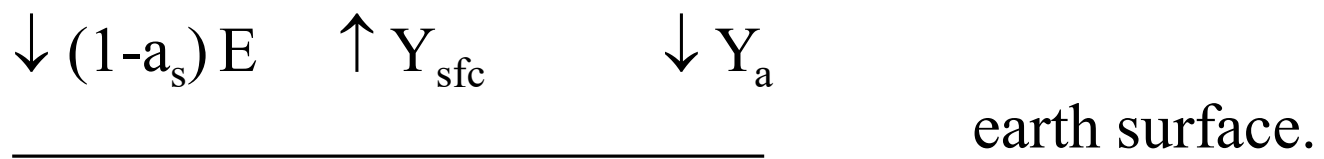
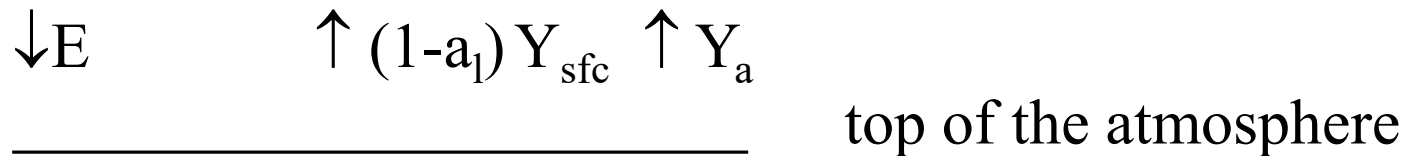
'ENERGY
CONSERVATION'

Selective Absorption

Atmosphere transmits visible and traps infrared

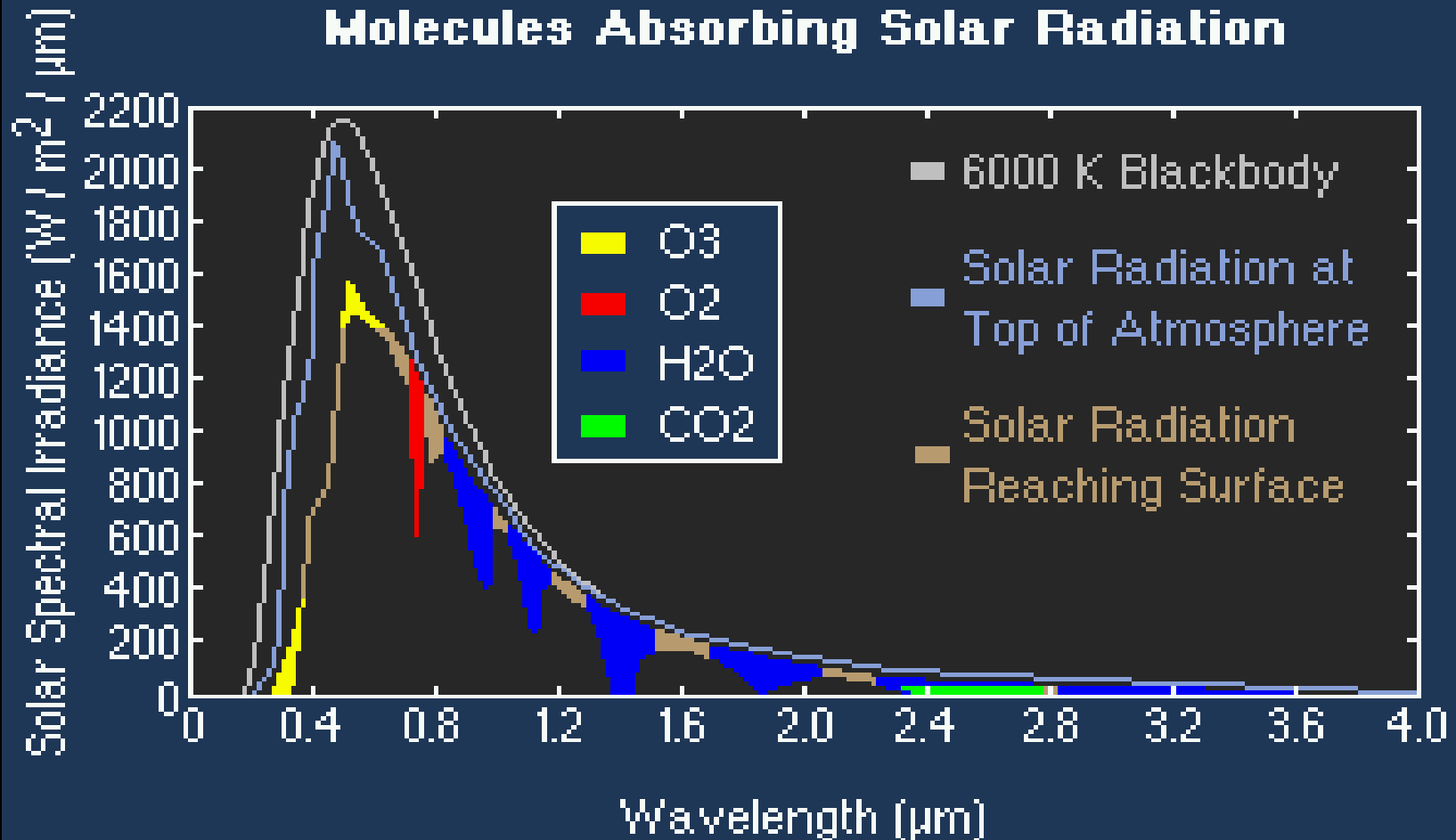
Incoming
solar

Outgoing IR

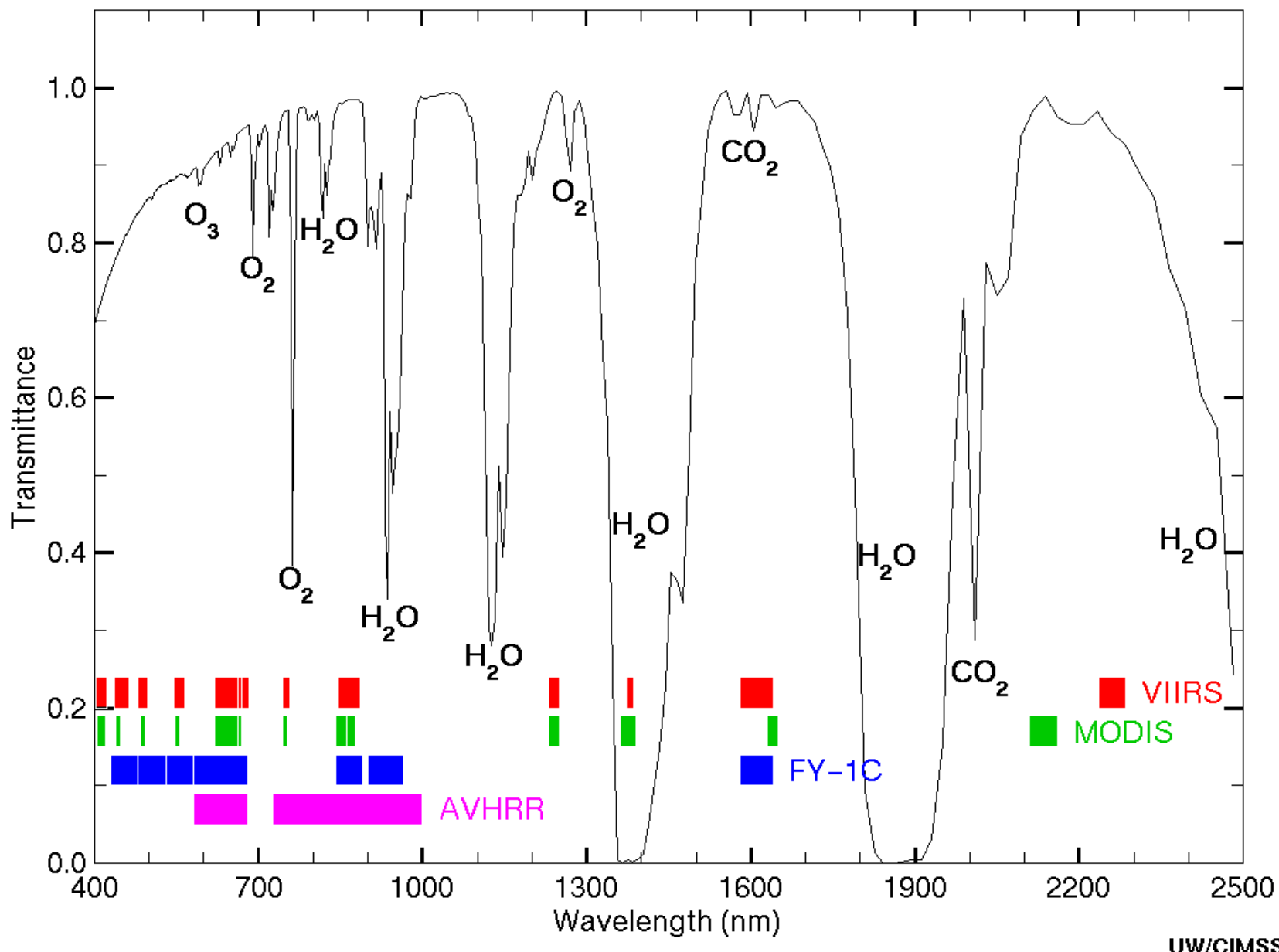


$$Y_{sfc} = \frac{(2-a_s)}{(2-a_L)} E = \sigma T_{sfc}^4 \text{ thus if } a_s < a_L \text{ then } Y_{sfc} > E$$

Solar Spectrum



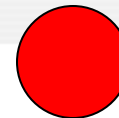
VIIRS, MODIS, FY-1C, AVHRR



Tools Settings

Band: 1 wavelength 0.65 μm

Ocean: Dark



Vegetated Surface: Dark

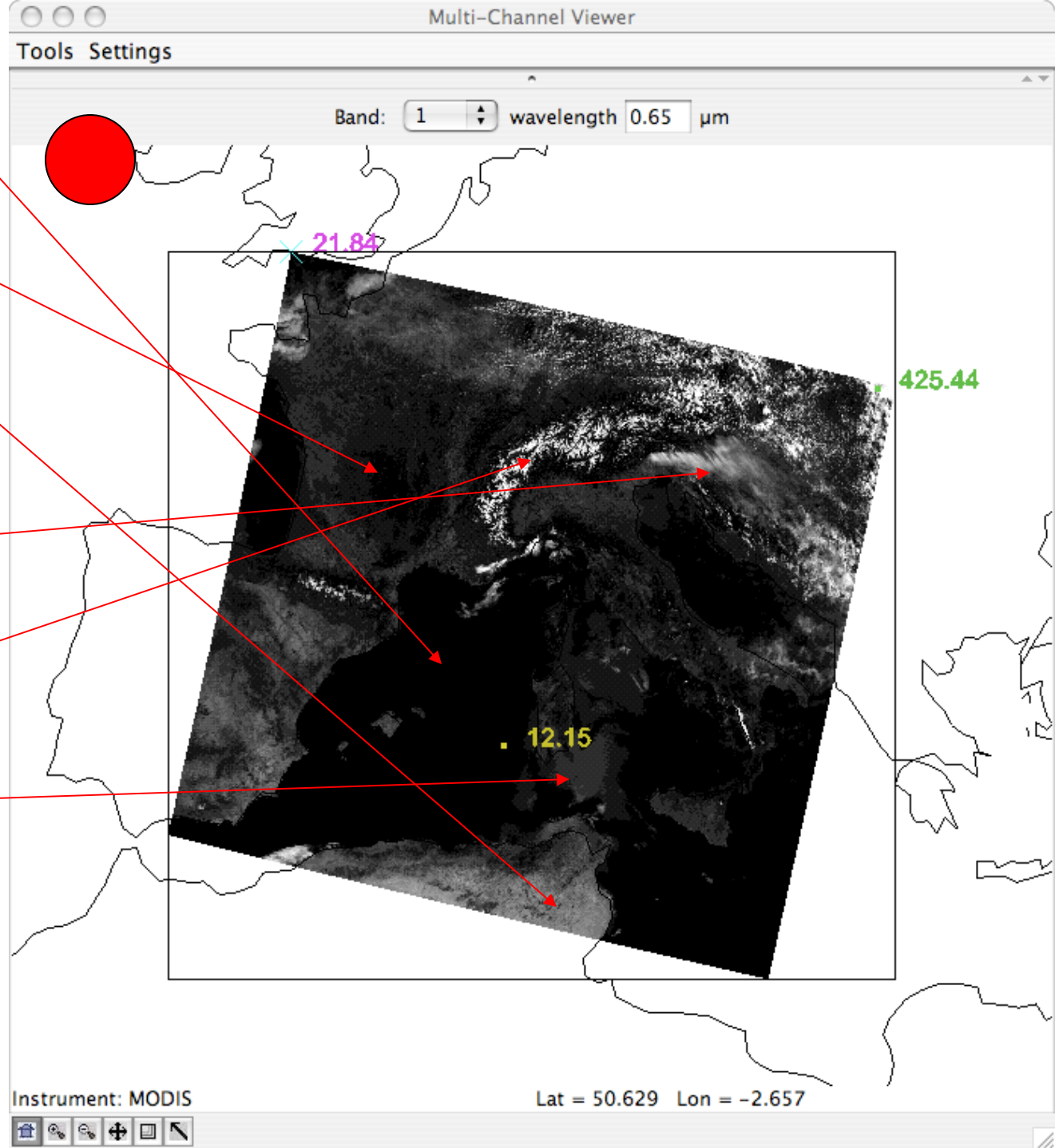
NonVegetated Surface: Dark

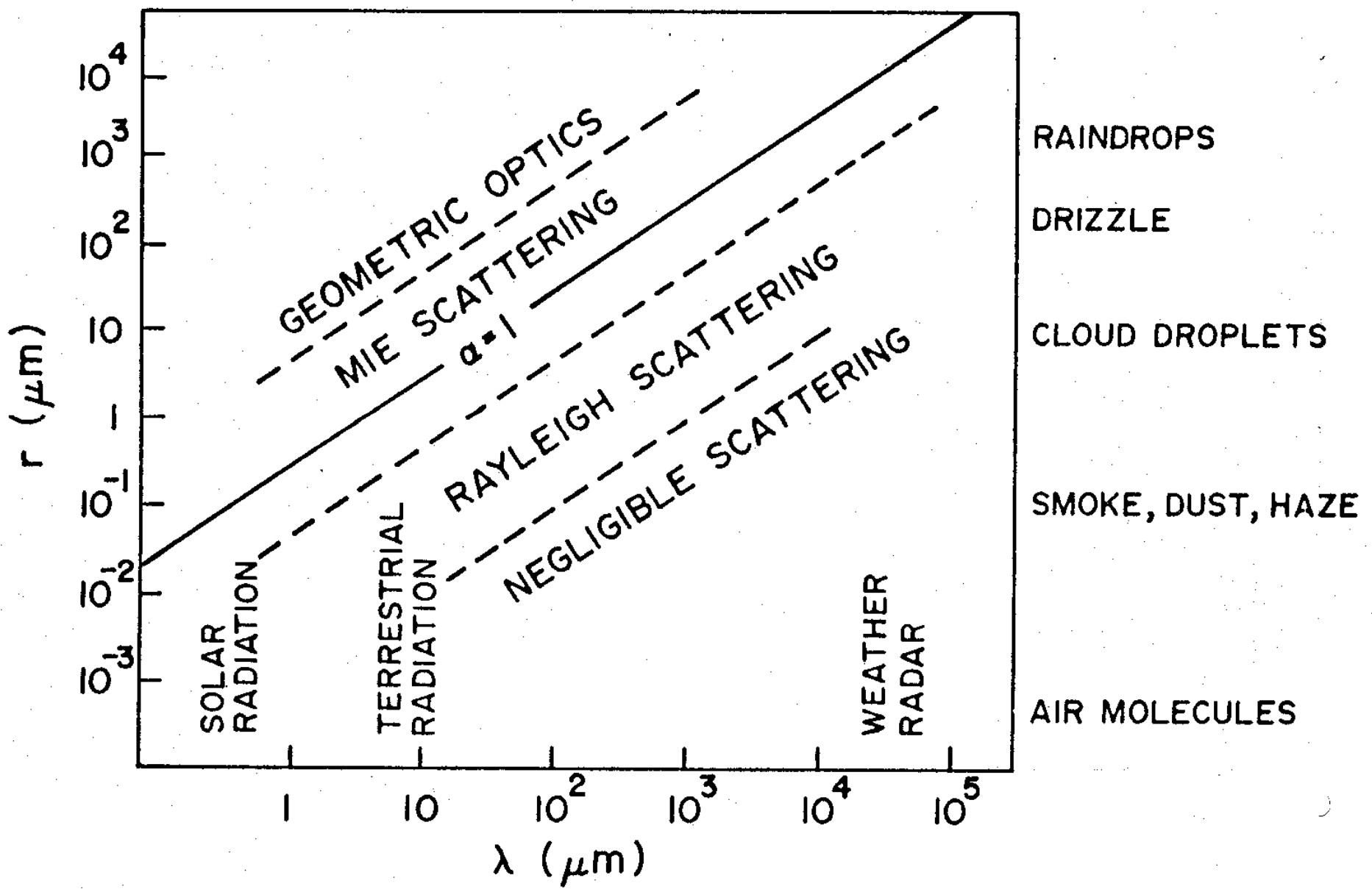
NonVegetated Surface: Brighter

Clouds: Bright

Snow: Bright

Sunglint

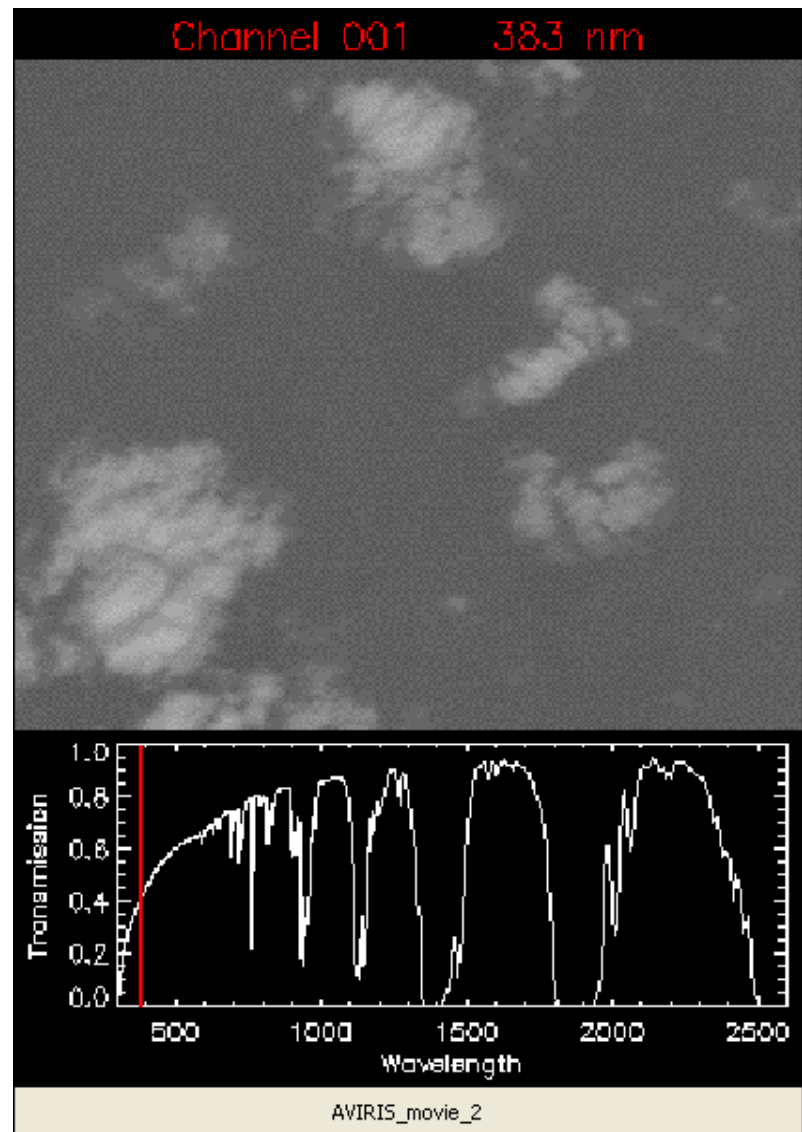
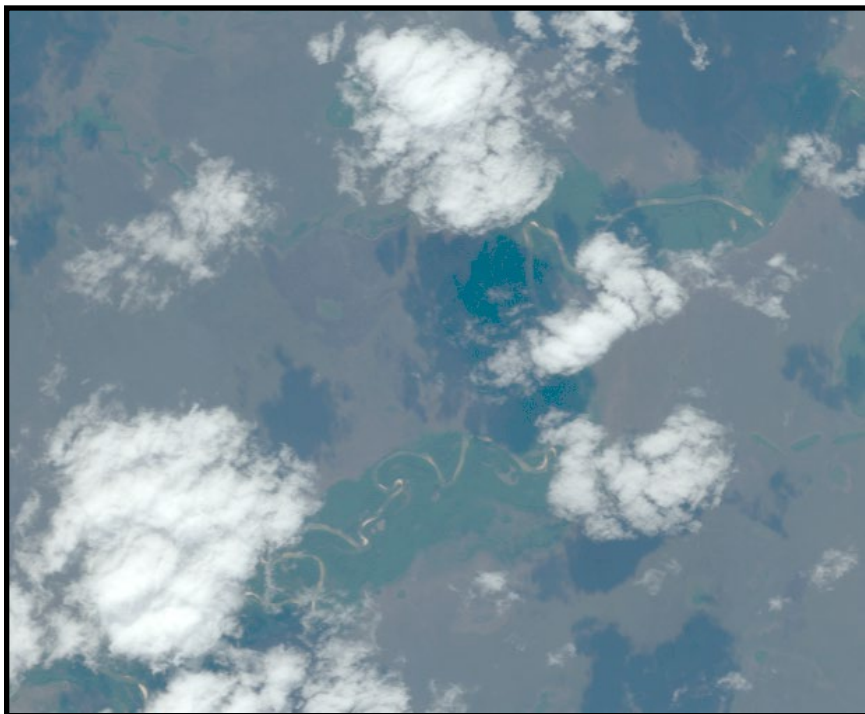




AVIRIS Movie #2

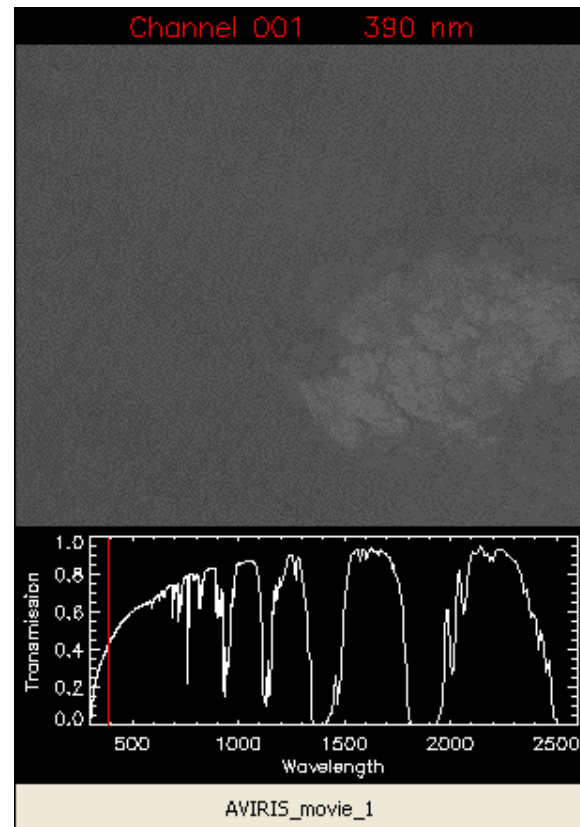
AVIRIS Image - Porto Nacional, Brazil
20-Aug-1995

224 Spectral Bands: 0.4 - 2.5 μm
Pixel: 20m x 20m Scene: 10km x 10km



AVIRIS Movie #1

AVIRIS Image - Linden CA 20-Aug-1992
224 Spectral Bands: 0.4 - 2.5 μm
Pixel: 20m x 20m Scene: 10km x 10km

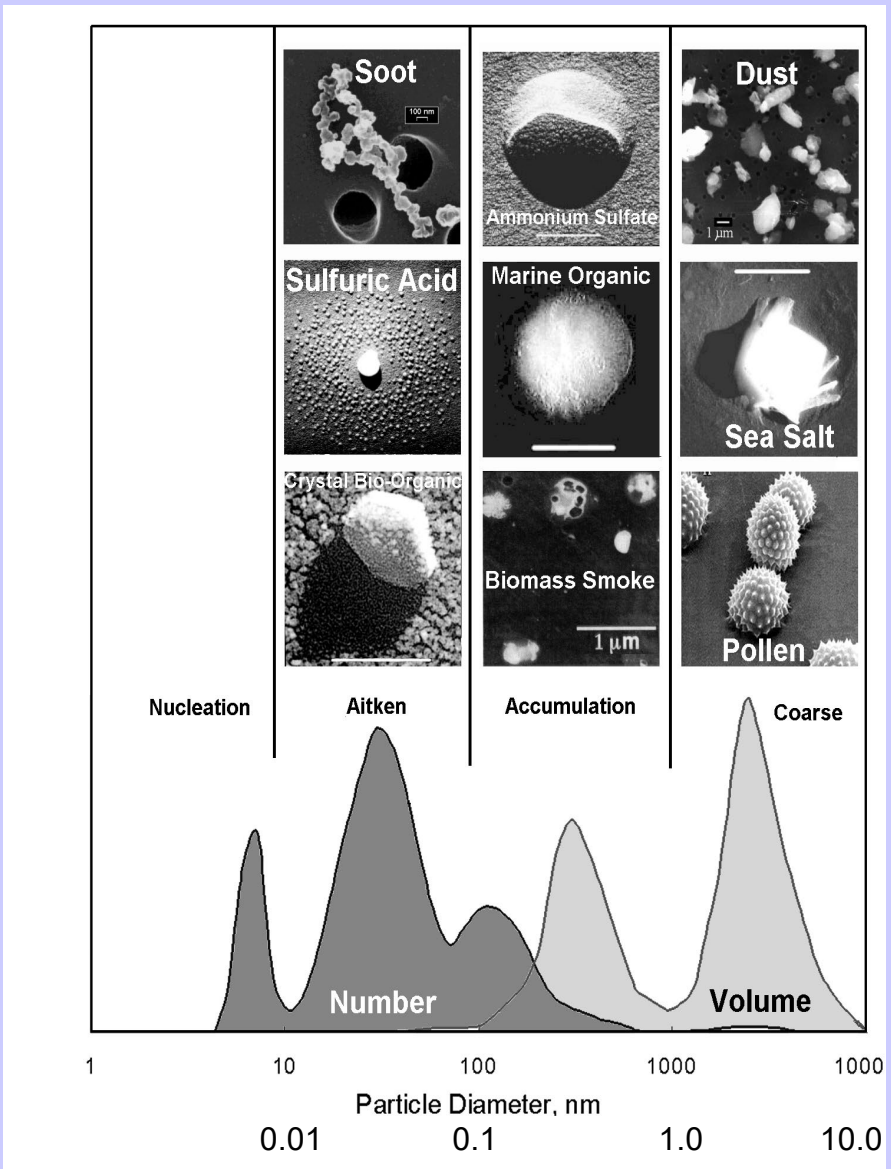


Aerosol Size Distribution

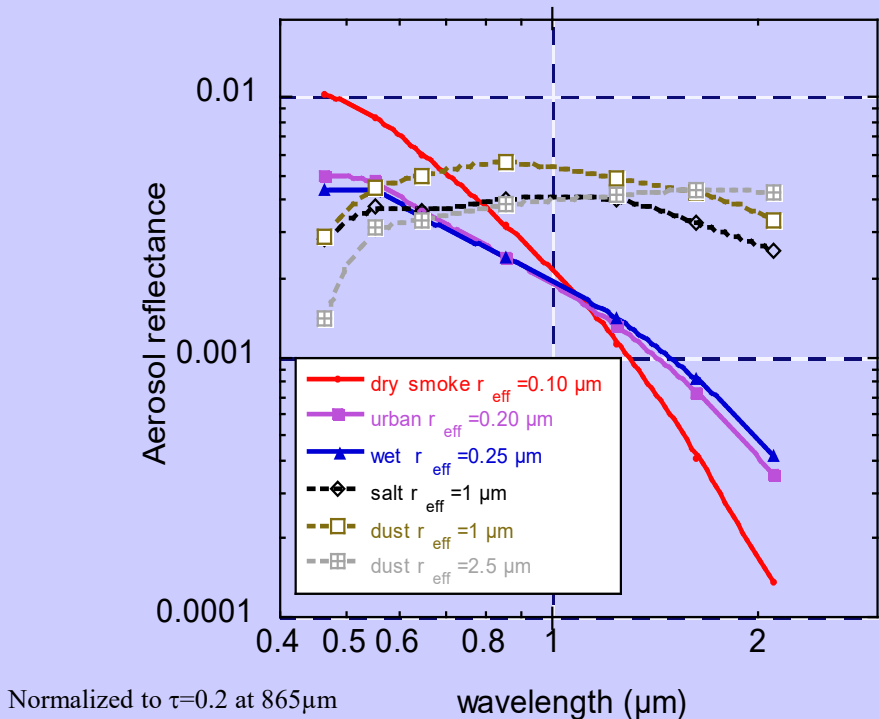
There are 3 modes :

- « **nucleation** »: radius is between 0.002 and 0.05 µm.
They result from combustion processes, photo-chemical reactions, etc.
- « **accumulation** »: radius is between 0.05 µm and 0.5 µm.
Coagulation processes.
- « **coarse** »: larger than 1 µm.
From mechanical processes like aeolian erosion.

« fine » particles (nucleation and accumulation) result from anthropogenic activities, coarse particles come from natural processes.



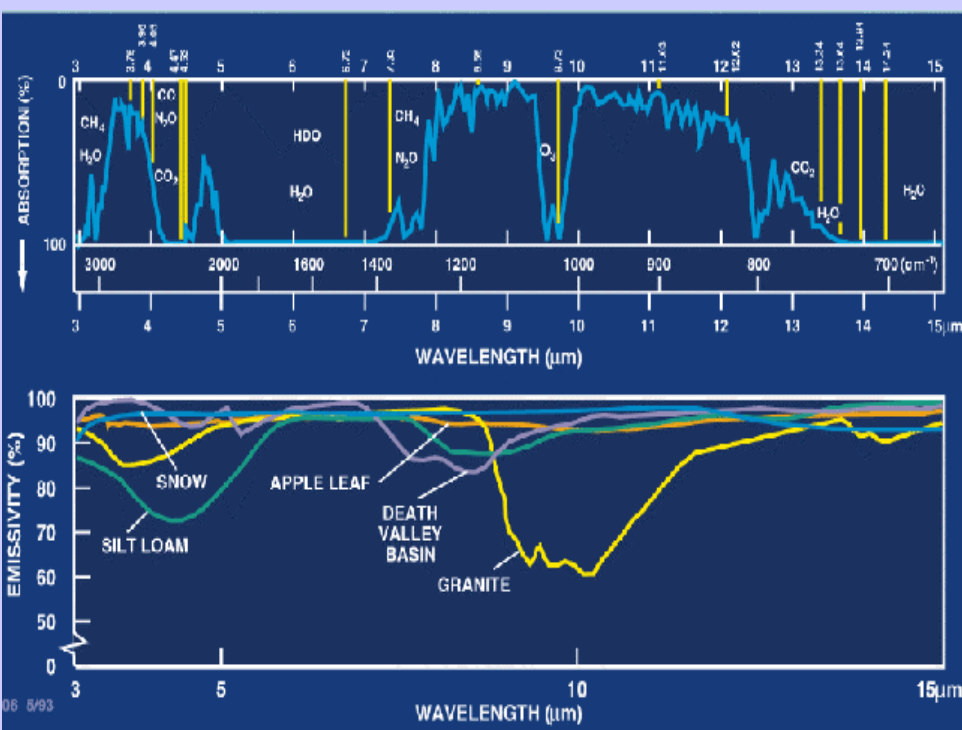
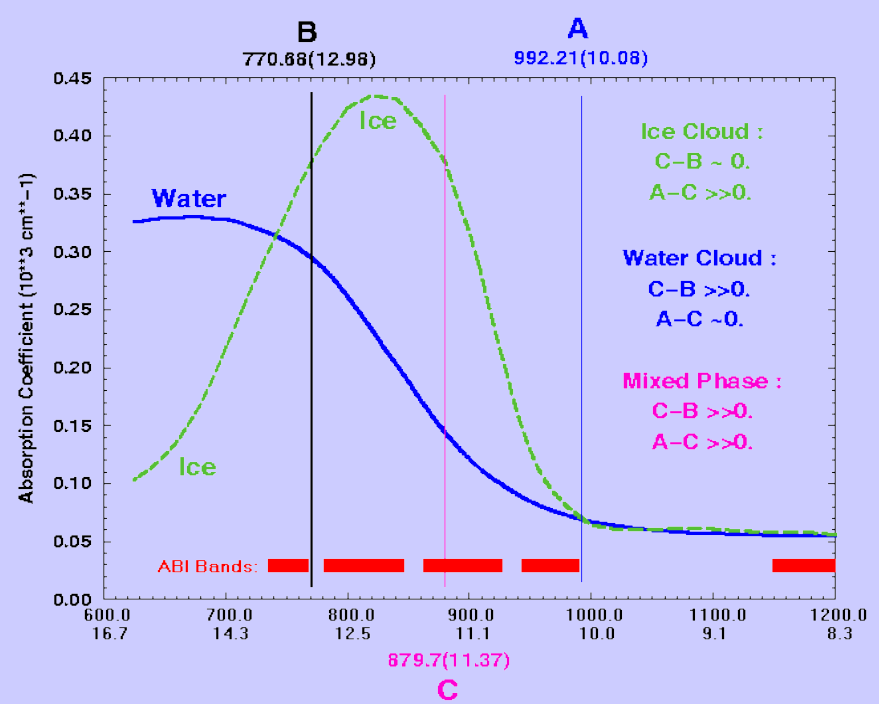
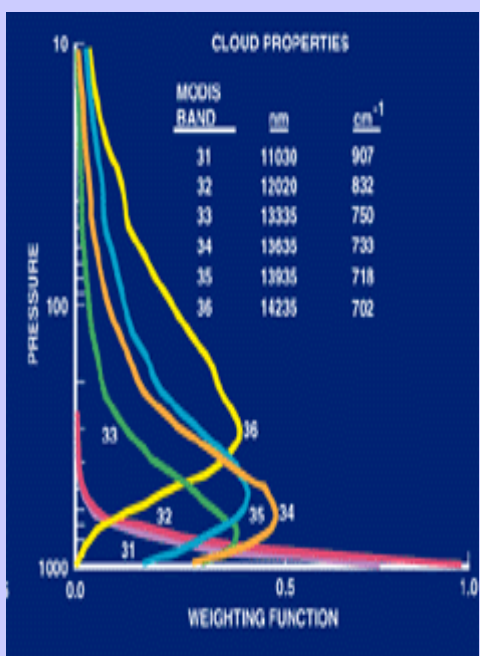
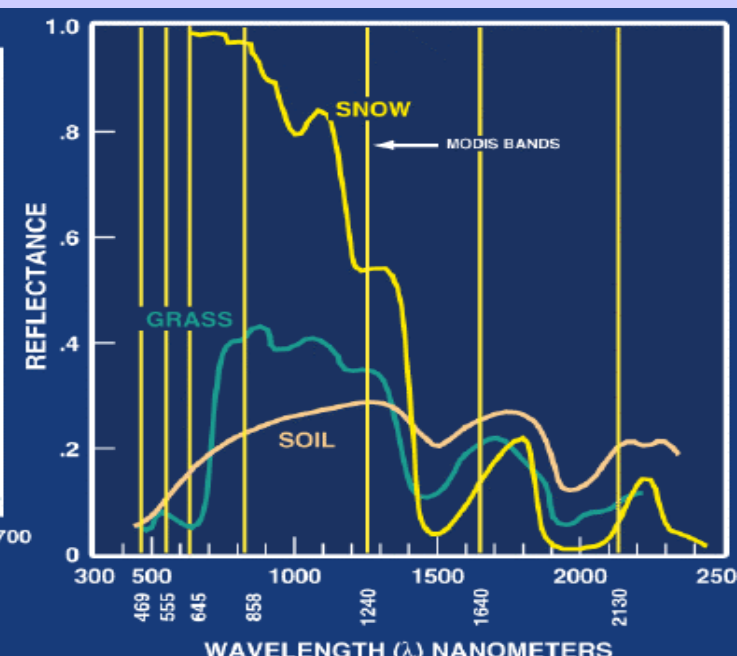
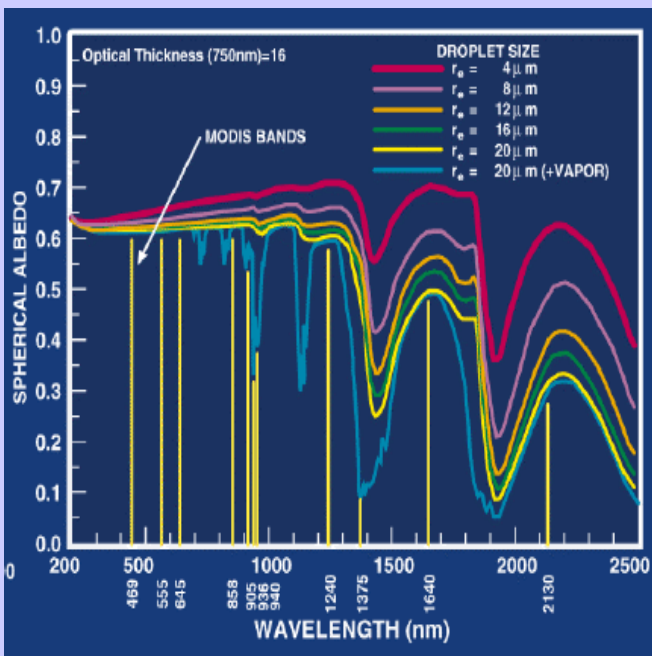
Aerosols over Ocean

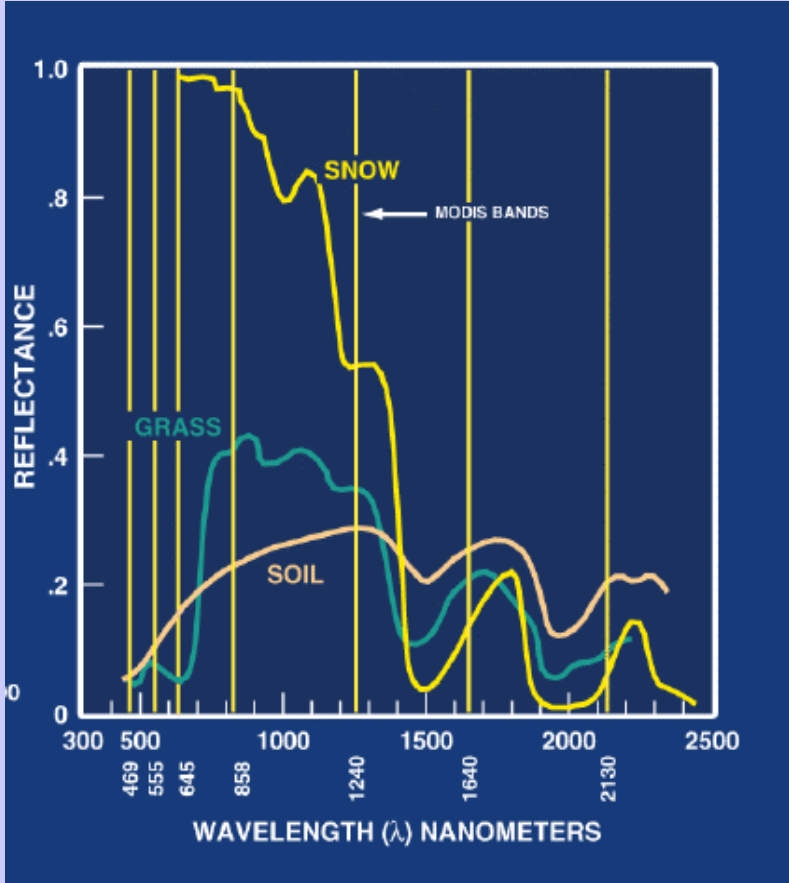


- Radiance data in 6 bands (550-2130nm).
- Spectral radiances (LUT) to derive the aerosol size distribution
- Two modes (accumulation $0.10-0.25\mu m$; coarse $1.0-2.5\mu m$); ratio is a free parameter
- Radiance at $865\mu m$ to derive τ

Ocean products :

- The total Spectral Optical thickness
- The effective radius
- The optical thickness of small & large modes/ratio between the 2 modes





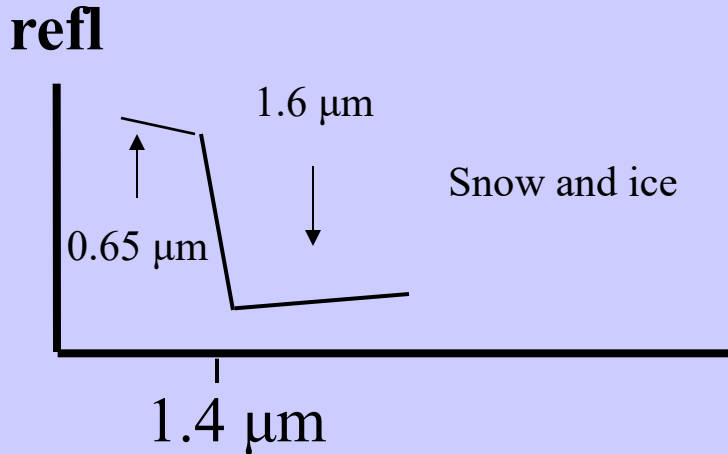
Investigating with Multi-spectral Combinations

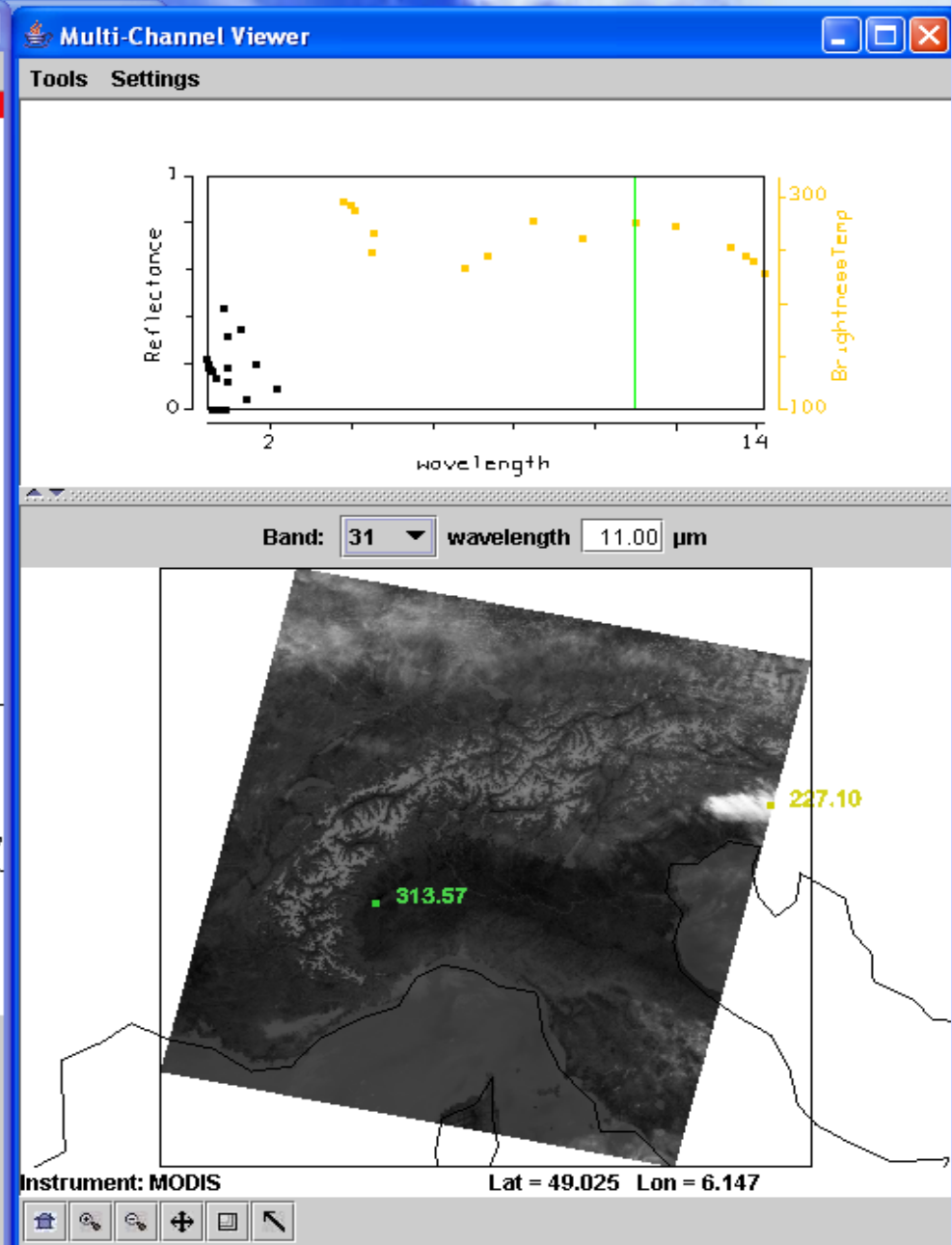
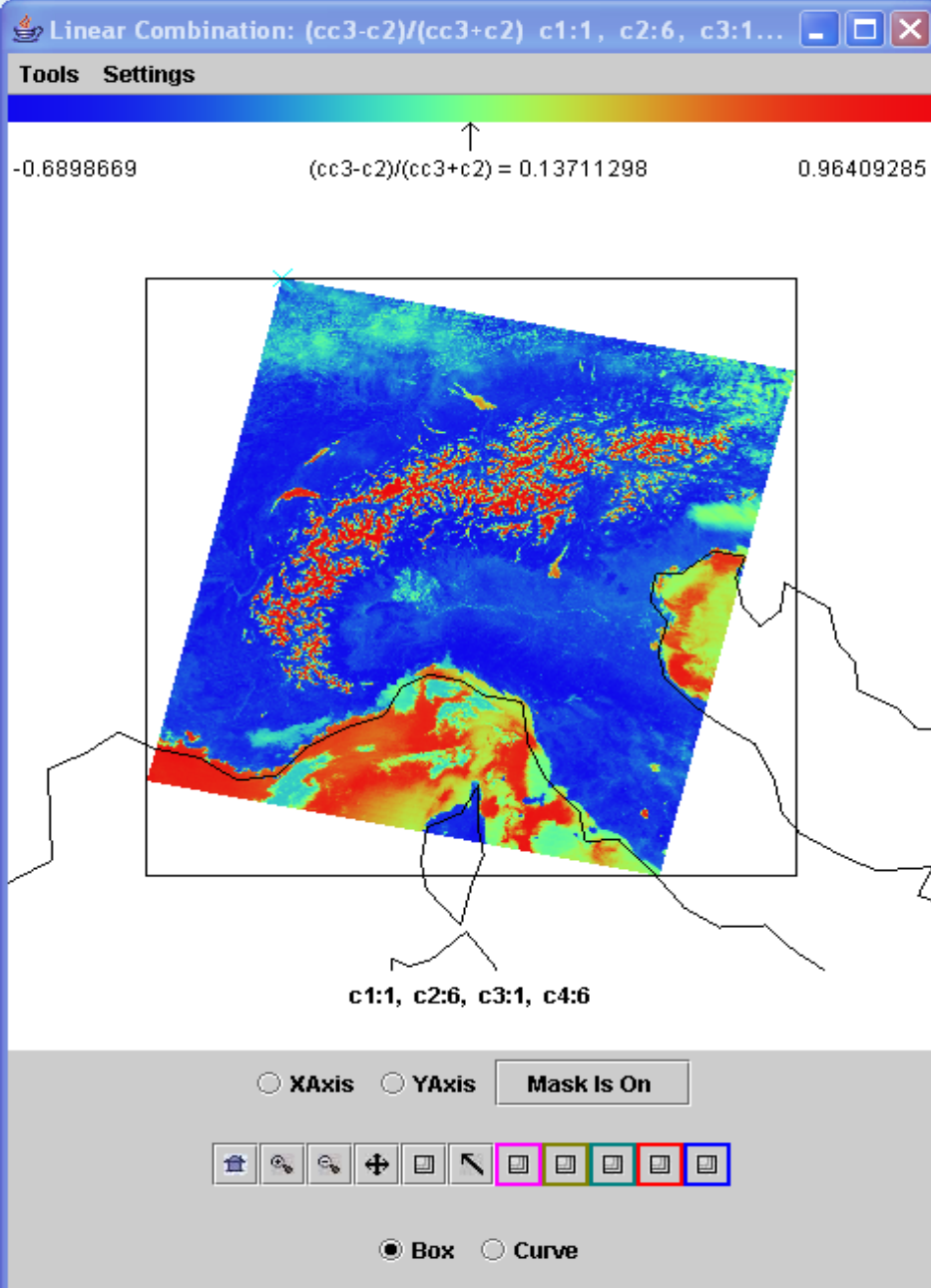
Given the spectral response of a surface or atmospheric feature

Select a part of the spectrum where the reflectance or absorption changes with wavelength

e.g. reflection from snow/ice

If $0.65 \mu\text{m}$ and $1.6 \mu\text{m}$ channels see the same reflectance than surface viewed is not snow;
if $1.6 \mu\text{m}$ sees considerably lower reflectance than $0.65 \mu\text{m}$ then surface might be snow



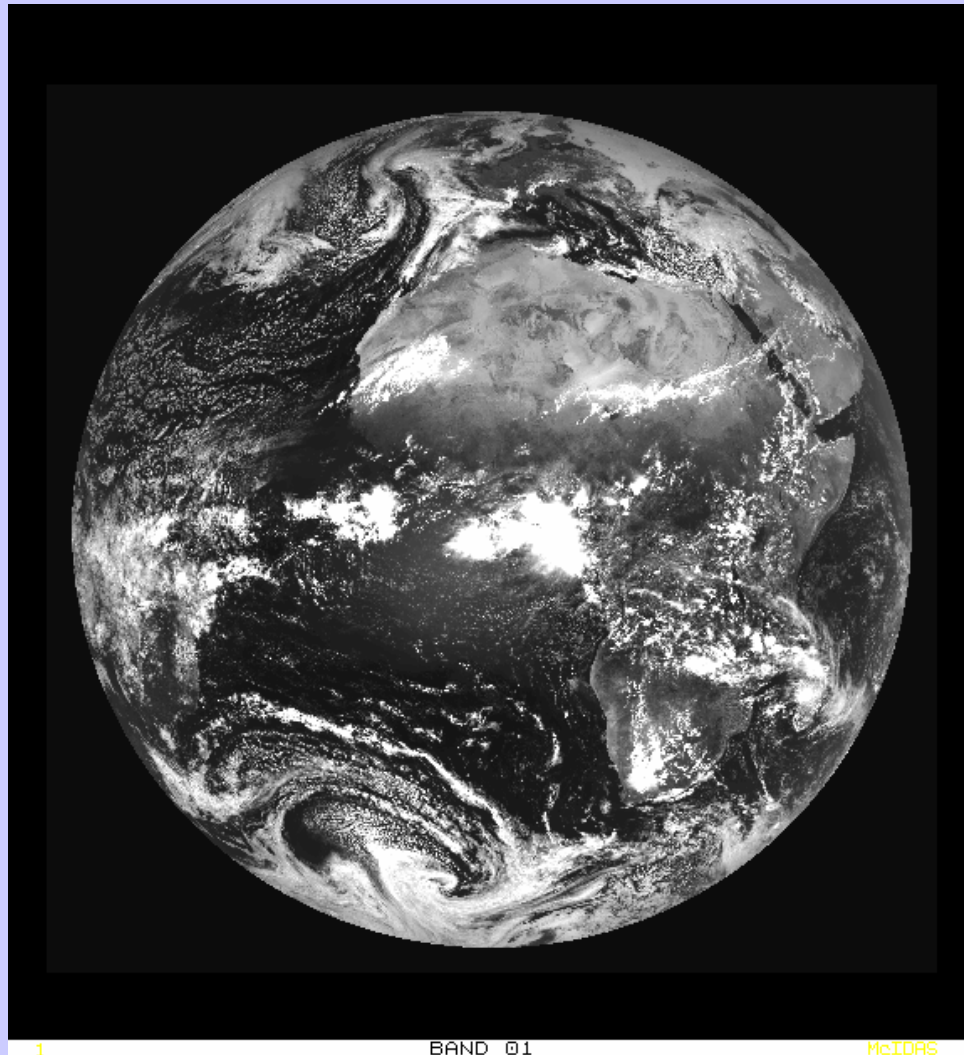


NDSI = $[r0.6-r1.6]/[r0.6+r1.6]$ is near one in snow in Alps

Cloud Mask Tests

- BT11 clouds over ocean
- BT13.9 high clouds
- BT6.7 high clouds
- BT3.9-BT11 broken or scattered clouds
- BT11-BT12 high clouds in tropics
- BT8.6-BT11 ice clouds
- BT6.7-BT11 or BT13.9-BT11 clouds in polar regions
- BT11+aPW(BT11-BT12) clouds over ocean
- r0.65 clouds over land
- r0.85 clouds over ocean
- r1.38 thin cirrus
- r1.6 clouds over snow, ice cloud
- r0.85/r0.65 or NDVI clouds over vegetation
- $\sigma(\text{BT11})$ clouds over ocean

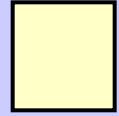
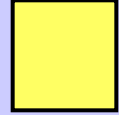
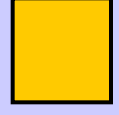
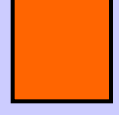
12 channel SEVIRI



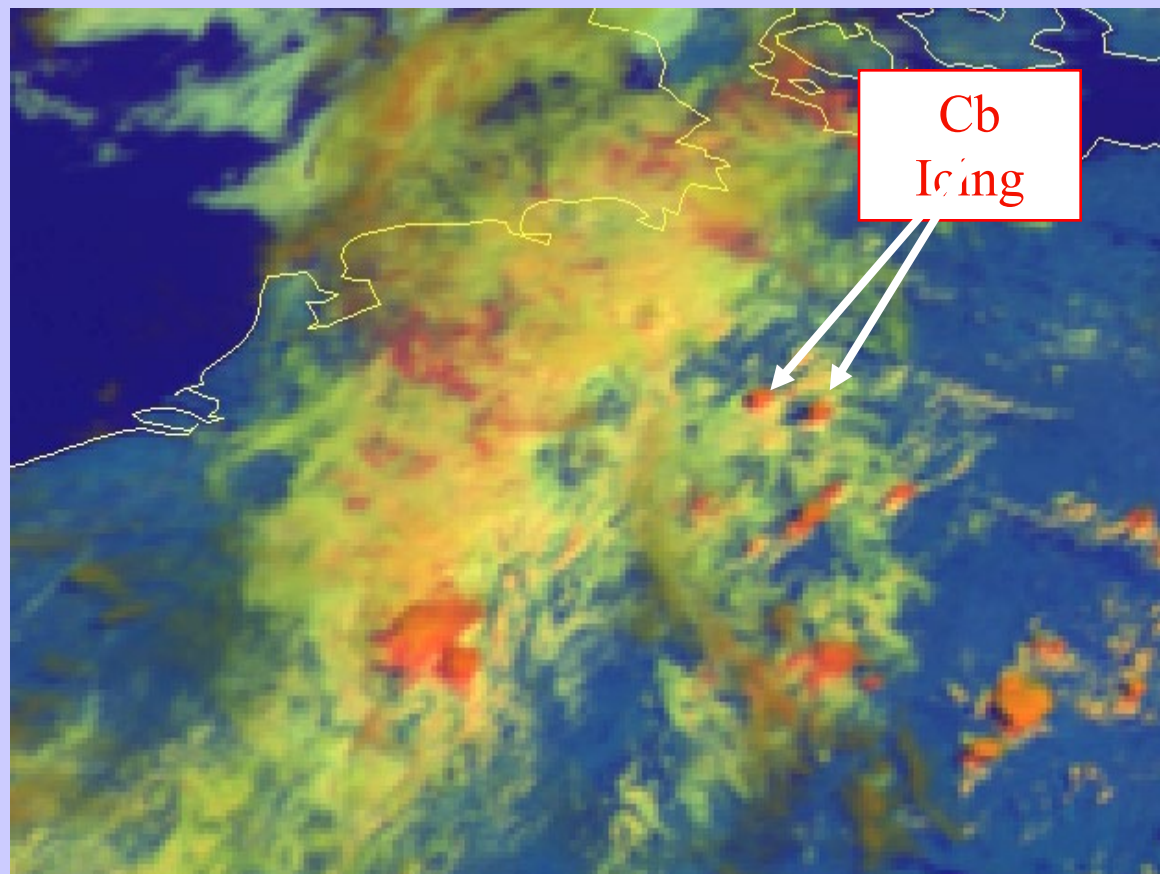
See image gallery at <http://www.eumetsat.int/idcplg>

Convective Initiation

RGB 0.6-1.6-10.8 um

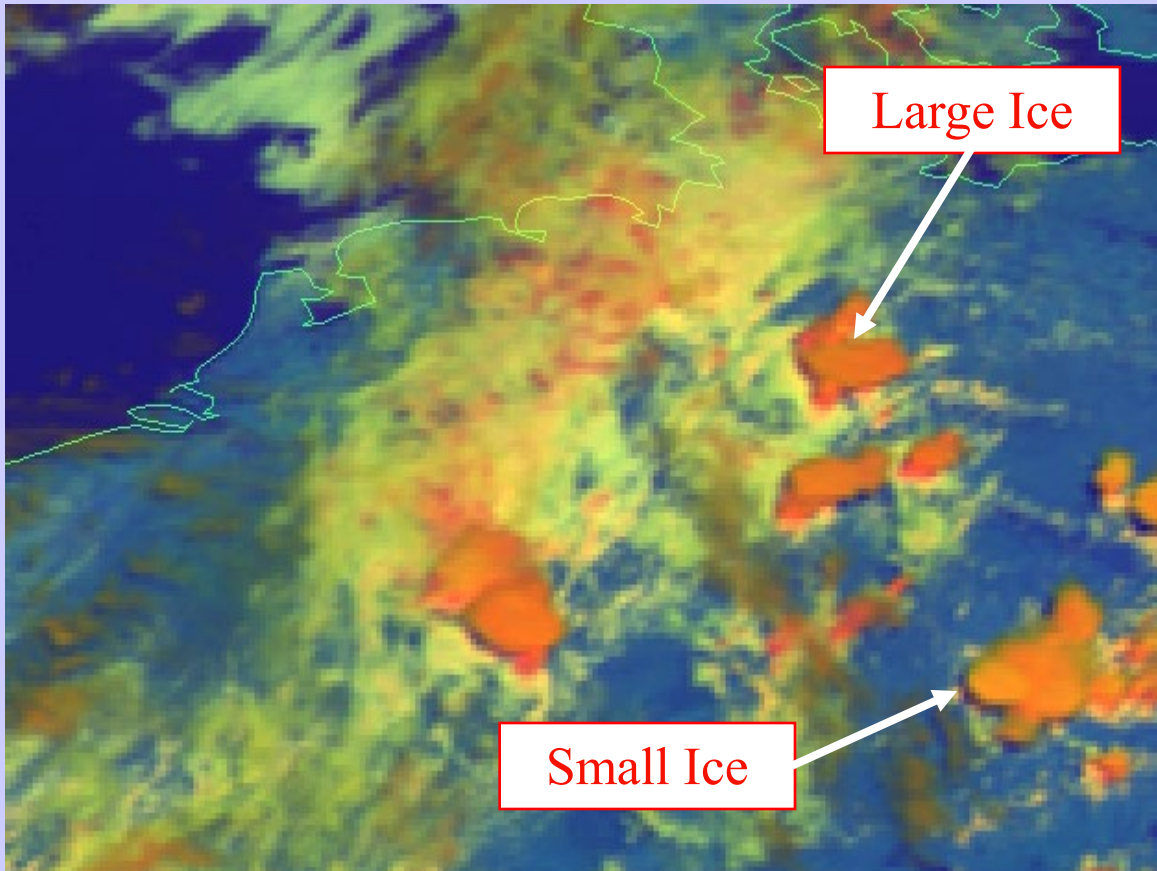
| | Red VIS0.6 | Green NIR1.6 | Blue IR10.8 | RGB | |
|--------------------------------------|---------------|-----------------|----------------|--------------------|---|
| I. Very early stage <i>yellow</i> | 255 | 255 | 200 | <i>white-light</i> |  |
| II. First convection | 255 | 255 | 100 | <i>yellow</i> |  |
| III. First icing | 255 | 200 | 0 | <i>orange</i> |  |
| IV. Large icing | 255 | 100 | 0 | <i>red-orange</i> |  |

First Icing



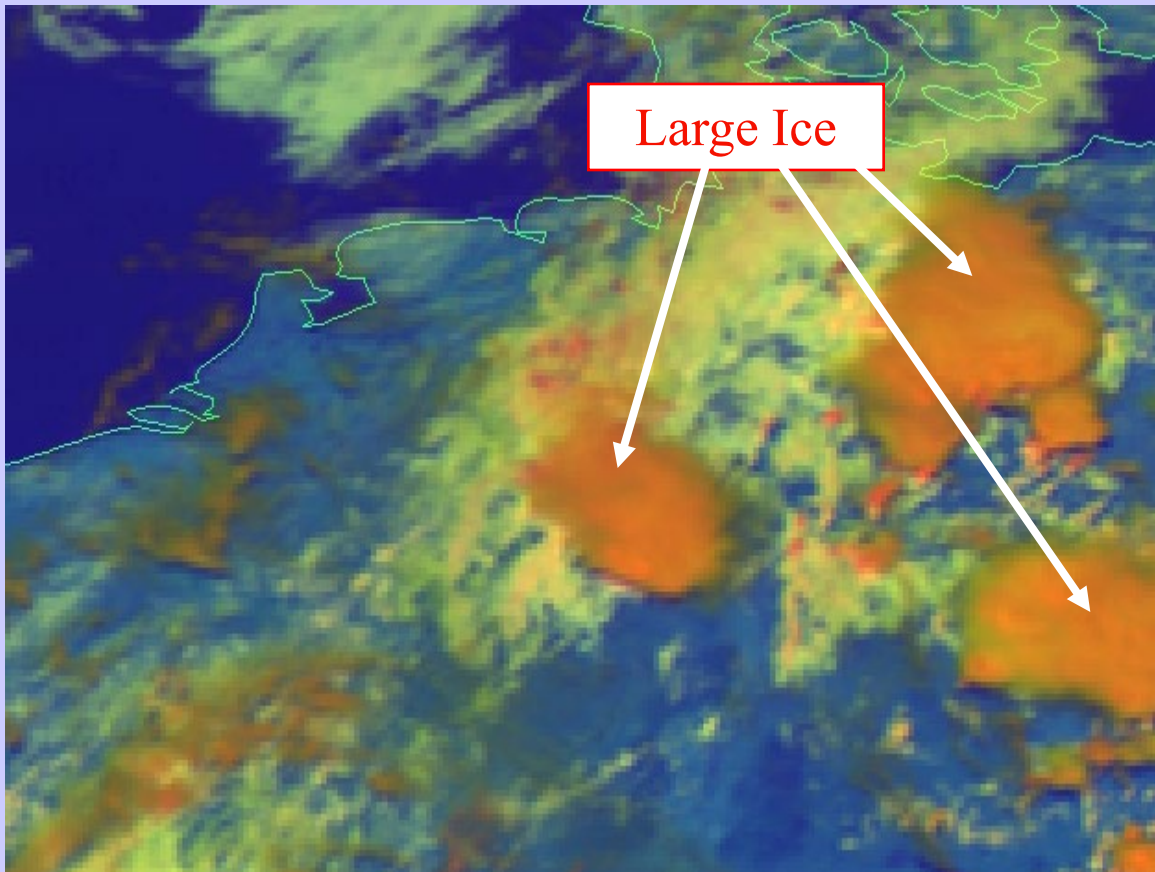
MSG-1, 5 June 2003, 10:30 UTC, RGB 01-03-09

Large Icing



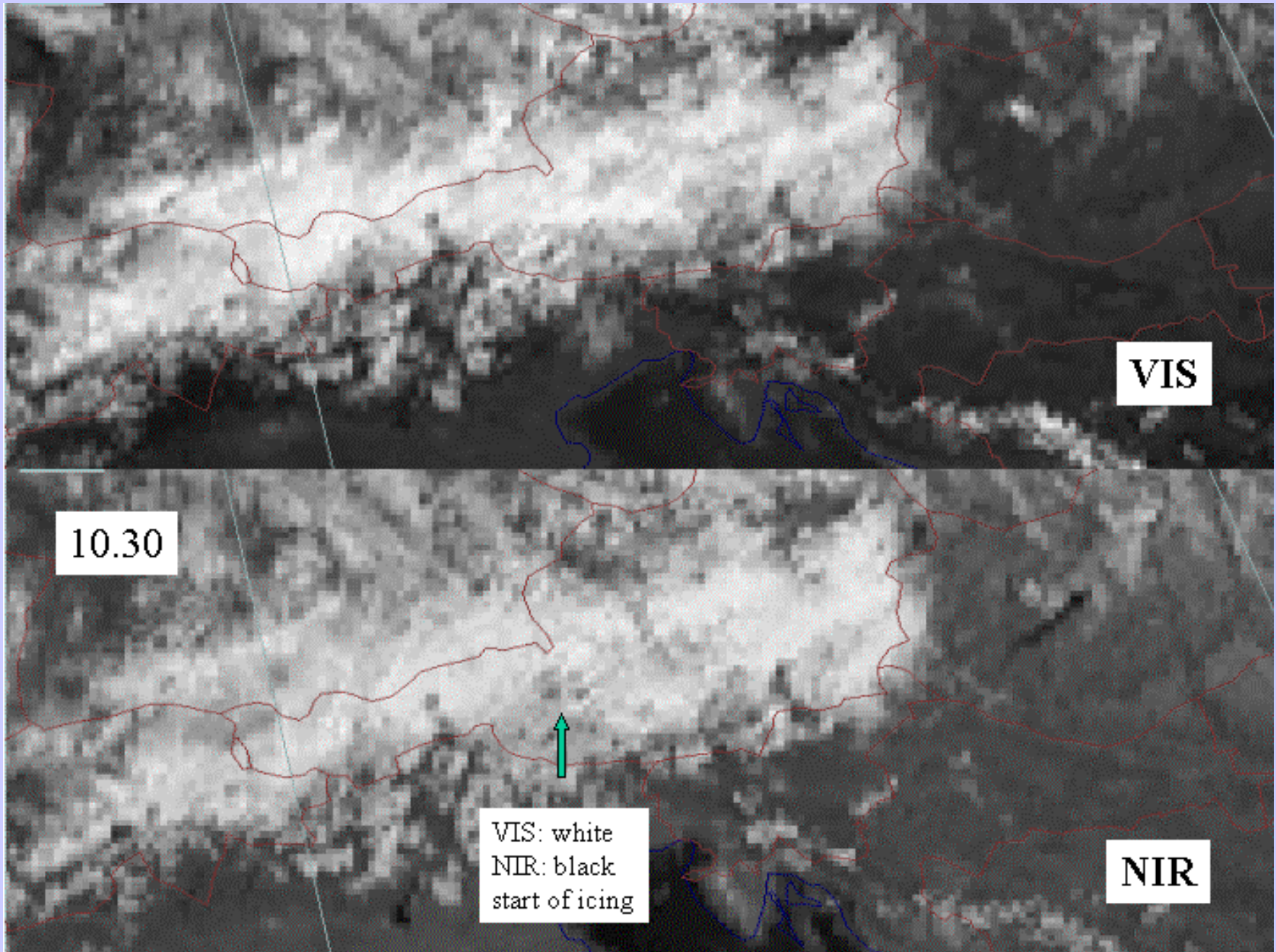
MSG-1, 5 June 2003, 11:30 UTC, RGB 01-03-09

Very Large Icing



MSG-1, 5 June 2003, 13:30 UTC, RGB 01-03-09

Meteosat-8 sees icing in clouds (Lutz et al)



RGB example

$$R = BT12.0 - BT10.8 \quad G = BT 10.8 - BT8.7 \quad B = BT10.8$$

microphysics RGB MSG Ch 10-9, 9-7, 9
dust, clouds, contrails, fog, ash, SO₂, low-level H₂O

| | |
|---|------------|
| R – optical thickness of cloud, Tsfc-Tcld | -4 to +2 |
| G – plus cloud phase | 0 to +6 |
| B – plus cloud top temp | 248 to 303 |

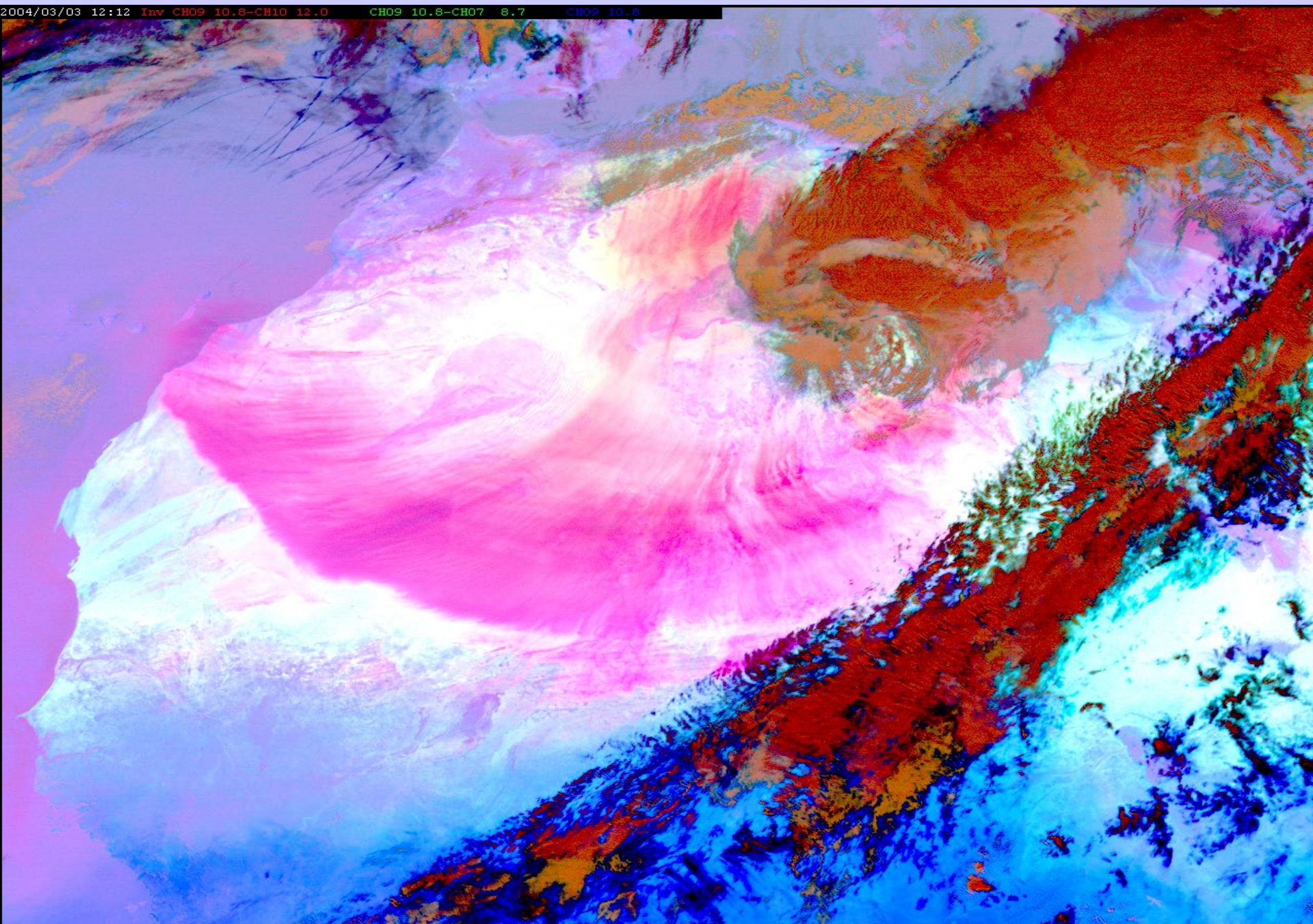
With emphasis on dust ($[BT12-BT11]>0$)
and thin ice clouds ($[BT12-BT11]<0$ & $[BT11-BT8.6]>0$)

| | |
|---|------------|
| R | -4 to +2 |
| G | 0 to +15 |
| B | 261 to 289 |

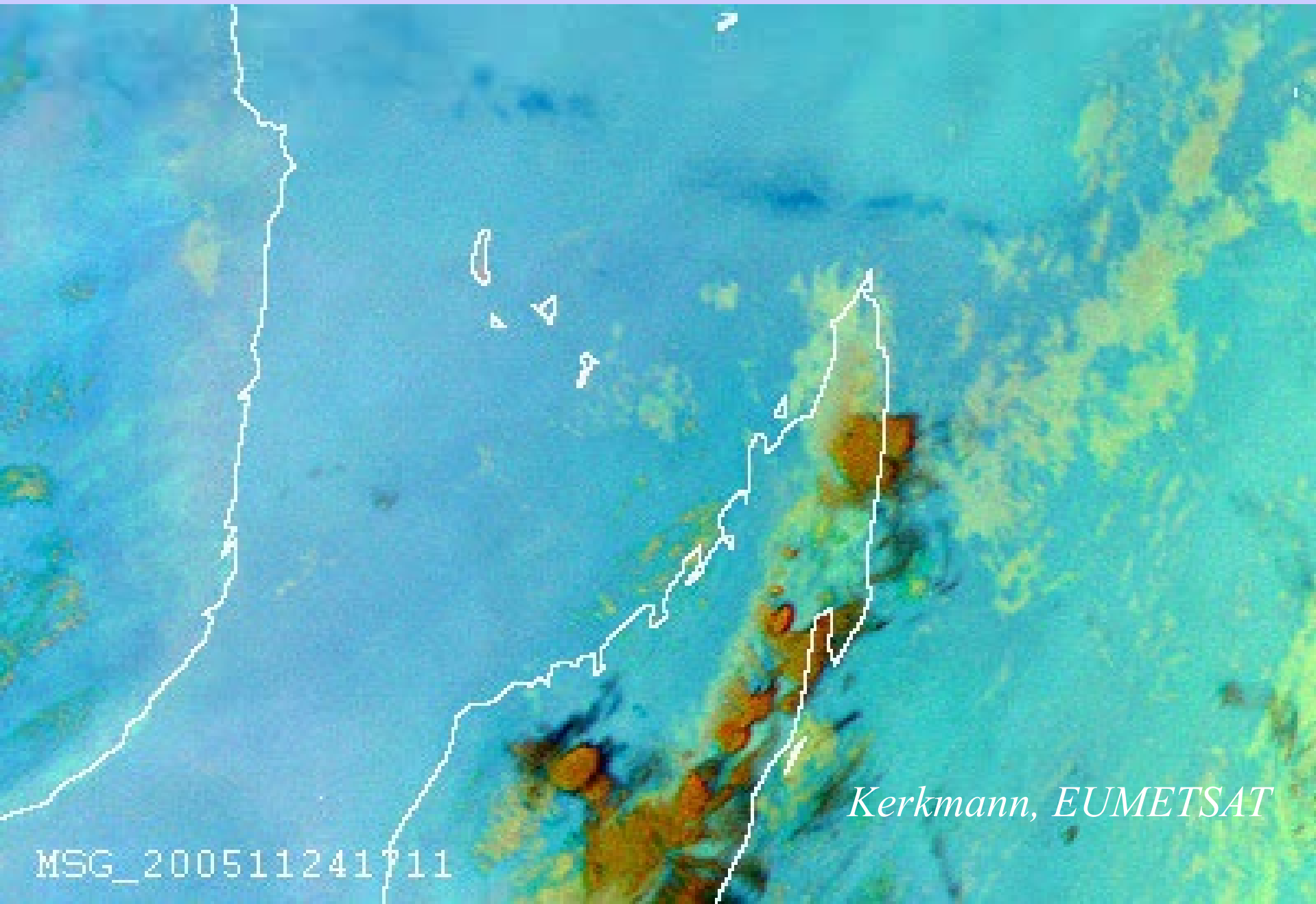
With emphasis on ash clouds ($[BT12-BT11]>0$)

| | |
|---|------------|
| R | -4 to +2 |
| G | -4 to +5 |
| B | 243 to 303 |

SEVIRI sees dust storm over Africa

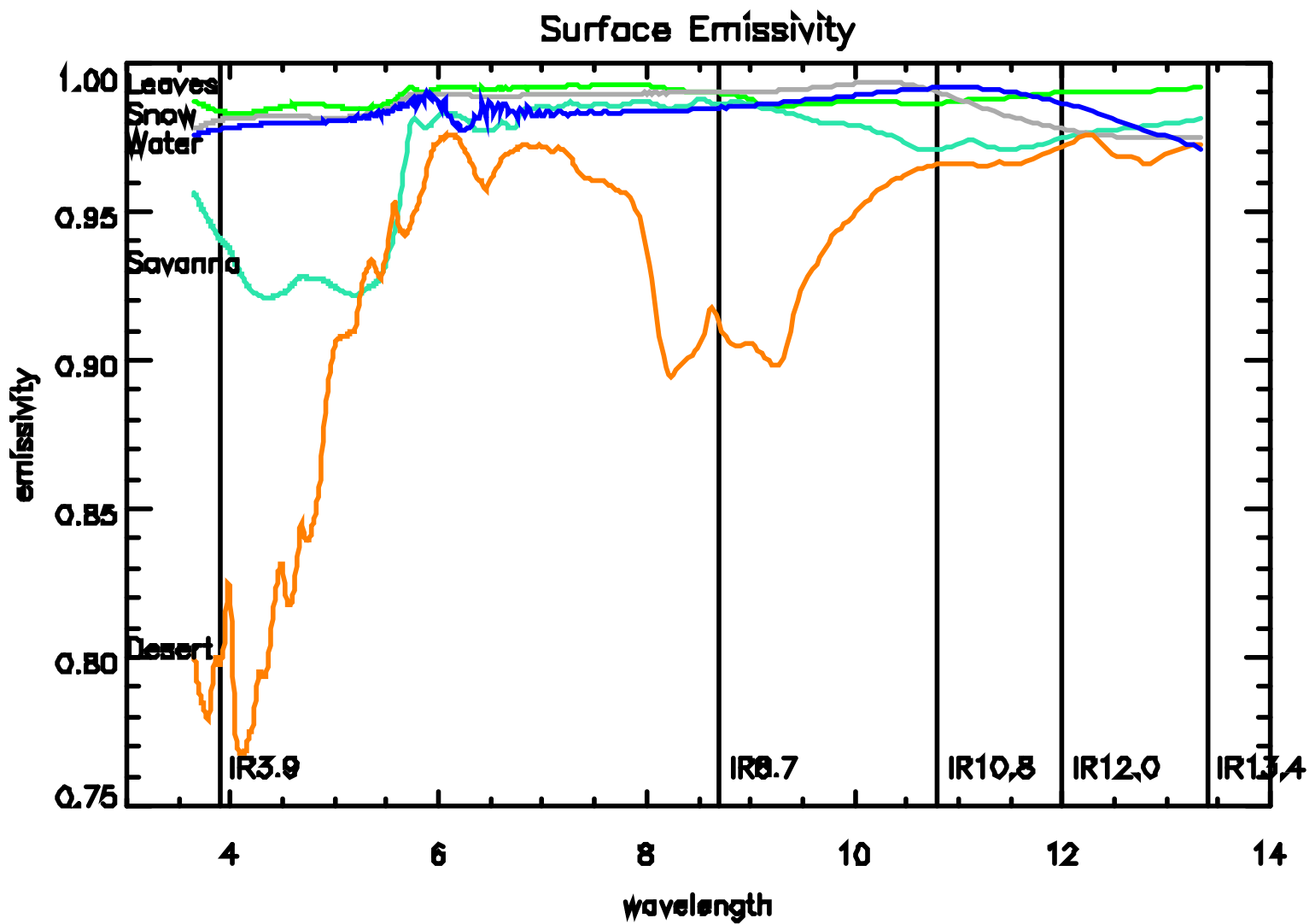


SEVIRI sees volcanic ash & SO₂ and downwind inhibition of convection



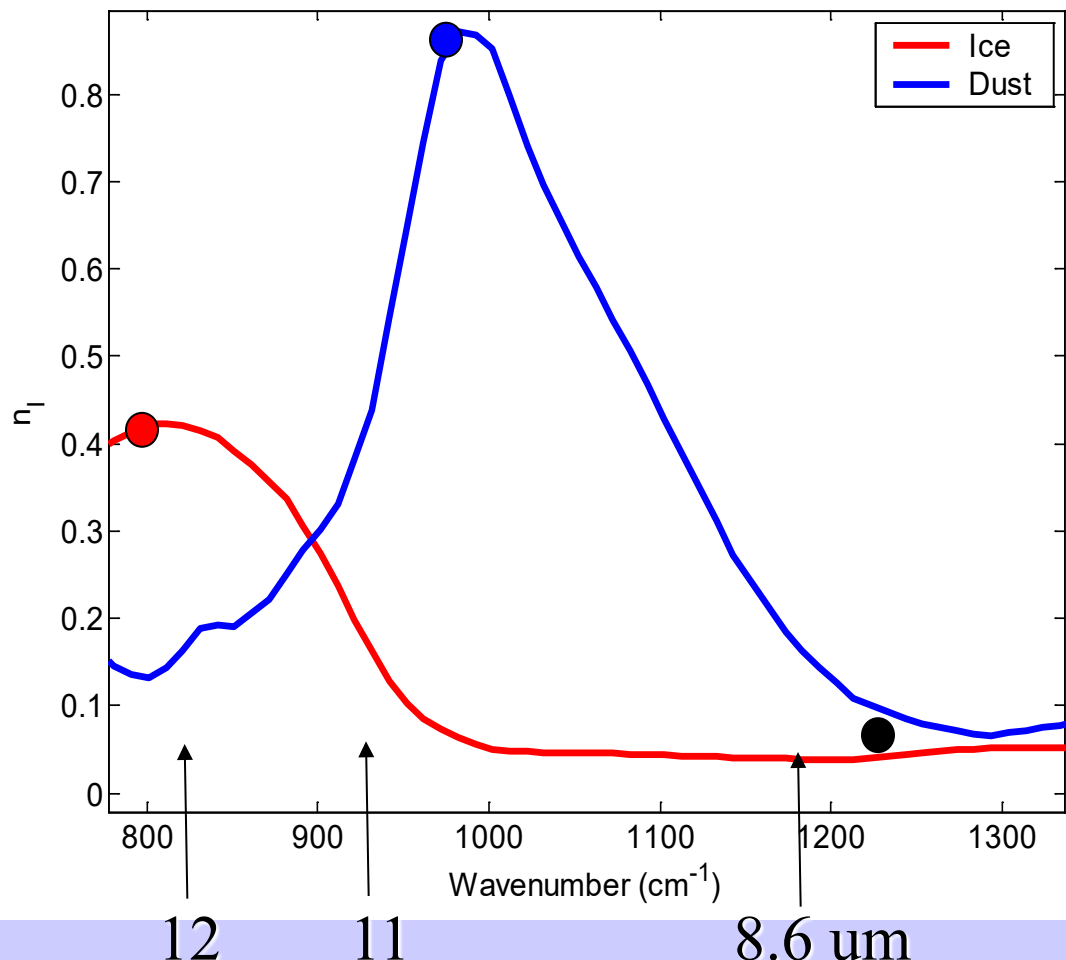
Kerkmann, EUMETSAT

MSG_200511241711



Dust and Cirrus Signals

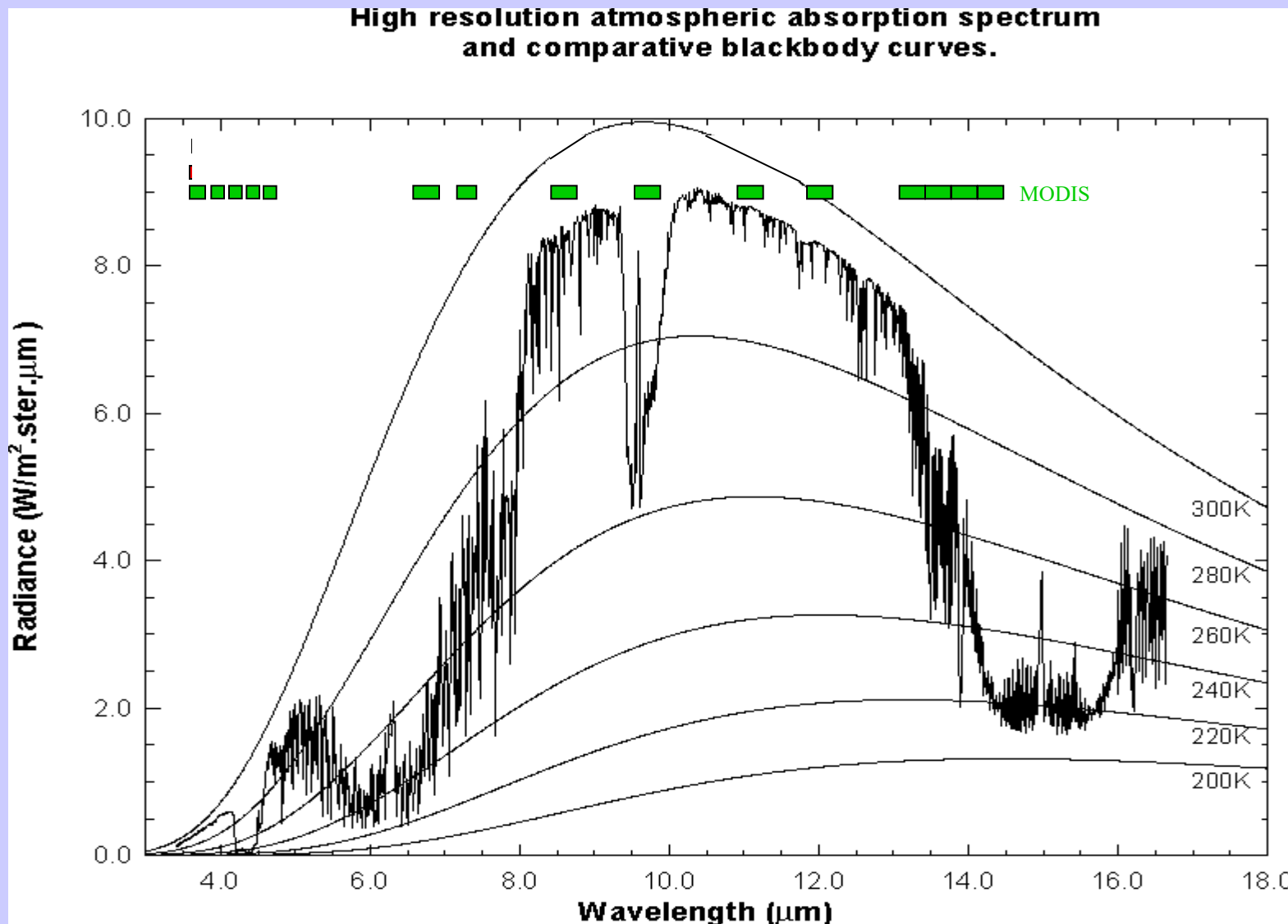
Imaginary Index of Refraction of Ice and Dust



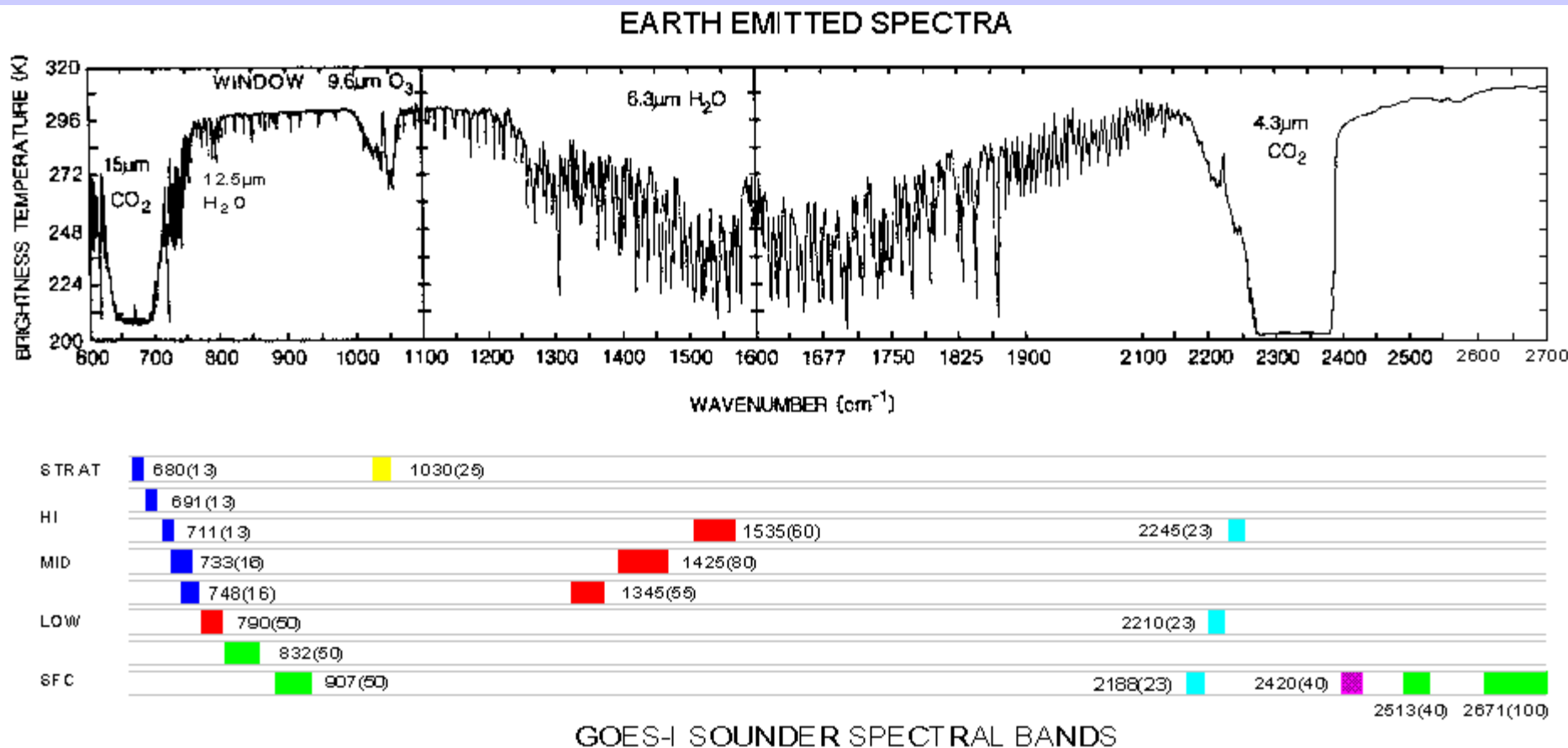
- Both ice and silicate absorption small in 1200 cm^{-1} window
- In the $800\text{-}1000 \text{ cm}^{-1}$ atmospheric window:
 - Silicate index *increases*
 - Ice index *decreases* with wavenumber

Volz, F.E. : Infrared optical constant of ammonium sulphate, Sahara Dust, volcanic pumice and flash, Appl Optics **12** 564-658 (1973)

MODIS IR Spectral Bands

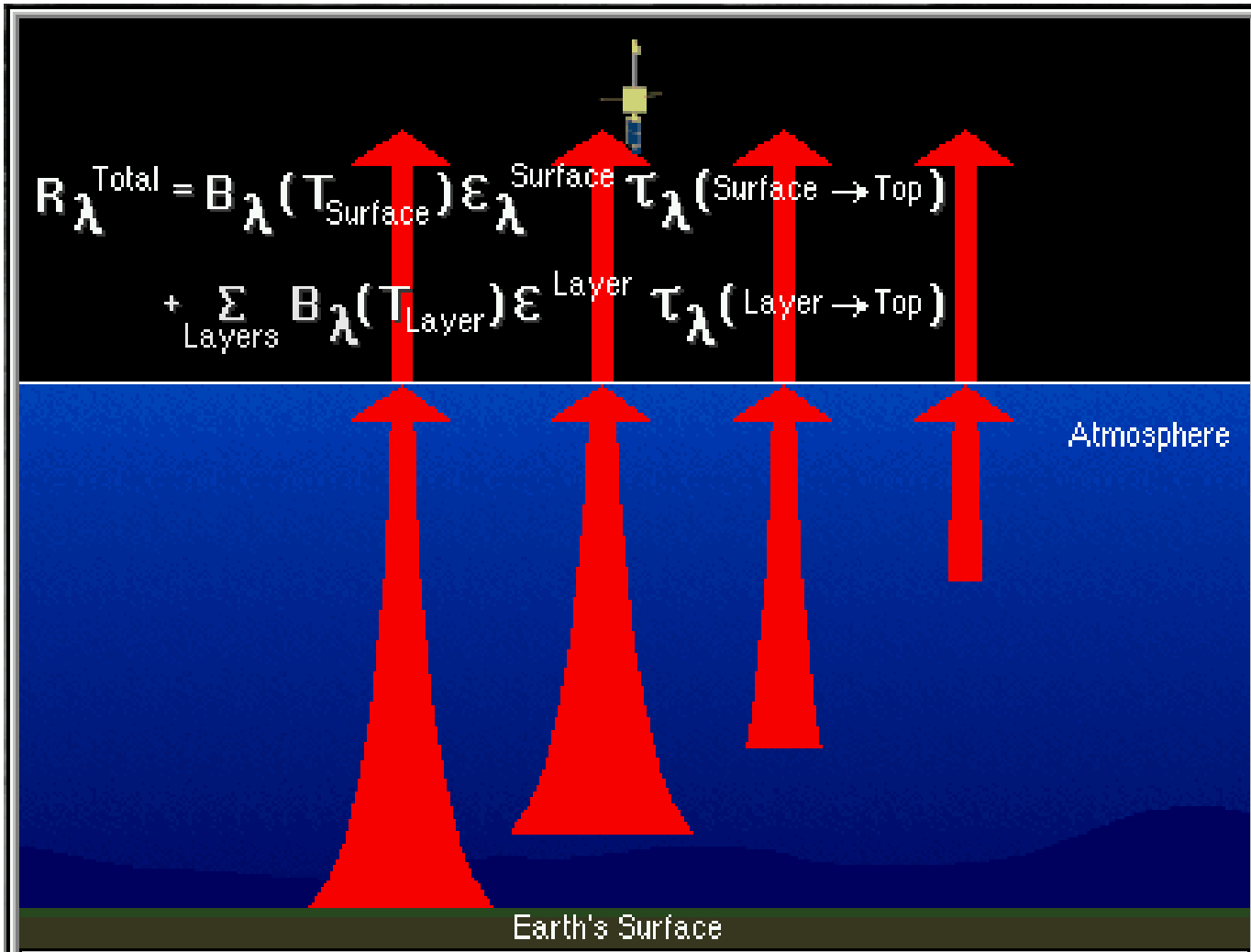


GOES Sounder Spectral Bands: 14.7 to 3.7 um and vis

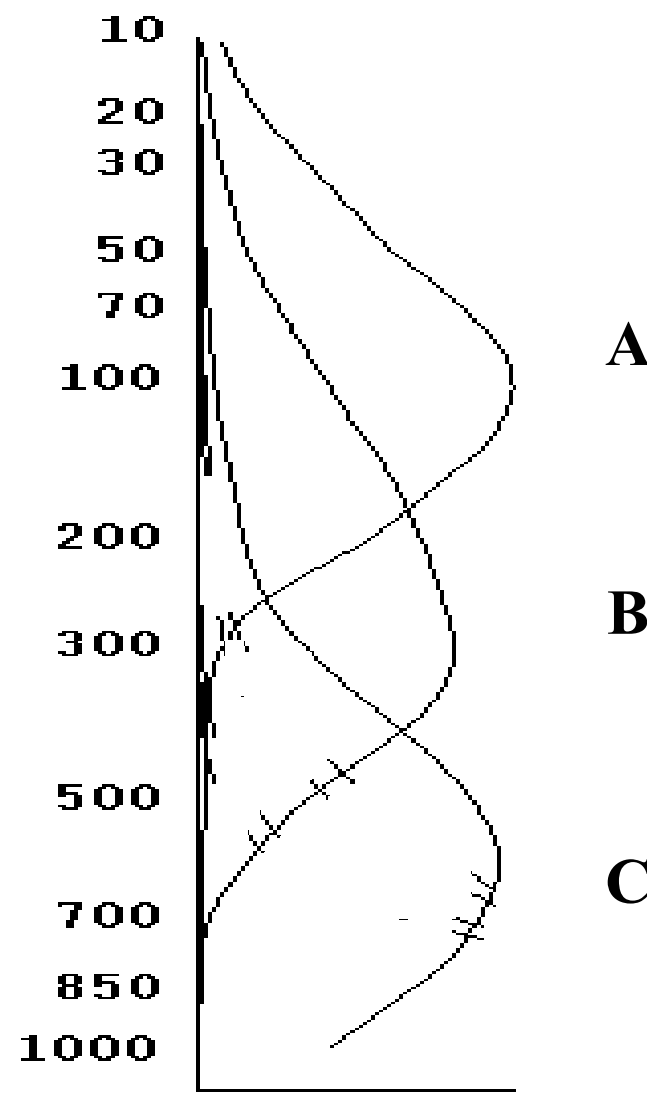
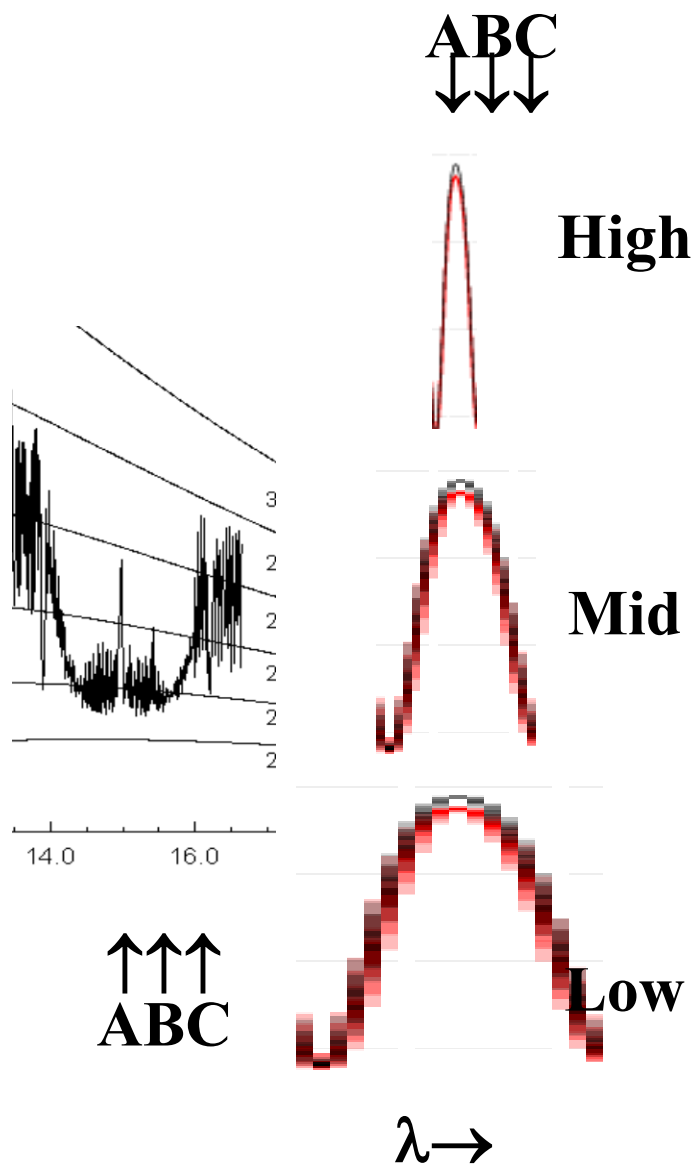


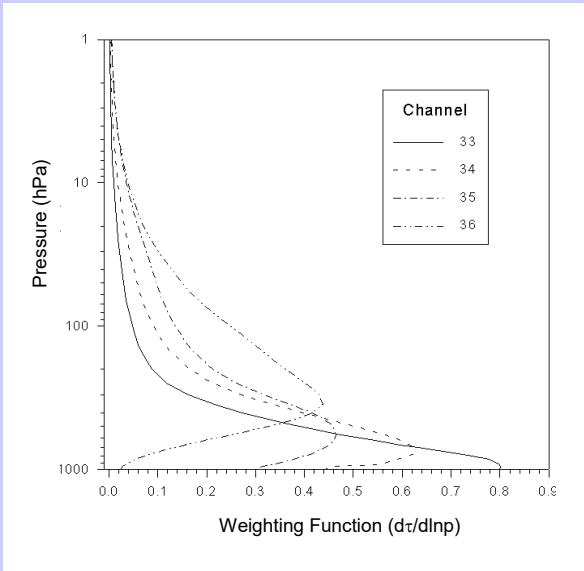
COOPERATIVE INSTITUTE FOR METEOROLOGICAL SATELLITE STUDIES

Radiative Transfer through the Atmosphere

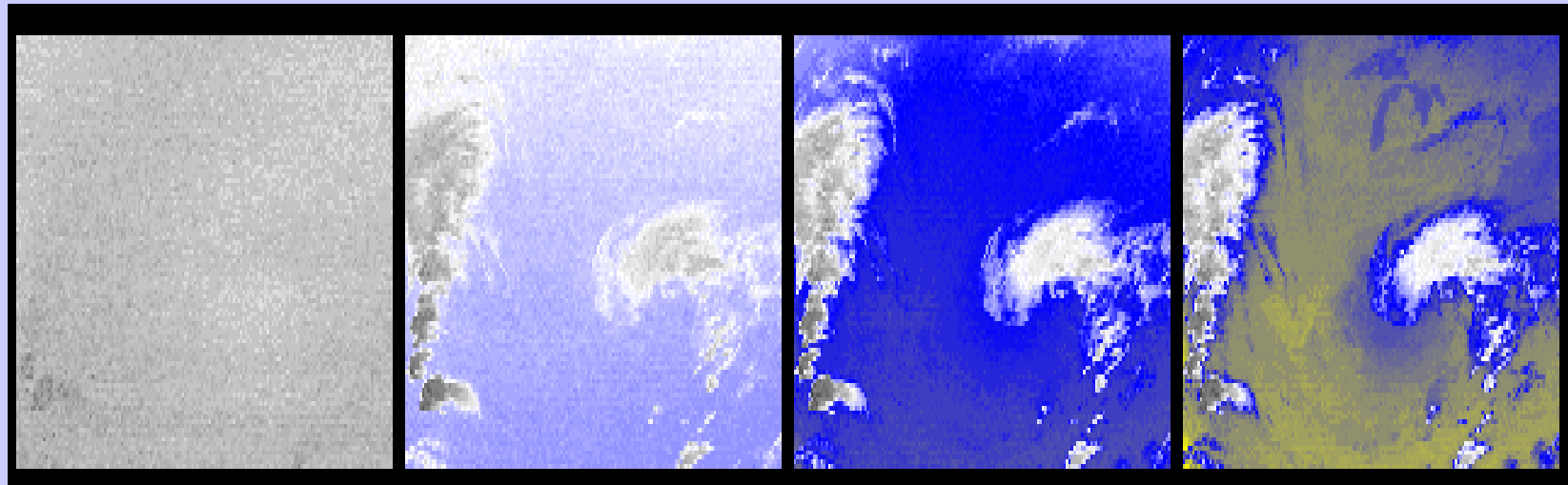


line broadening with pressure helps to explain weighting functions





**CO₂ channels see different layers
in the atmosphere**



14.2 um

13.9 um

13.6 um

13.3 um

Radiative Transfer Equation

When reflection from the earth surface is also considered, the RTE for infrared radiation can be written

$$I_\lambda = \varepsilon_\lambda^{\text{sfc}} B_\lambda(T_s) \tau_\lambda(p_s) + \int_{p_s}^0 B_\lambda(T(p)) F_\lambda(p) [d\tau_\lambda(p)/dp] dp$$

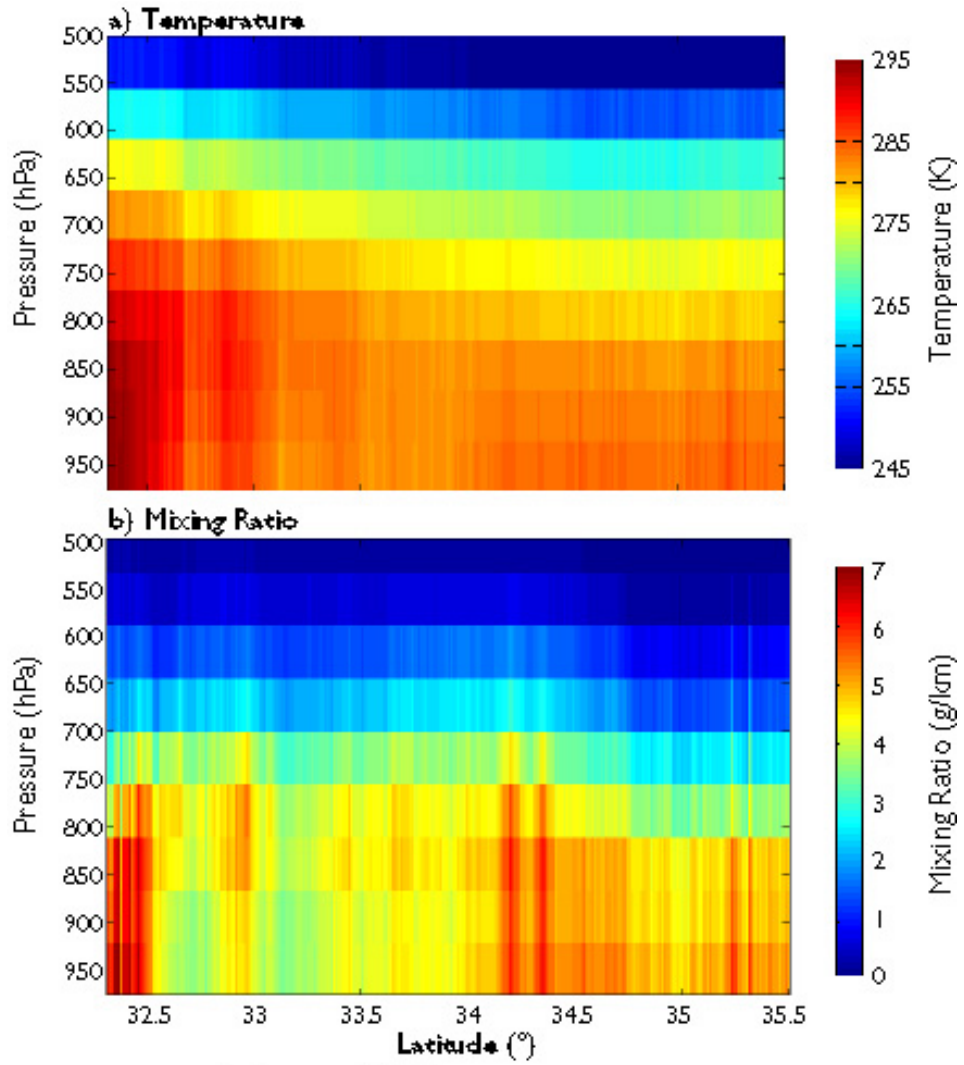
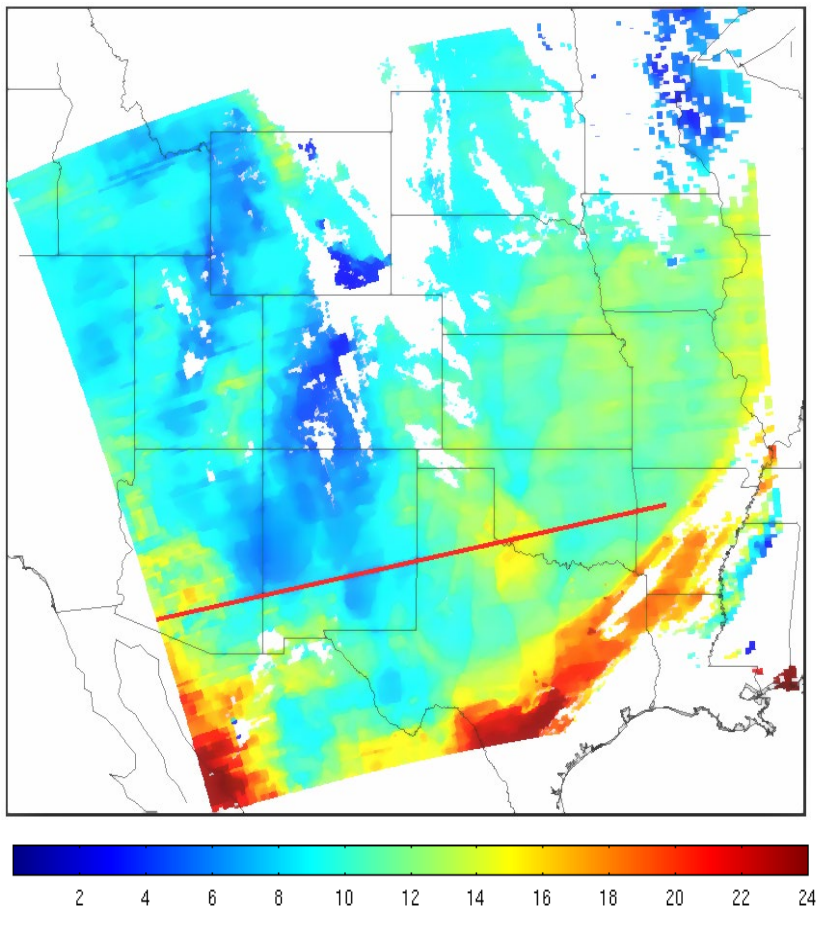
where

$$F_\lambda(p) = \{ 1 + (1 - \varepsilon_\lambda) [\tau_\lambda(p_s) / \tau_\lambda(p)]^2 \}$$

The first term is the spectral radiance emitted by the surface and attenuated by the atmosphere, often called the boundary term and the second term is the spectral radiance emitted to space by the atmosphere directly or by reflection from the earth surface.

The atmospheric contribution is the weighted sum of the Planck radiance contribution from each layer, where the weighting function is $[d\tau_\lambda(p)/dp]$. This weighting function is an indication of where in the atmosphere the majority of the radiation for a given spectral band comes from.

MODIS TPW



Clear sky layers of temperature and moisture on 2 June 2001

RTE in Cloudy Conditions

$$I_\lambda = \eta \underset{\lambda}{\int} I_{\lambda}^{cd} + (1 - \eta) \underset{\lambda}{\int} I^c \quad \text{where } cd = \text{cloud, } c = \text{clear, } \eta = \text{cloud fraction}$$

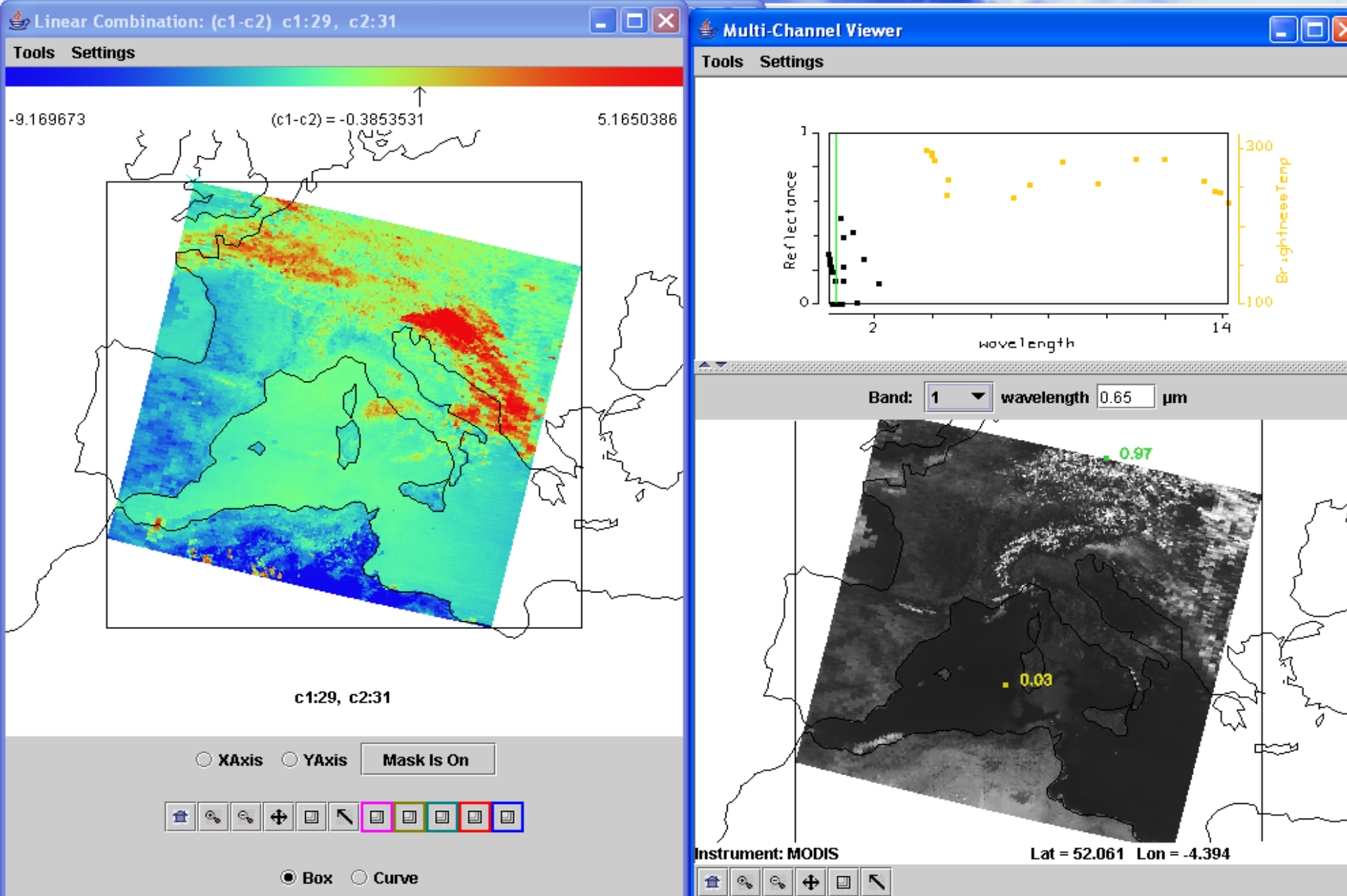
$$I^c = B_\lambda(T_s) \tau_\lambda(p_s) + \int_{p_s}^0 B_\lambda(T(p)) d\tau_\lambda .$$

$$\begin{aligned} \underset{\lambda}{\int} I_{\lambda}^{cd} &= (1 - \varepsilon_\lambda) B_\lambda(T_s) \tau_\lambda(p_s) + (1 - \varepsilon_\lambda) \int_{p_s}^{p_c} B_\lambda(T(p)) d\tau_\lambda \\ &\quad + \varepsilon_\lambda B_\lambda(T(p_c)) \tau_\lambda(p_c) + \int_{p_c}^0 B_\lambda(T(p)) d\tau_\lambda \end{aligned}$$

ε_λ is emittance of cloud. First two terms are from below cloud, third term is cloud contribution, and fourth term is from above cloud. After rearranging

$$I_\lambda - I_\lambda^c = \eta \varepsilon_\lambda \int_{p_s}^{p_c} \tau(p) \frac{dB_\lambda}{dp} dp .$$

Techniques for dealing with clouds fall into three categories: (a) searching for cloudless fields of view, (b) specifying cloud top pressure and sounding down to cloud level as in the cloudless case, and (c) employing adjacent fields of view to determine clear sky signal from partly cloudy observations.



Ice clouds are revealed with BT8.6-BT11>0 & water clouds and fog show in r0.65

Cloud Properties

RTE for cloudy conditions indicates dependence of cloud forcing (observed minus clear sky radiance) on cloud amount ($\eta\varepsilon_\lambda$) and cloud top pressure (p_c)

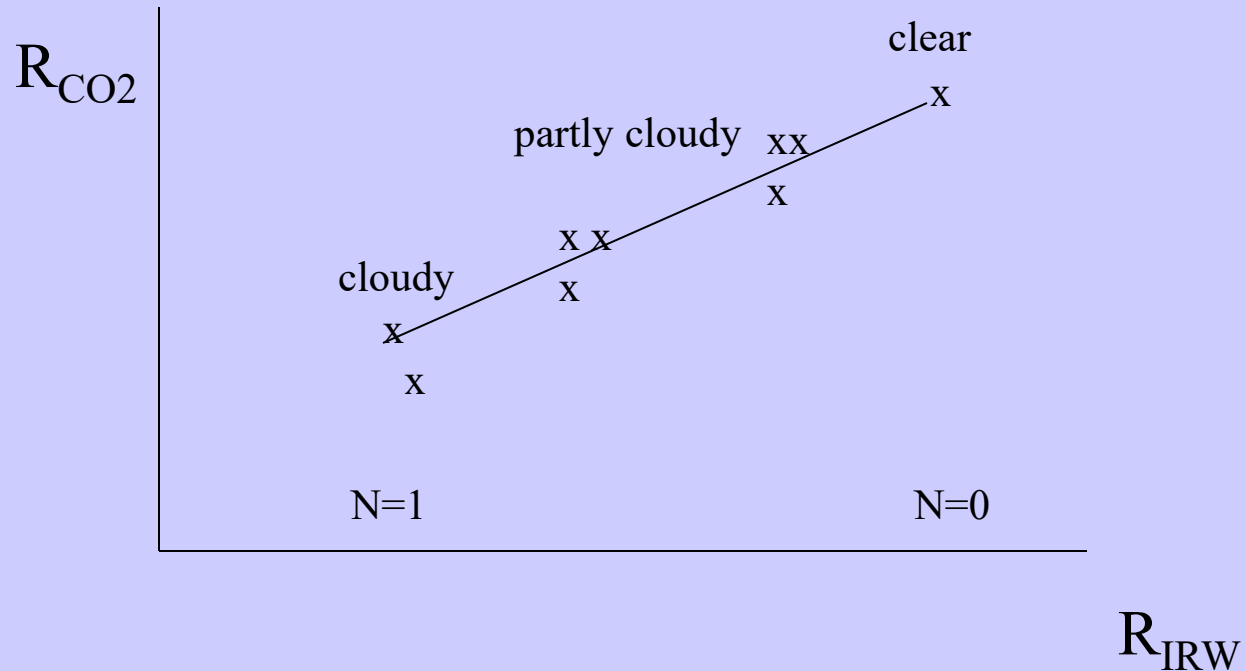
$$(I_\lambda - I_\lambda^{\text{clr}}) = \eta\varepsilon_\lambda \int_{p_s}^{p_c} \tau_\lambda dB_\lambda .$$

Higher colder cloud or greater cloud amount produces greater cloud forcing; dense low cloud can be confused for high thin cloud. Two unknowns require two equations.

p_c can be inferred from radiance measurements in two spectral bands where cloud emissivity is the same. $\eta\varepsilon_\lambda$ is derived from the infrared window, once p_c is known. This is the essence of the CO₂ slicing technique.

Cloud Clearing

For a single layer of clouds, radiances in one spectral band vary linearly with those of another as cloud amount varies from one field of view (fov) to another



Clear radiances can be inferred by extrapolating to cloud free conditions.

Moisture

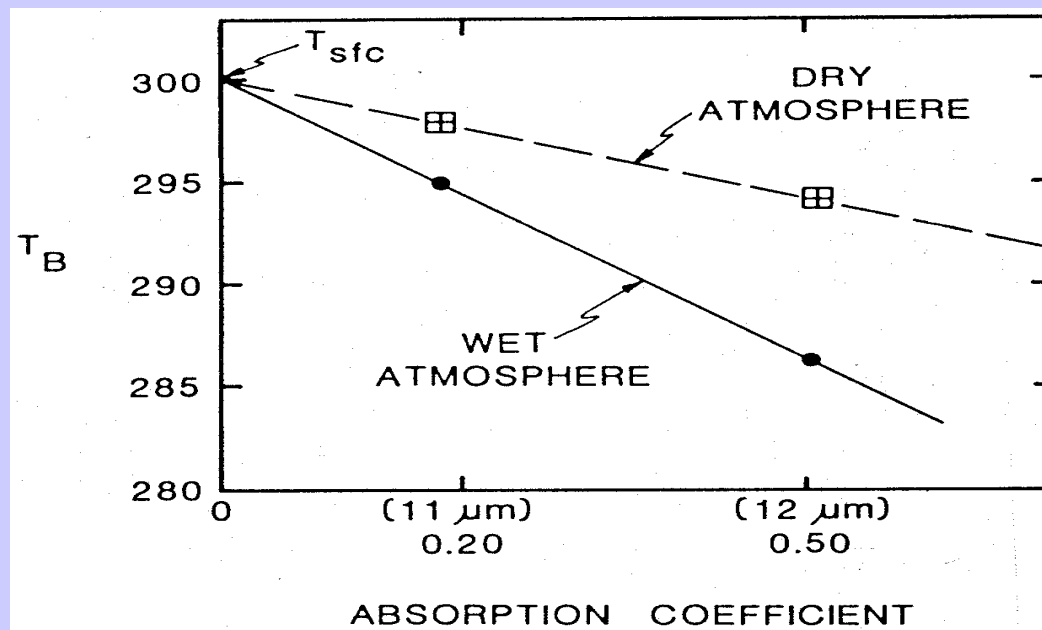
Moisture attenuation in atmospheric windows varies linearly with optical depth.

$$- k_\lambda u$$

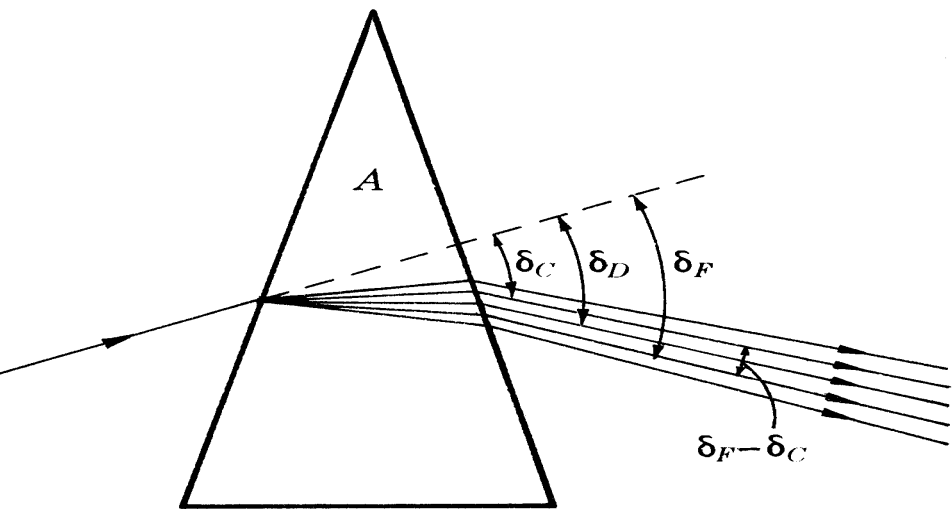
$$\tau_\lambda = e^{-k_\lambda u} = 1 - k_\lambda u$$

For same atmosphere, deviation of brightness temperature from surface temperature is a linear function of absorbing power. Thus moisture corrected SST can inferred by using split window measurements and extrapolating to zero k_λ

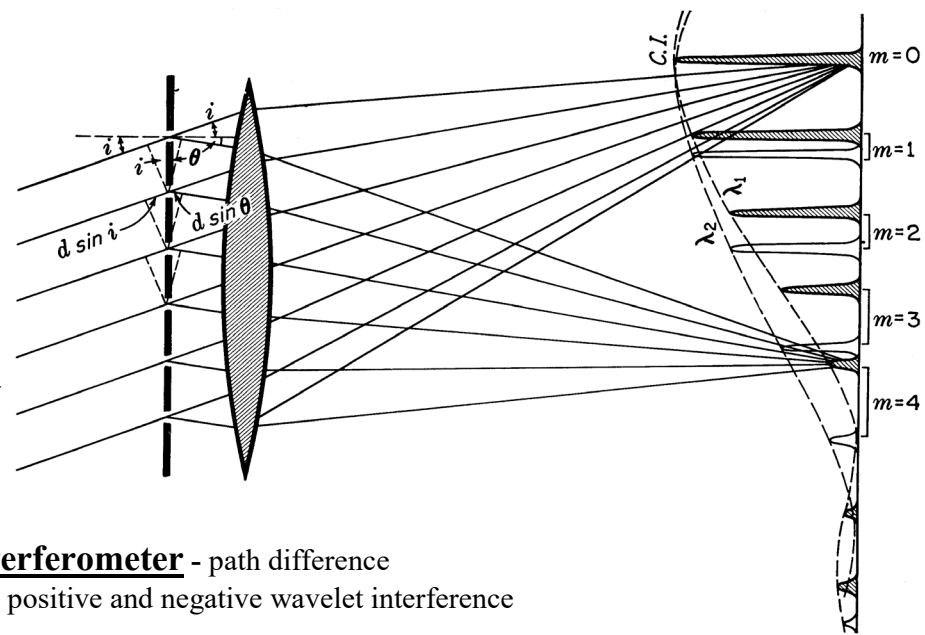
Moisture content of atmosphere inferred from slope of linear relation.



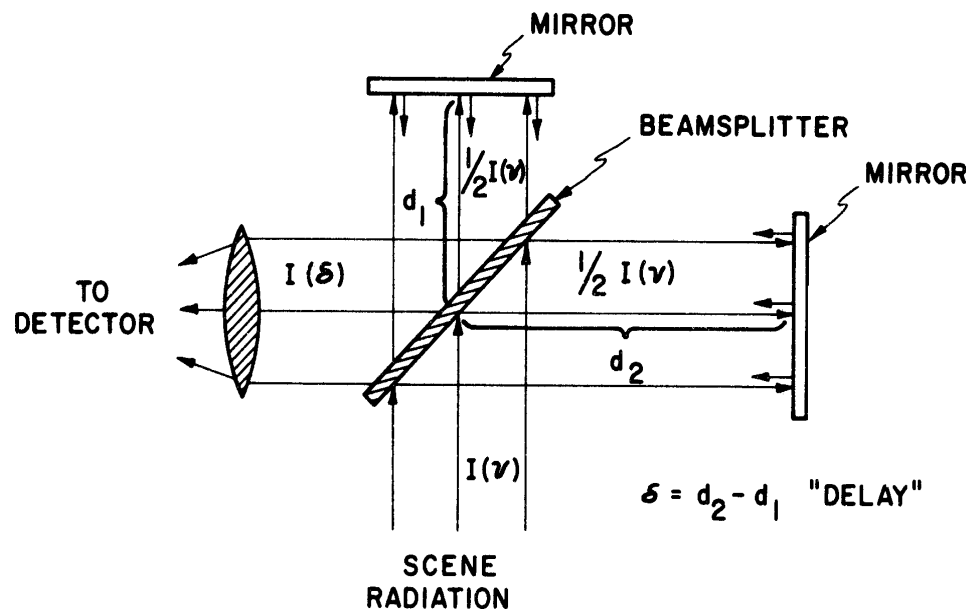
Spectral Separation with a Prism: longer wavelengths deflected less



Spectral Separation with a Grating: path difference from slits produces positive and negative wavelet interference on screen

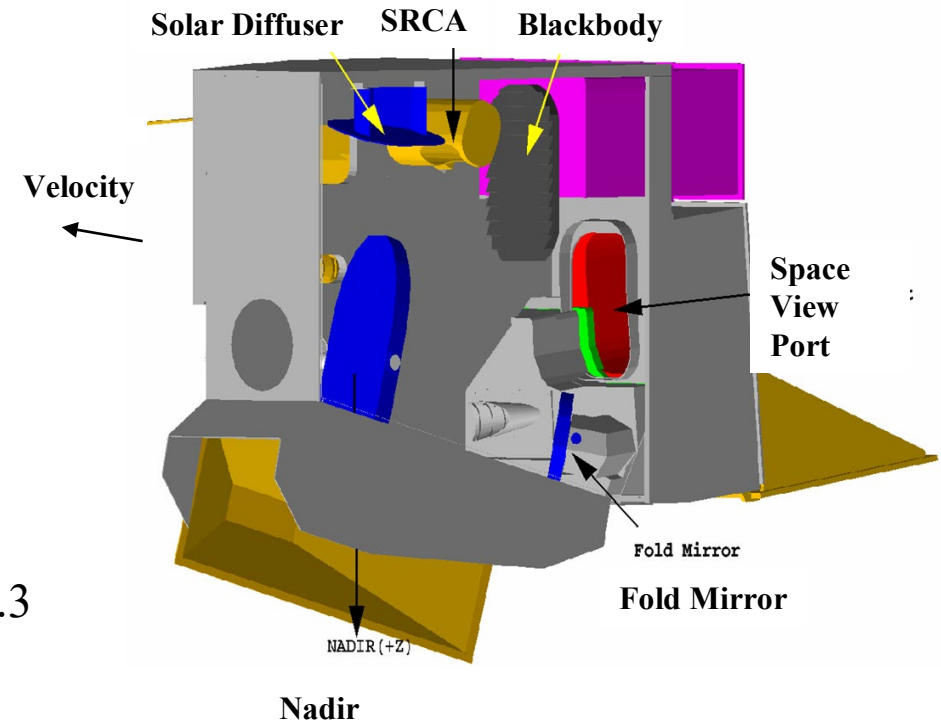


Spectral Separation with an Interferometer - path difference (or delay) from two mirrors produces positive and negative wavelet interference

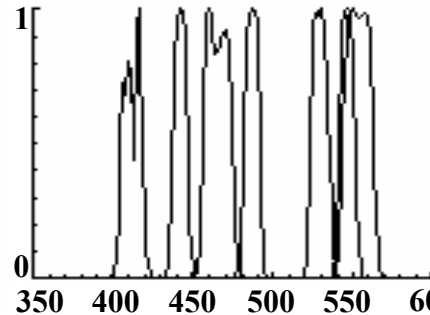


MODIS Instrument Overview

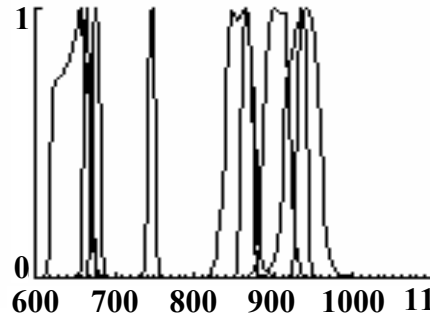
- 36 spectral bands (490 detectors) cover wavelength range from 0.4 to 14.5 μm
- Spatial resolution at nadir: 250m (2 bands), 500m (5 bands) and 1000m
- 4 FPAs: VIS, NIR, SMIR, LWIR
- On-Board Calibrators: SD/SDSM, SRCA, and BB (plus space view)
- 12 bit (0-4095) dynamic range
- 2-sided Paddle Wheel Scan Mirror scans 2330 km swath in 1.47 sec
- Day data rate = 10.6 Mbps; night data rate = 3.3 Mbps (100% duty cycle, 50% day and 50% night)



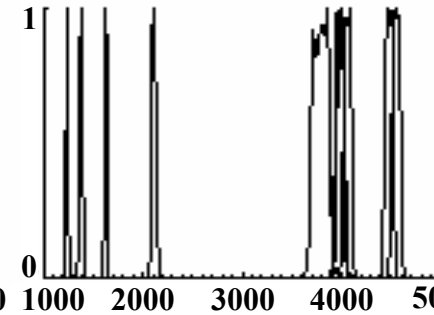
VIS



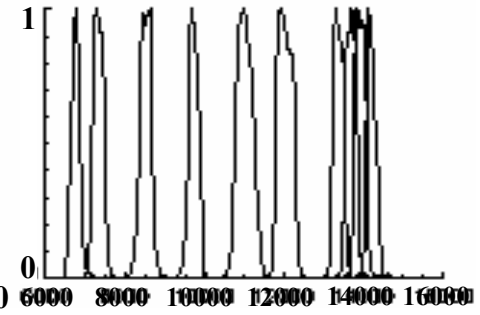
NIR



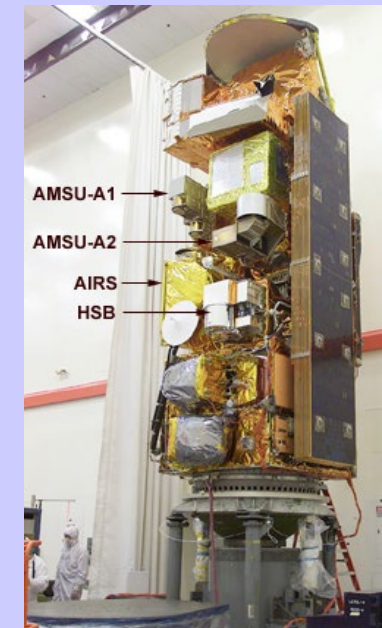
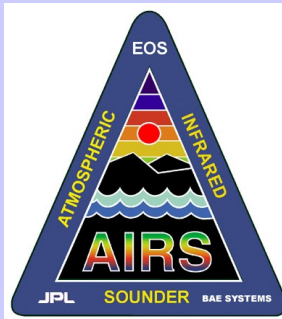
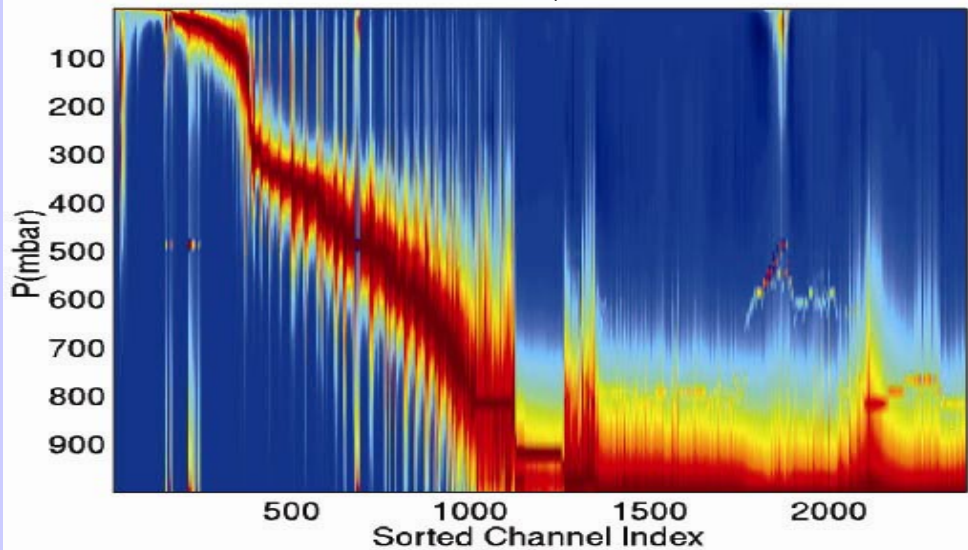
S/MWIR



LWIR



temperature weighting functions sorted by pressure of their peak (blue = 0)



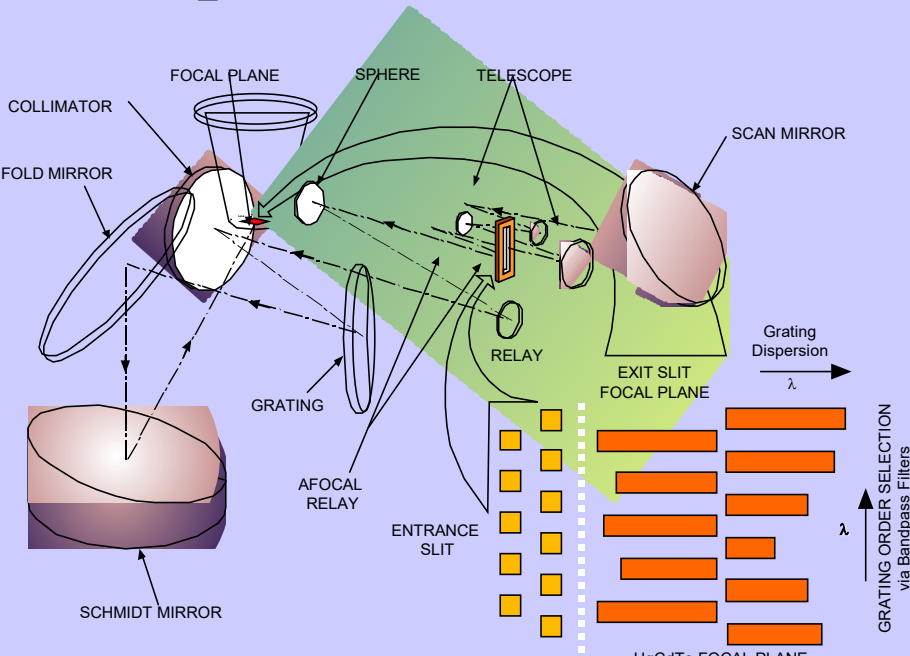
AIRS On Aqua

Instrument

- Hyperspectral radiometer with **resolution of $0.5 - 2 \text{ cm}^{-1}$**
- Extremely well calibrated pre-launch
- **Spectral range: $650 - 2700 \text{ cm}^{-1}$**
- Associated microwave instruments (AMSU, HSB)

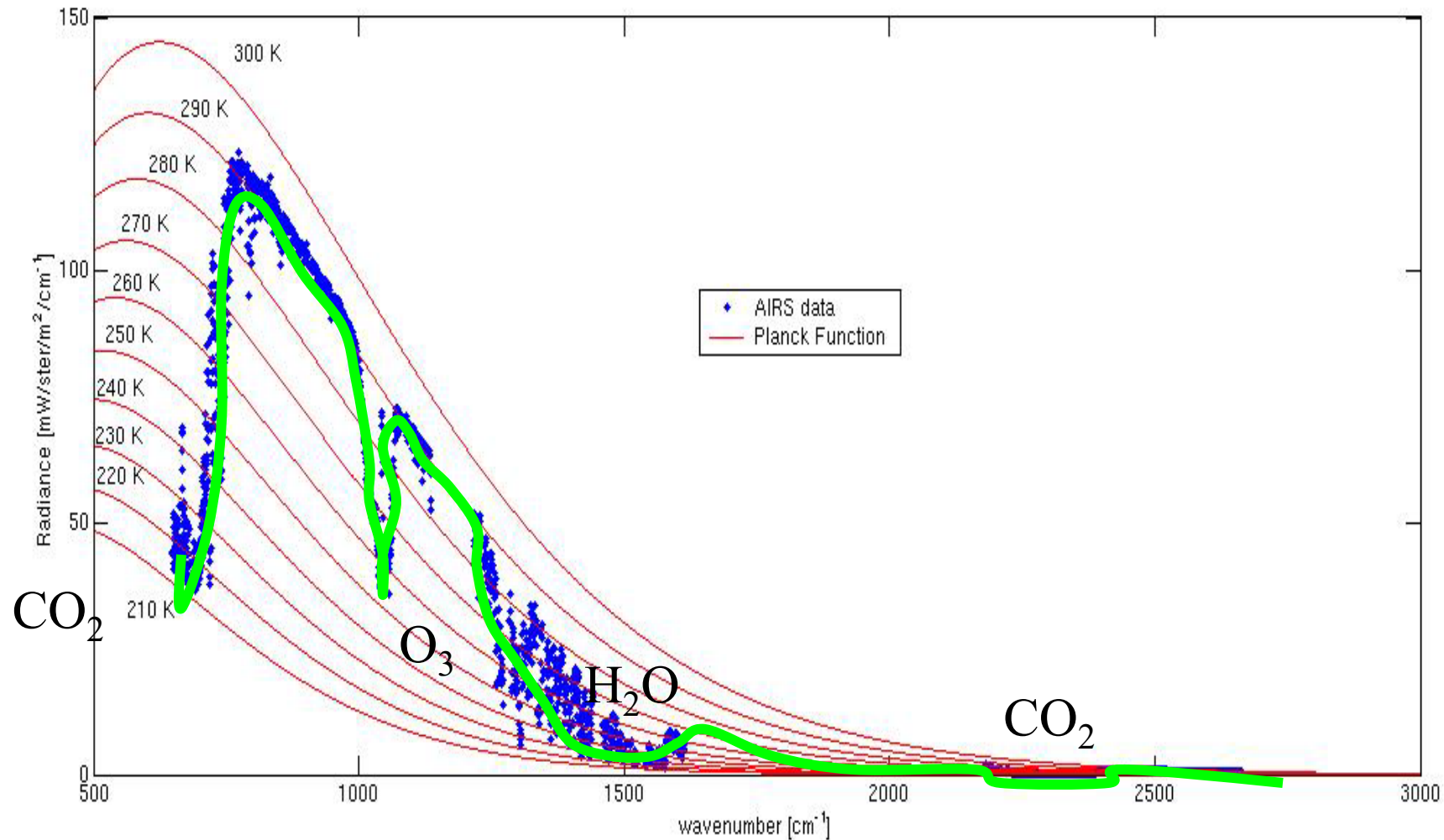
Design

- Grating Spectrometer passively cooled to 160K, stabilized to 30 mK
- **PV and PC HdCdTe focal plane cooled to 60K** with redundant active pulse tube cryogenic coolers
- **Focal plane has ~5000 detectors**, 2378 channels. PV detectors (all below 13 microns) are doubly redundant. Two channels per resolution element ($n/D_n = 1200$)
- 310 K Blackbody and space view provides radiometric calibration
- Paralyene coating on calibration mirror and upwelling radiation provides spectral calibration
- **NEDT (per resolution element) ranges from 0.05K to 0.5K**

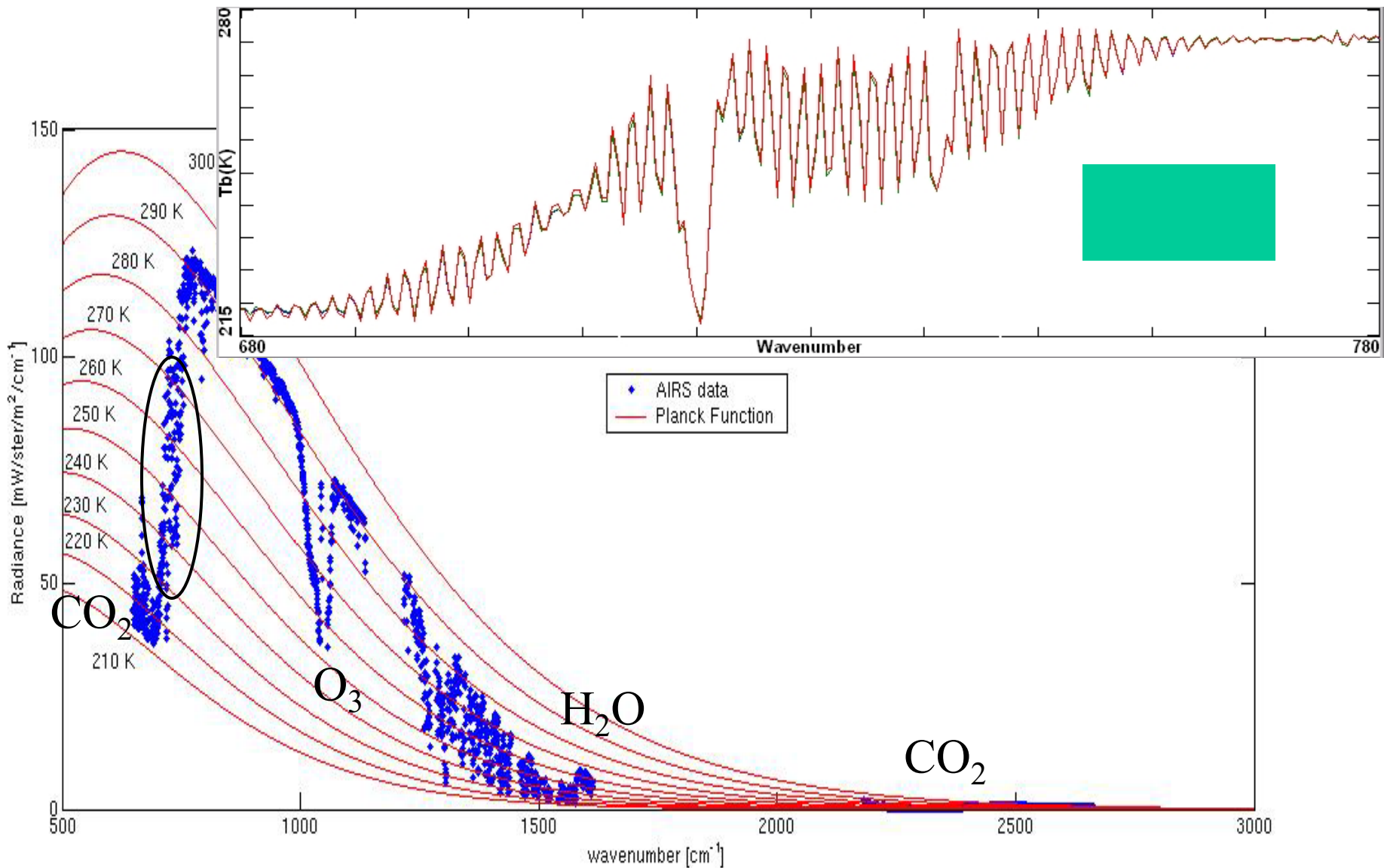


Spectral filters at each entrance slit and over each FPA array isolate color band (grating order) of interest

Vibrational Lines

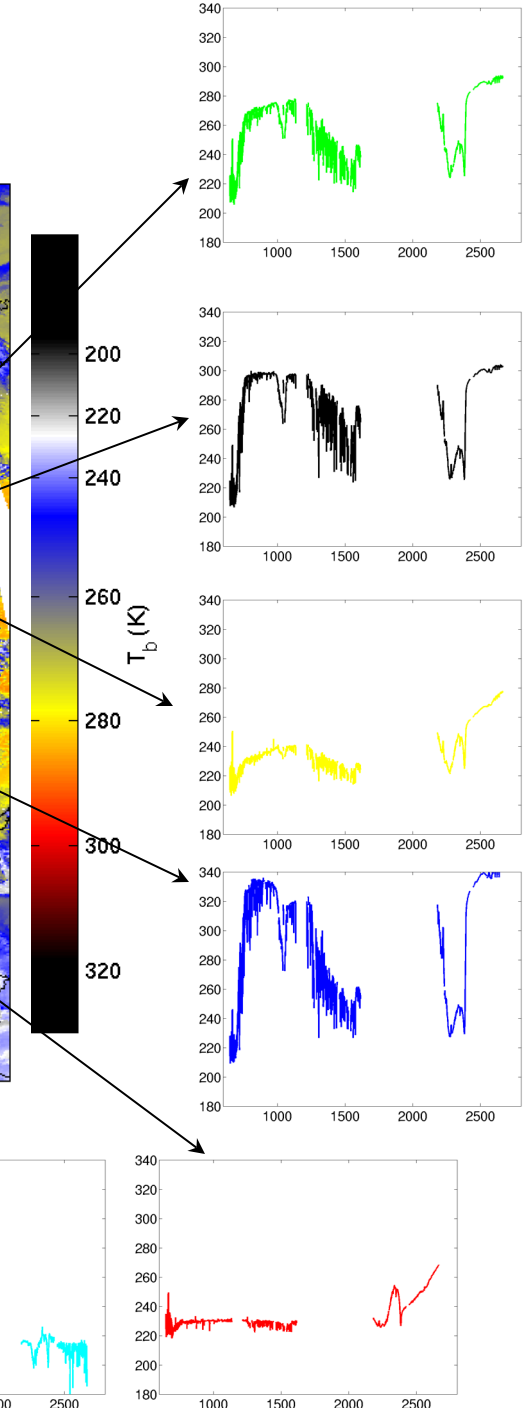
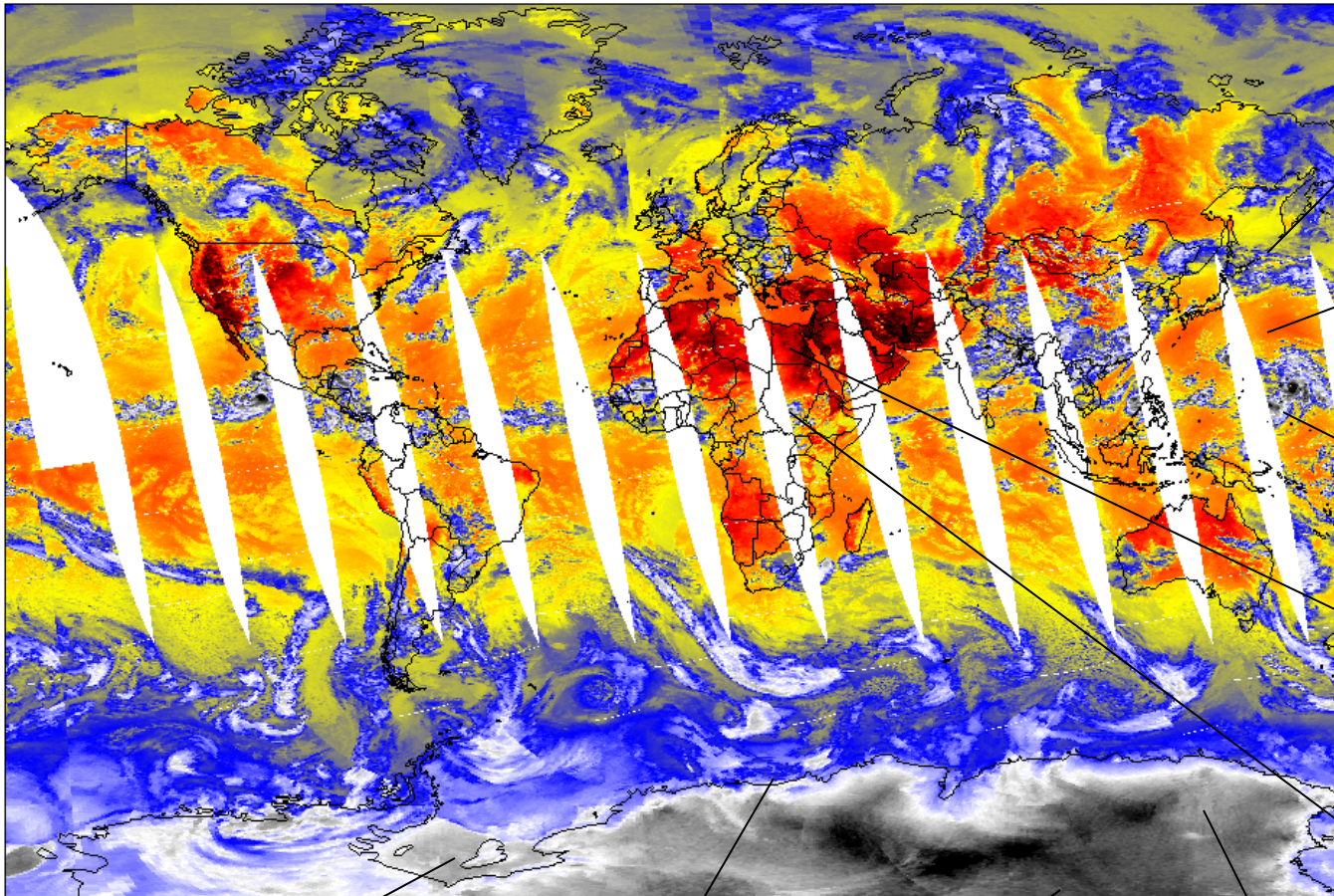


Rotational Lines

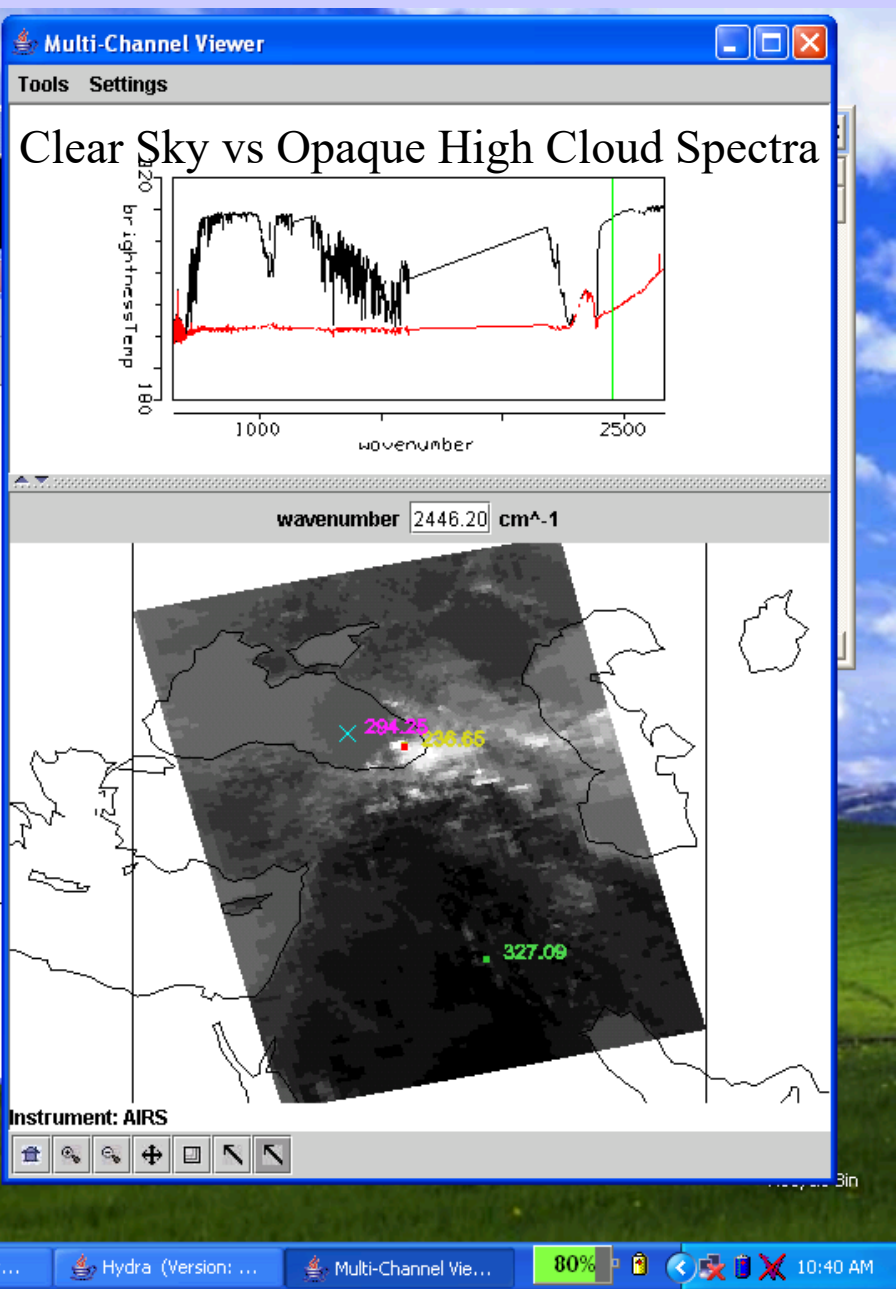
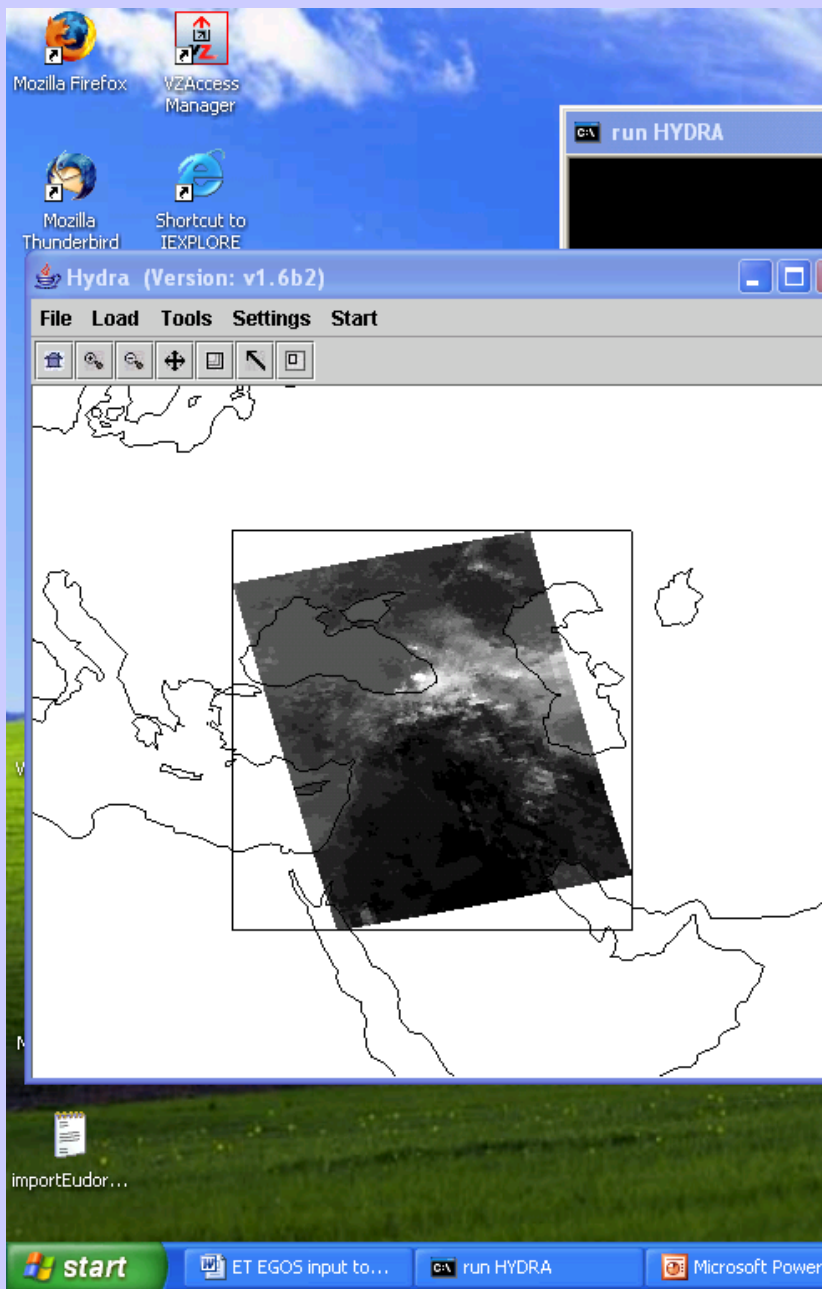


AIRS Spectra from around the Globe

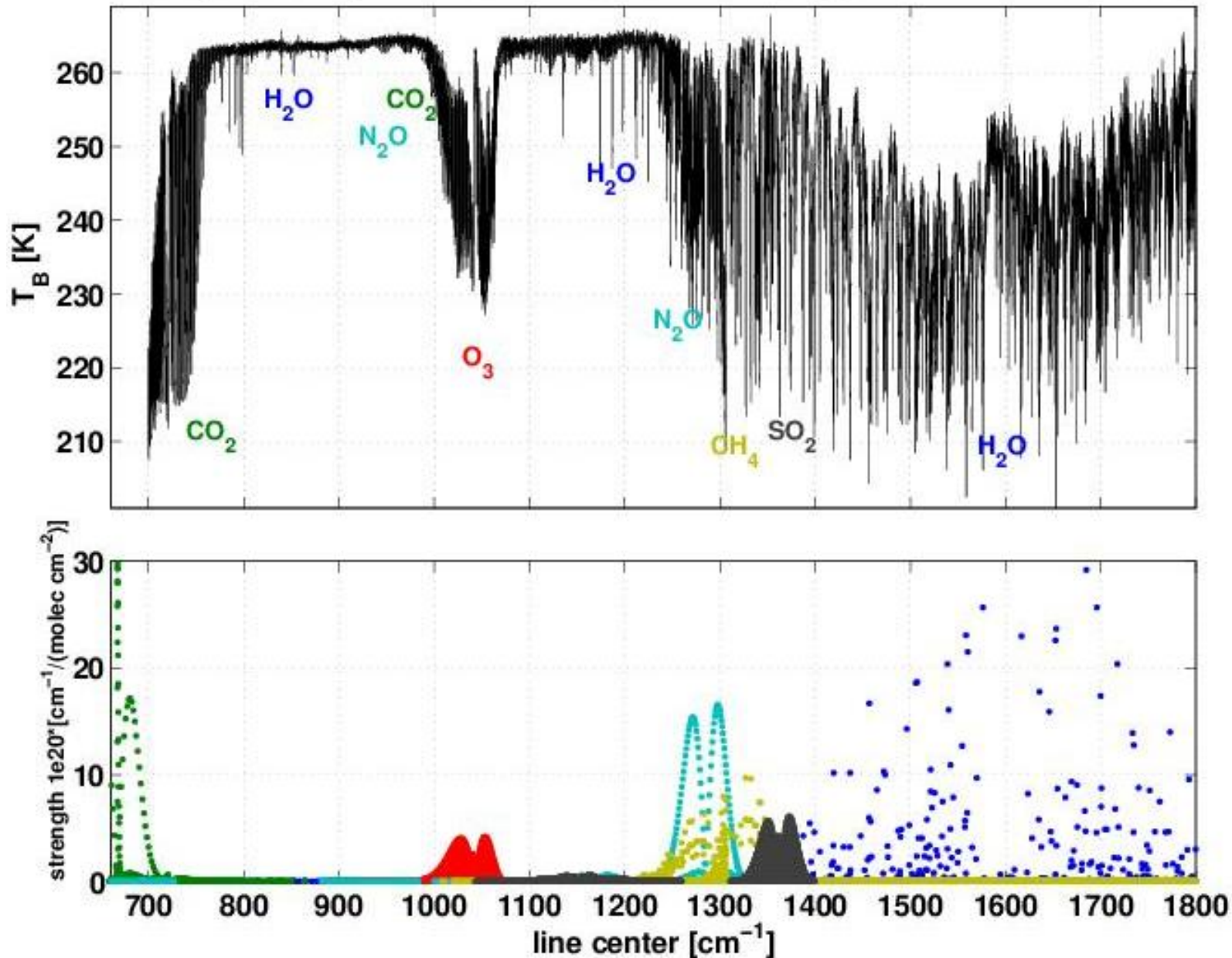
20-July-2002 Ascending LW_Window

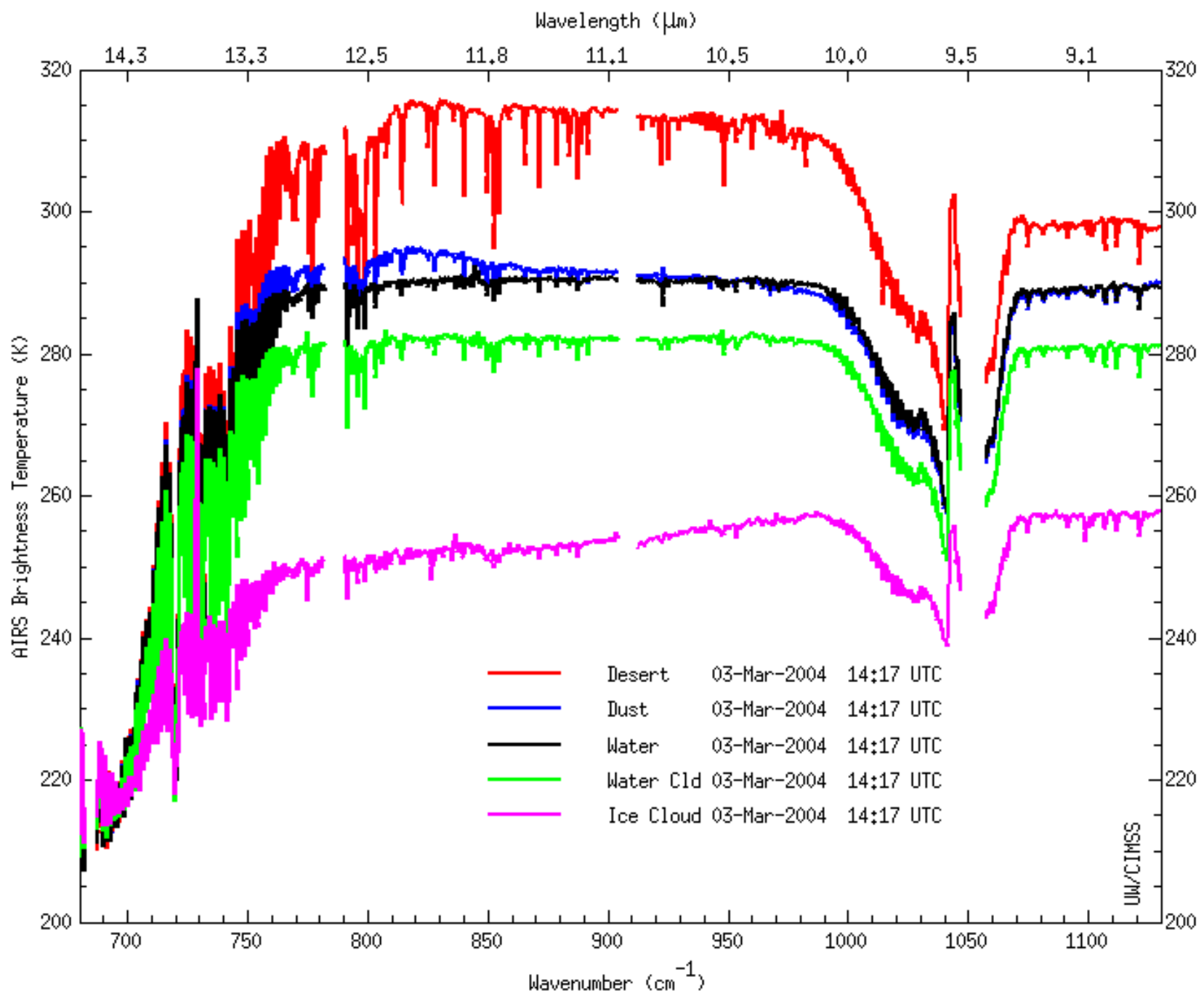


AIRS data from 28 Aug 2005



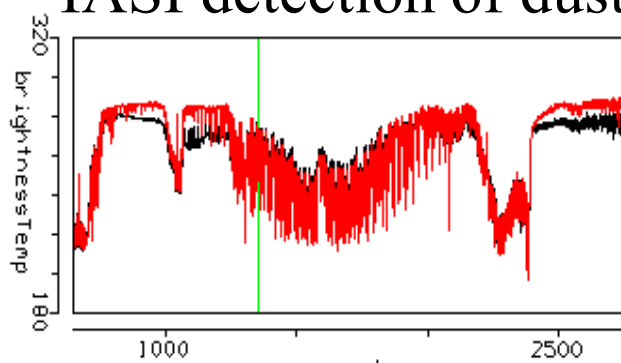
IMG spectrum (WINCE, 970128 over Nebraska) and HITRAN database



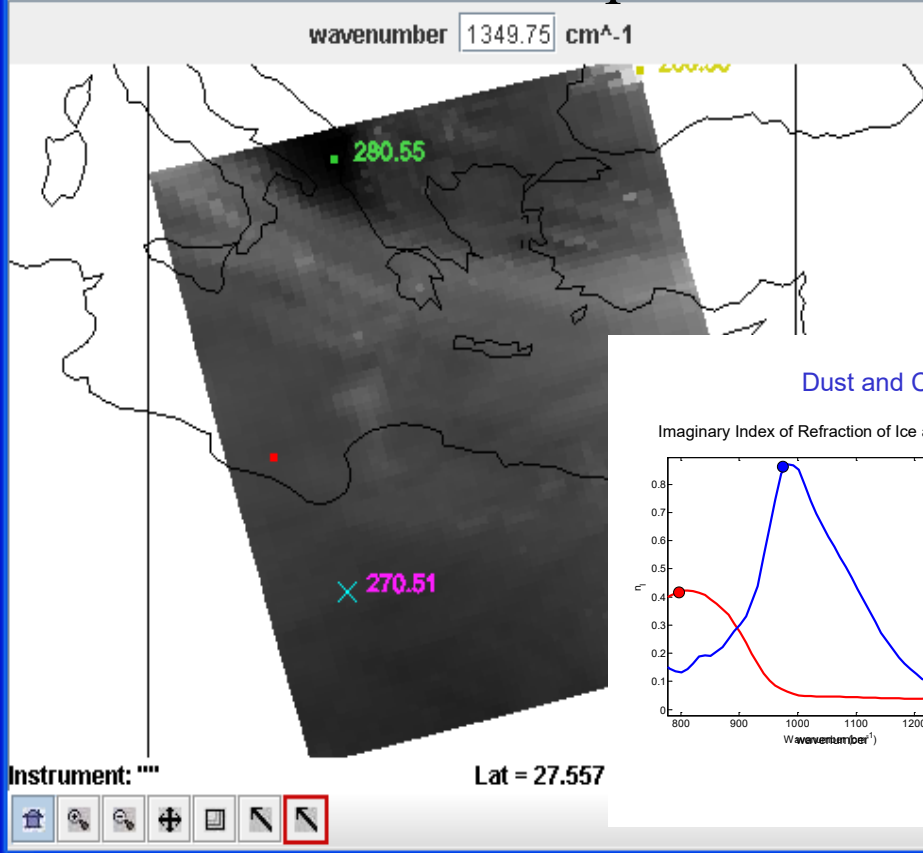


Tools Settings Import

IASI detection of dust

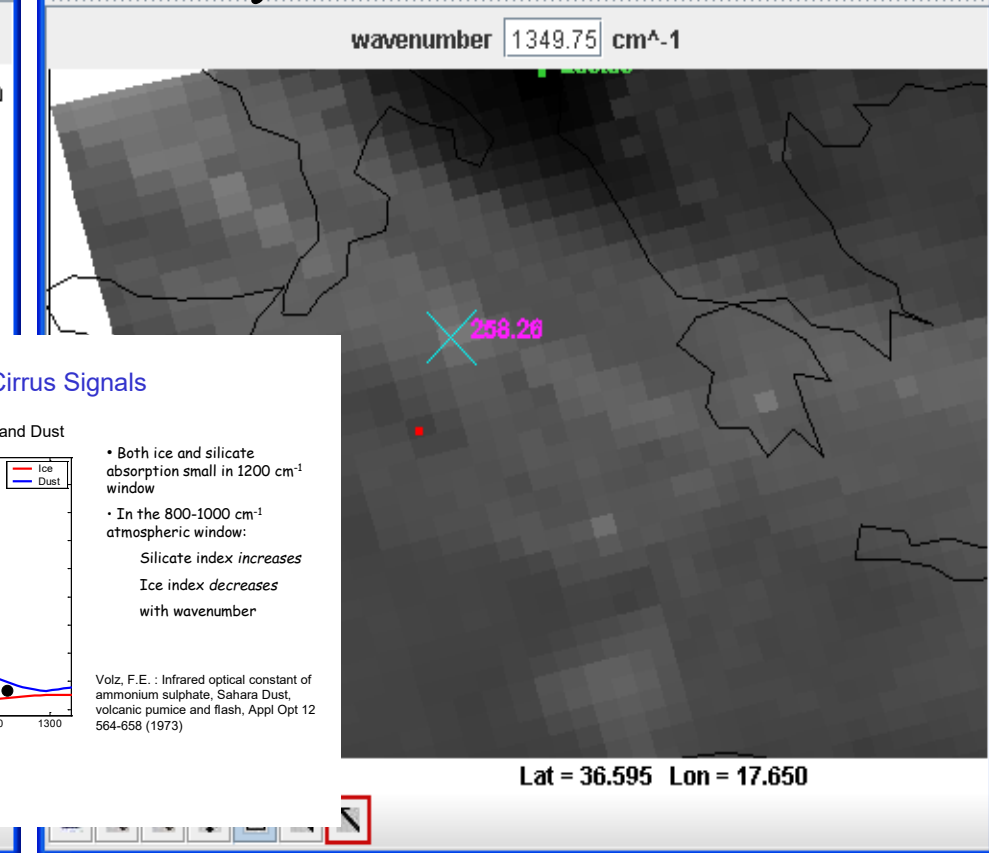
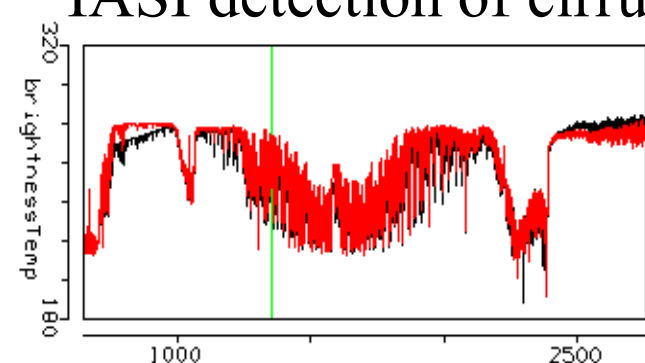


red spectrum is from nearby clear fov



Tools Settings Import

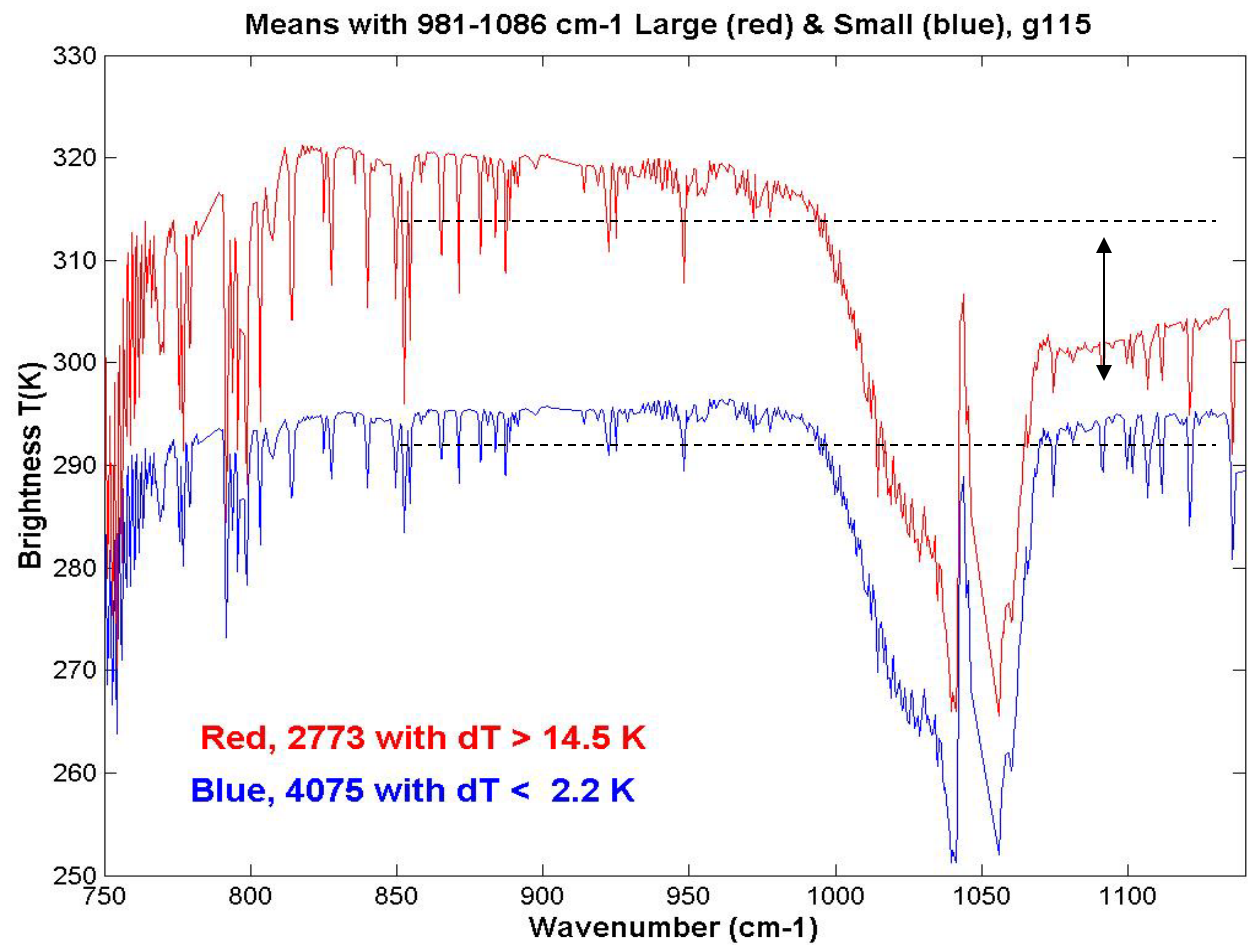
IASI detection of cirrus



Inferreding surface properties with AIRS high spectral resolution data

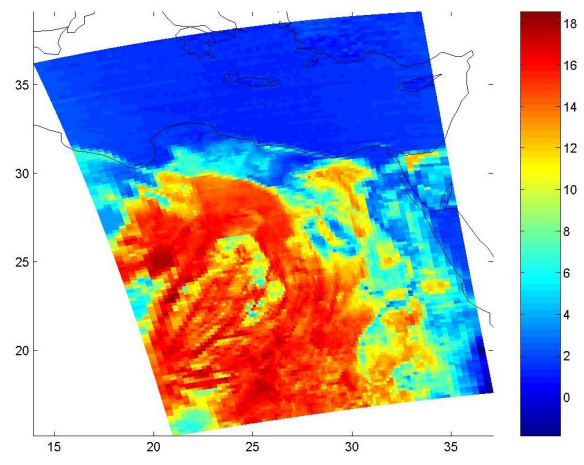
Barren region detection if $T(1086 \text{ cm}^{-1}) < T(981 \text{ cm}^{-1})$

Barren vs Water/Vegetated

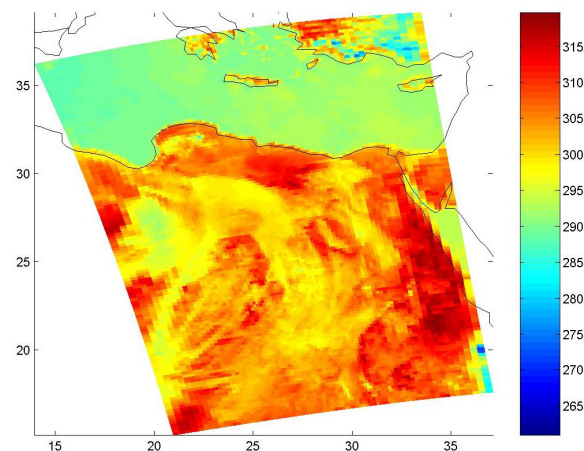


AIRS data from 14 June 2002

$T(981 \text{ cm}^{-1}) - T(1086 \text{ cm}^{-1})$

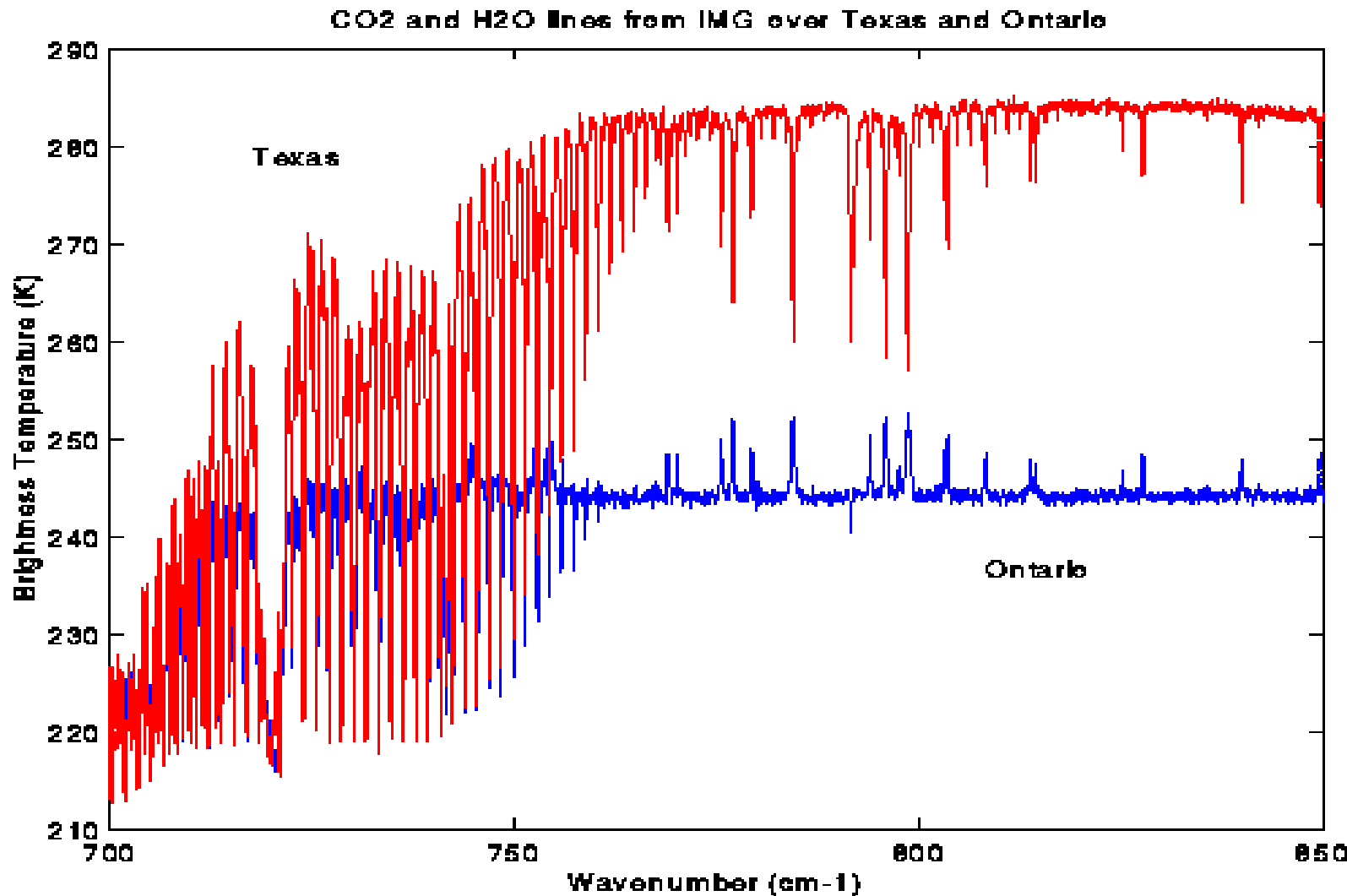


$T(1086 \text{ cm}^{-1})$

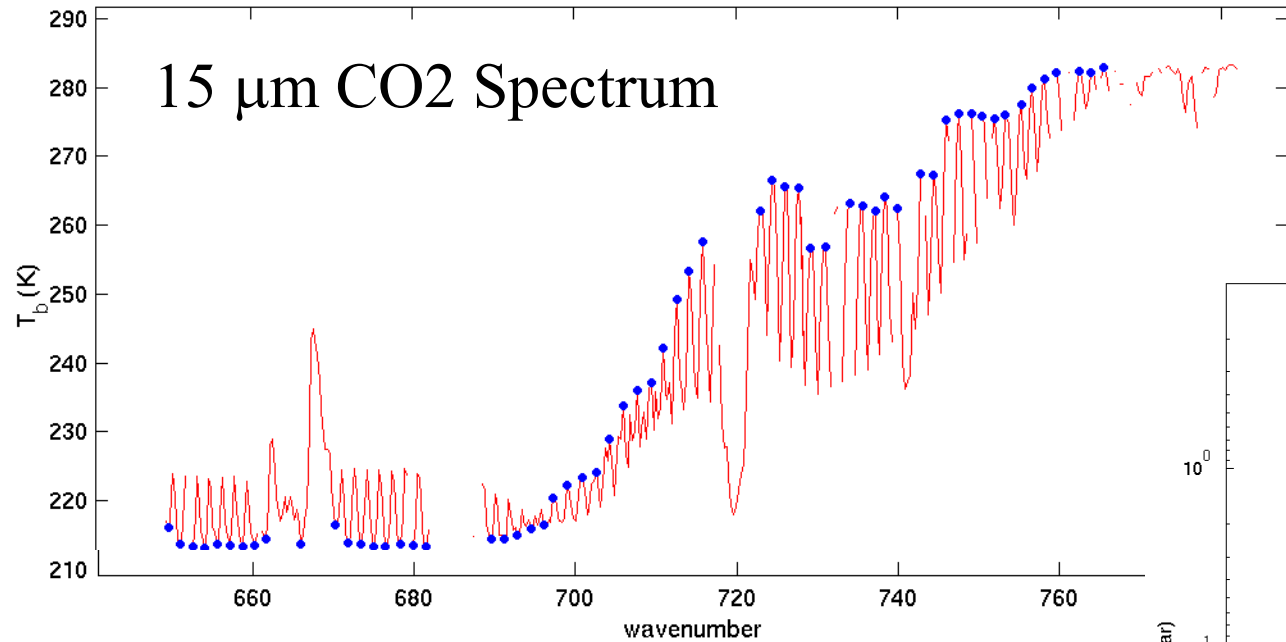


Sensitivity of High Spectral Resolution to Boundary Layer Inversions and Surface/atmospheric Temperature differences

(from IMG Data, October, December 1996)

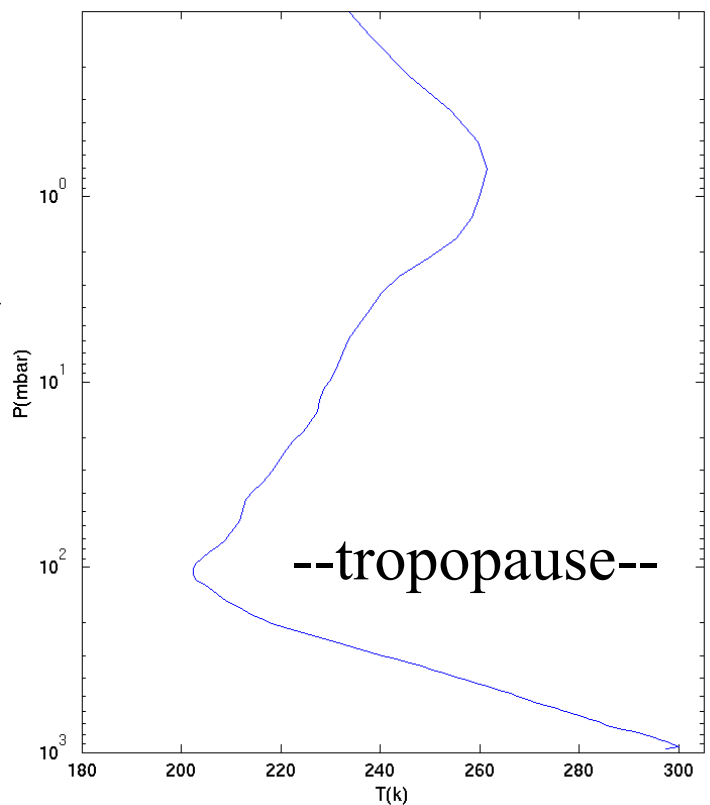


Twisted Ribbon formed by CO₂ spectrum: Tropopause inversion causes On-line & off-line patterns to cross

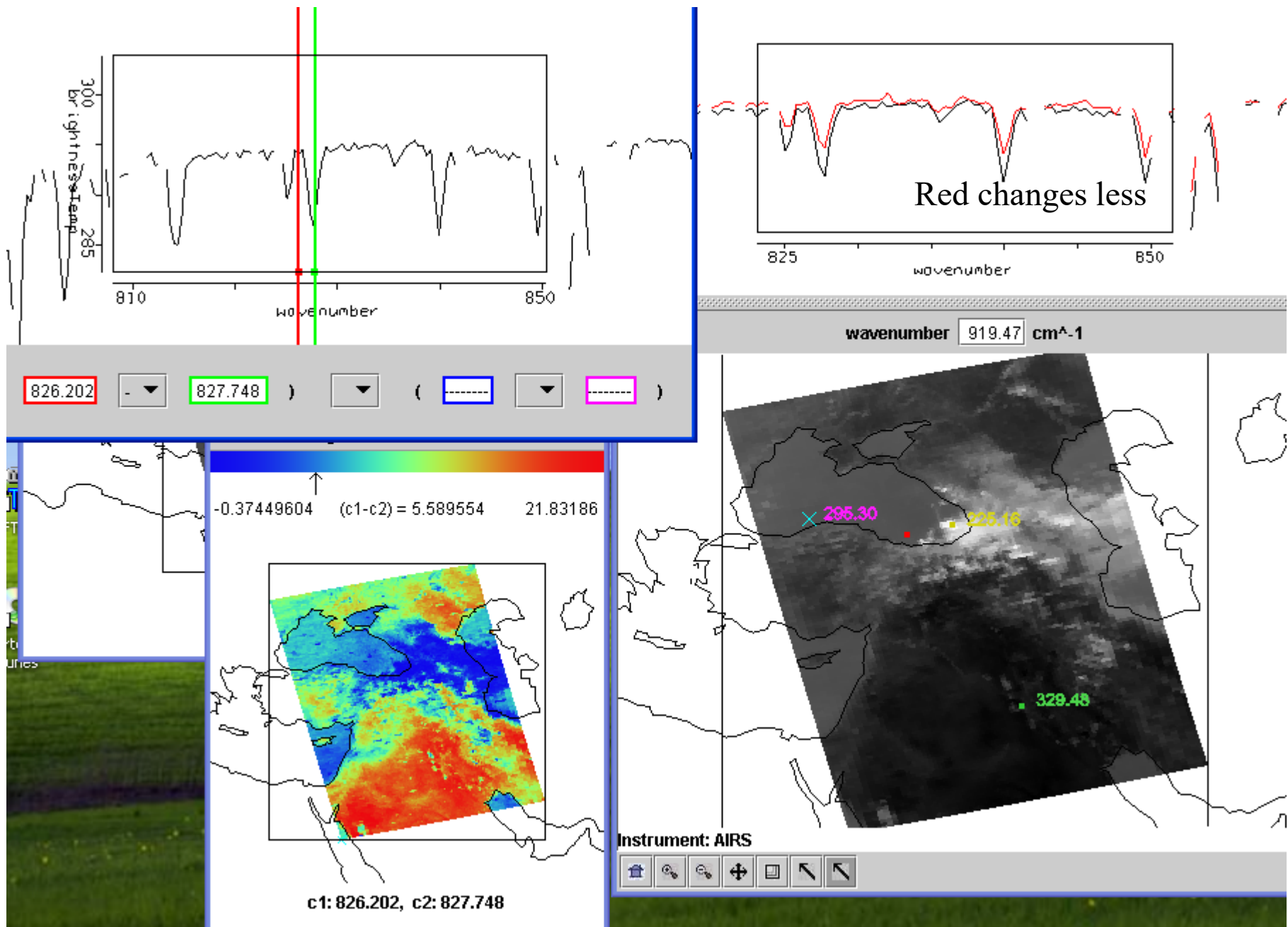


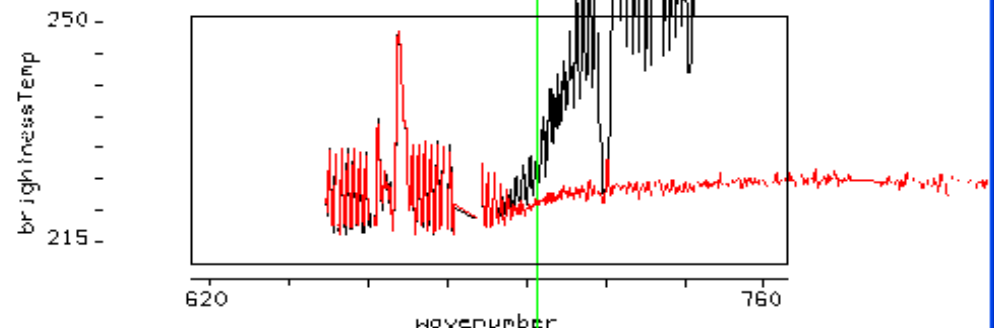
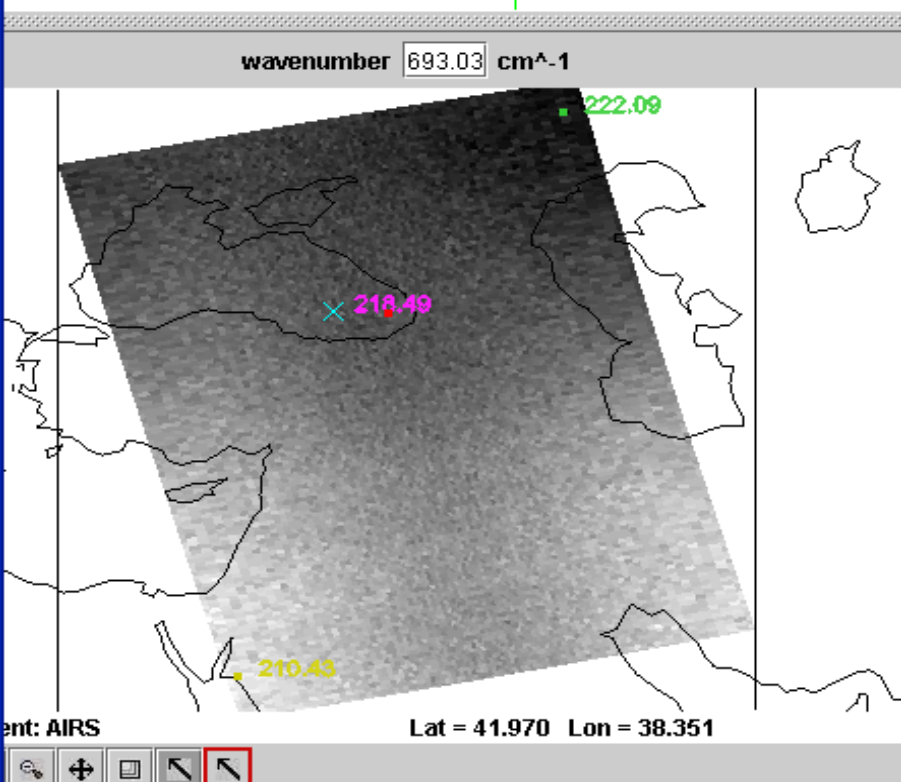
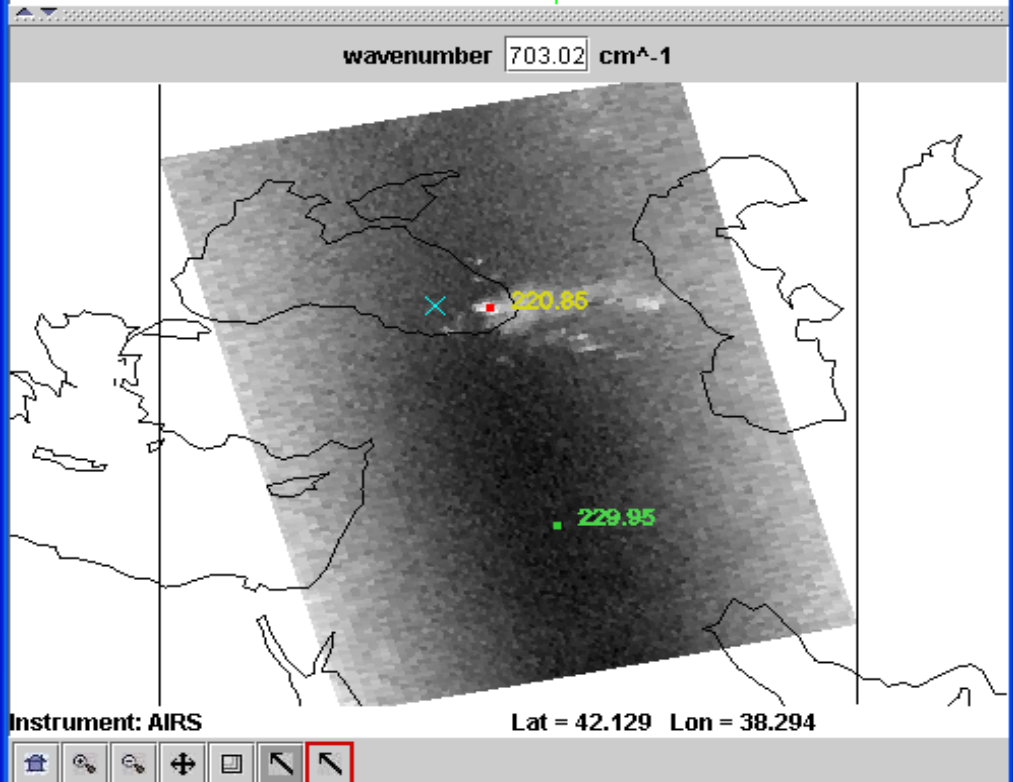
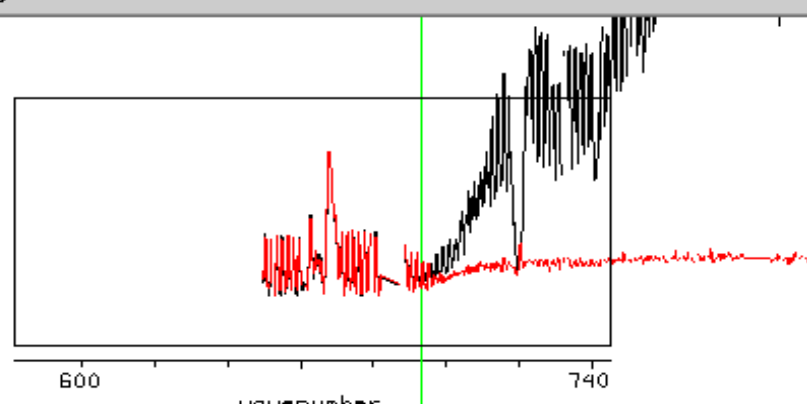
Blue between-line T_b
warmer for tropospheric channels,
colder for stratospheric channels

Signature not available at low resolution



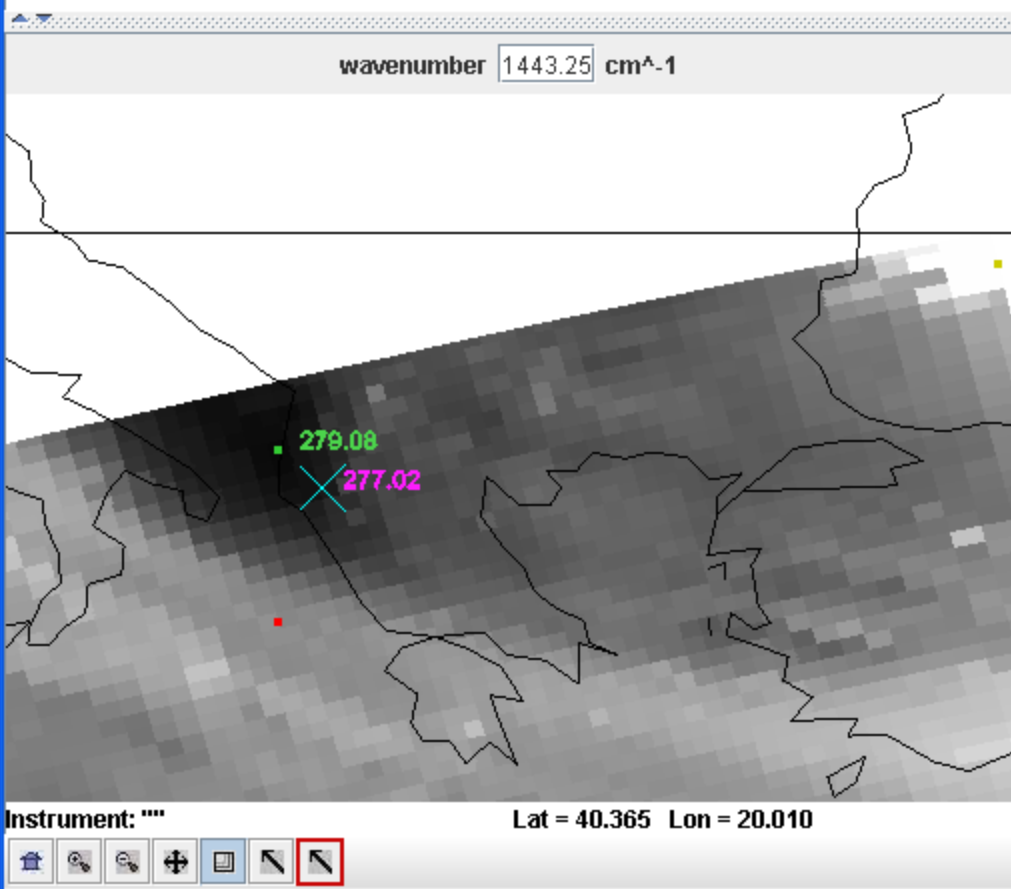
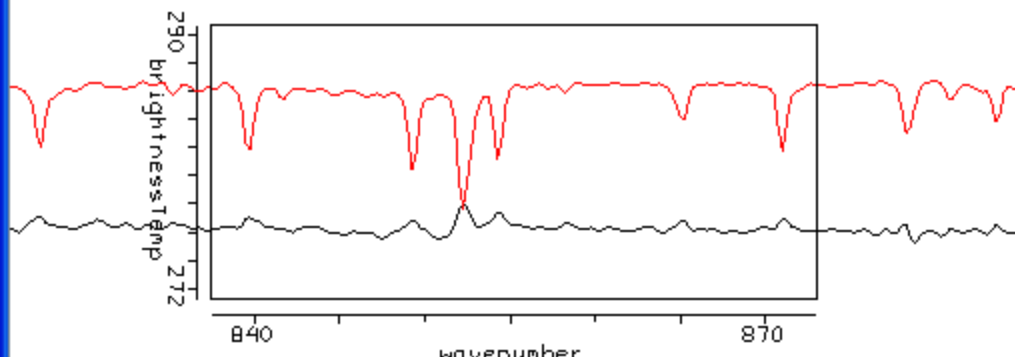
Offline-Online in LW IRW showing low level moisture



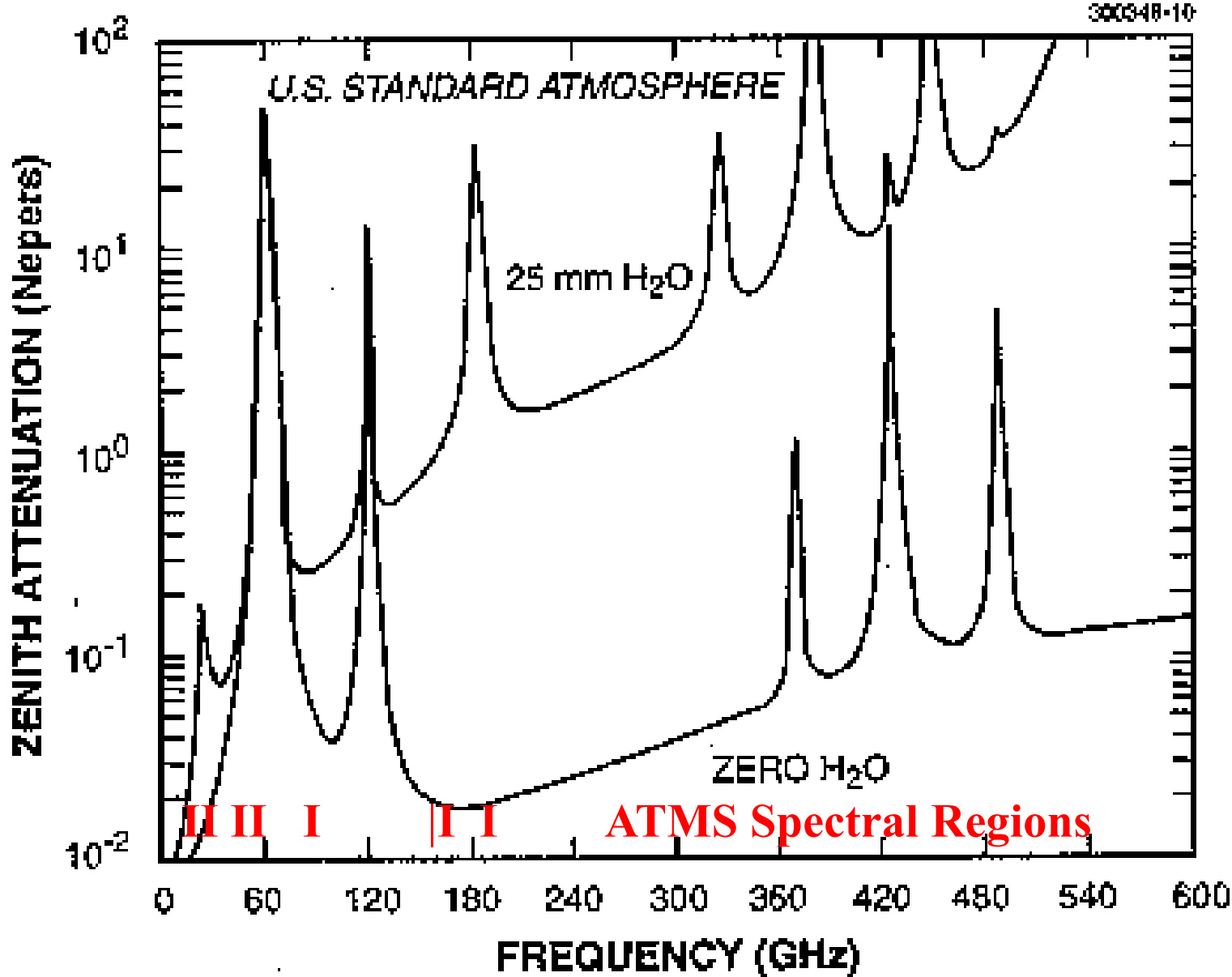
Tools **Settings****Settings**

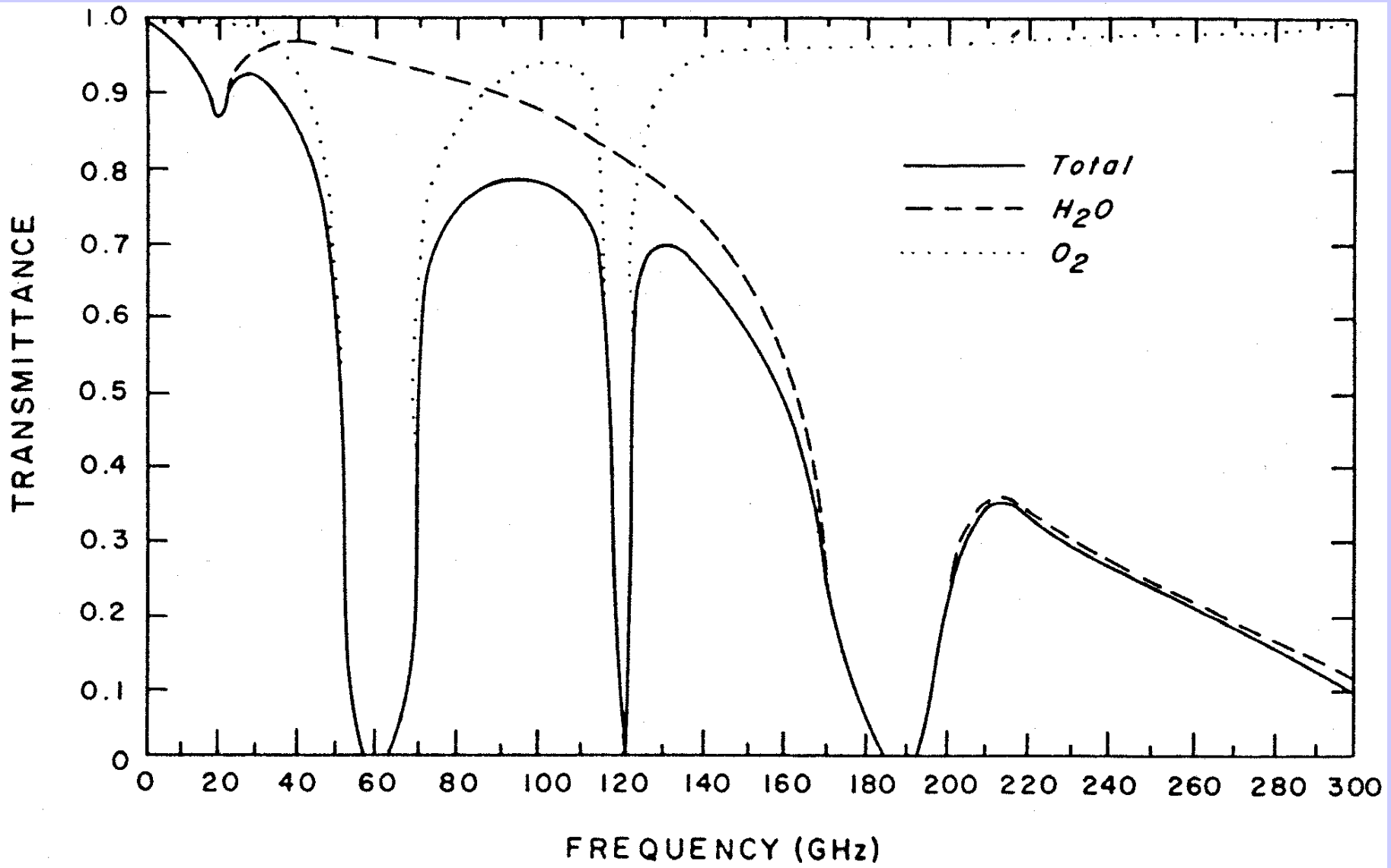
Cld and clr spectra in CO₂ absorption separate when weighting functions sink to cloud level

Tools Settings Import



IASI sees
low level inversion
over land





Radiation is governed by Planck's Law

$$B(\lambda, T) = c_1 / \{ \lambda^5 [e^{c_2 / \lambda T} - 1] \}$$

In microwave region $c_2 / \lambda T \ll 1$ so that

$$e^{-c_2 / \lambda T} = 1 + c_2 / \lambda T + \text{second order}$$

And classical Rayleigh Jeans radiation equation emerges

$$B_\lambda(T) \approx [c_1 / c_2] [T / \lambda^4]$$

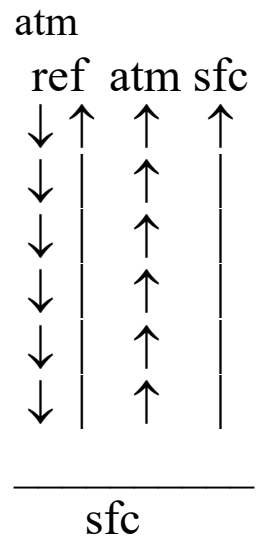
Radiance is linear function of brightness temperature.

Microwave Form of RTE

$$I_{\lambda}^{\text{sfc}} = \frac{1}{\lambda} \varepsilon_{\lambda} B_{\lambda}(T_s) \tau_{\lambda}(p_s) + (1 - \varepsilon_{\lambda}) \tau_{\lambda}(p_s) \int_0^{p_s} B_{\lambda}(T(p)) \frac{\partial \tau'_{\lambda}(p)}{\partial \ln p} d \ln p$$

$$I_{\lambda} = \varepsilon_{\lambda} B_{\lambda}(T_s) \tau_{\lambda}(p_s) + (1 - \varepsilon_{\lambda}) \tau_{\lambda}(p_s) \int_0^{p_s} B_{\lambda}(T(p)) \frac{\partial \tau'_{\lambda}(p)}{\partial \ln p} d \ln p$$

$$+ \int_{p_s}^{\infty} B_{\lambda}(T(p)) \frac{\partial \tau_{\lambda}(p)}{\partial \ln p} d \ln p$$



In the microwave region $c_2/\lambda T \ll 1$, so the Planck radiance is linearly proportional to the temperature

$$B_{\lambda}(T) \approx [c_1 / c_2] [T / \lambda^4]$$

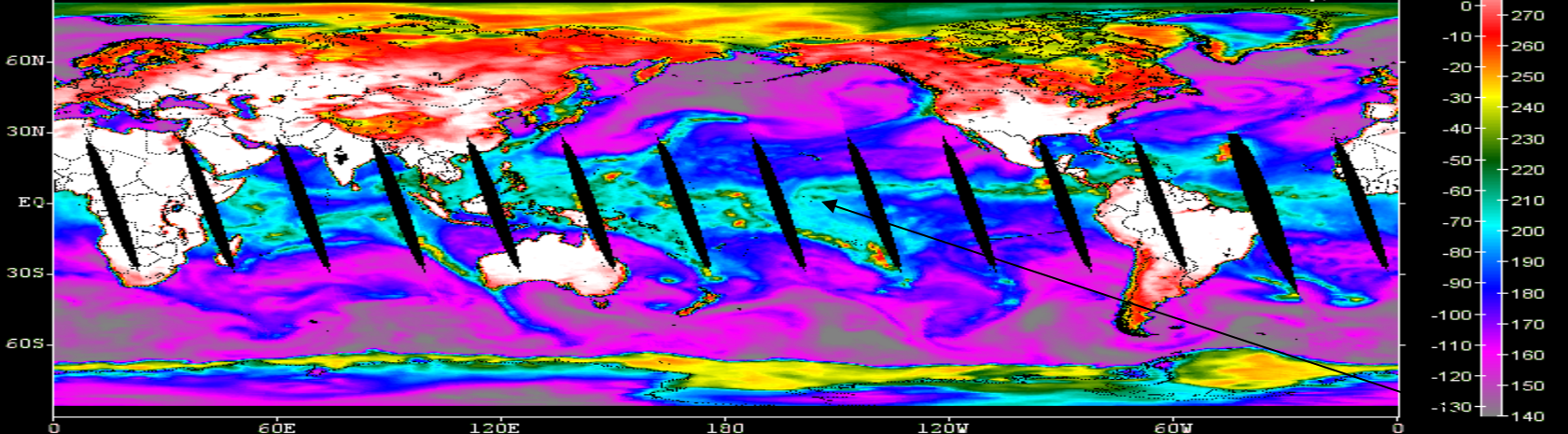
So

$$T_{b\lambda} = \varepsilon_{\lambda} T_s(p_s) \tau_{\lambda}(p_s) + \int_{p_s}^{\infty} T(p) F_{\lambda}(p) \frac{\partial \tau_{\lambda}(p)}{\partial \ln p} d \ln p$$

where

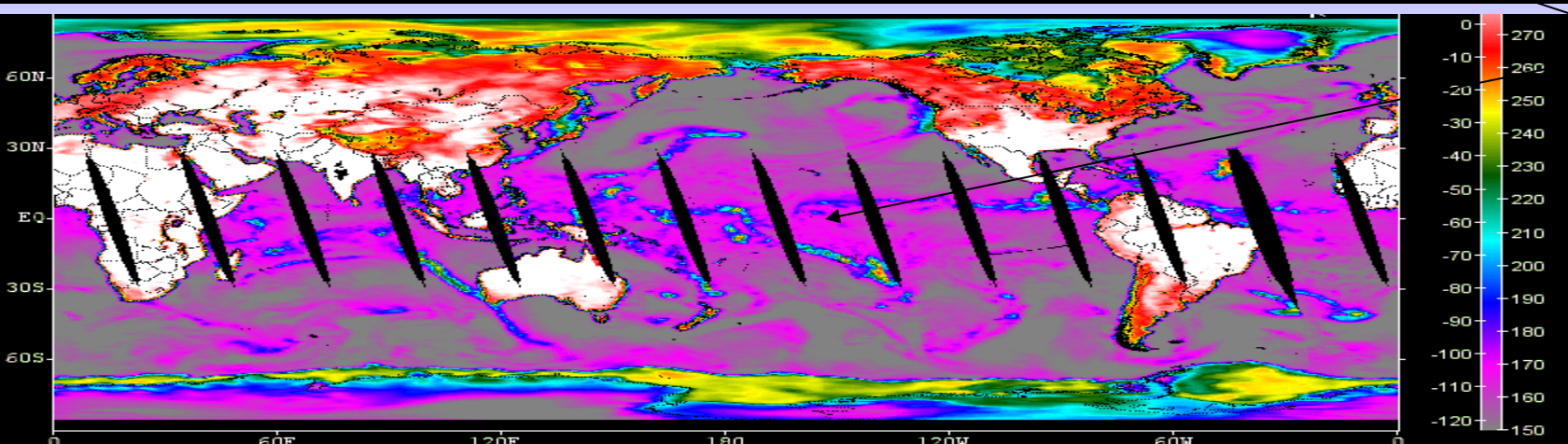
$$F_{\lambda}(p) = \left\{ 1 + (1 - \varepsilon_{\lambda}) \left[\frac{\tau_{\lambda}(p_s)}{\tau_{\lambda}(p)} \right]^2 \right\} .$$

AMSU
23.8
dirty
window

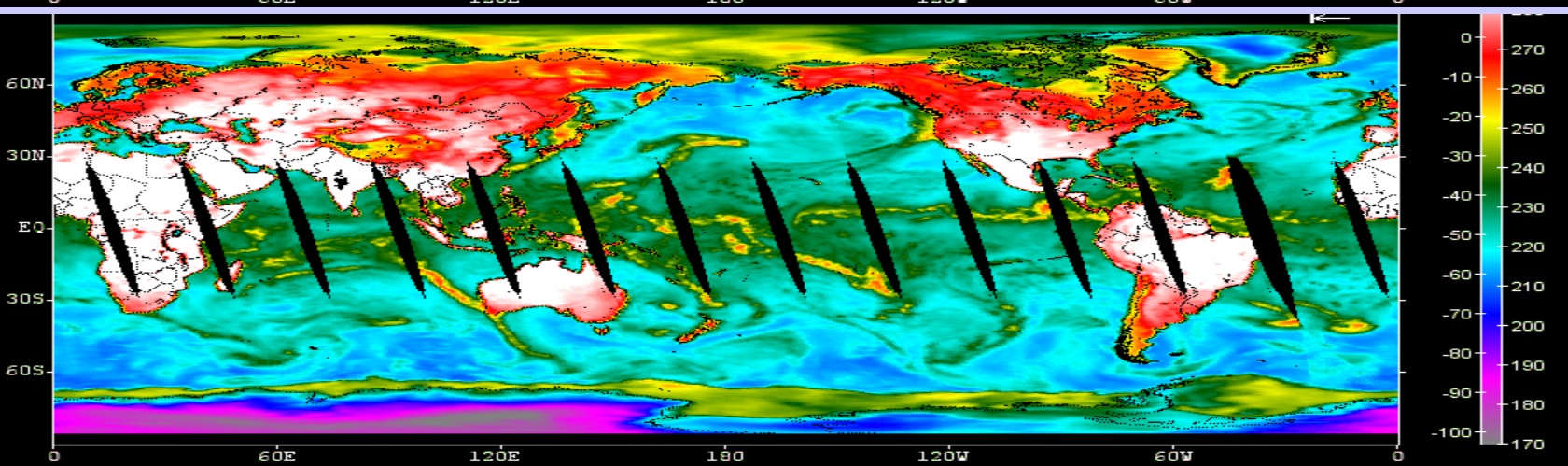


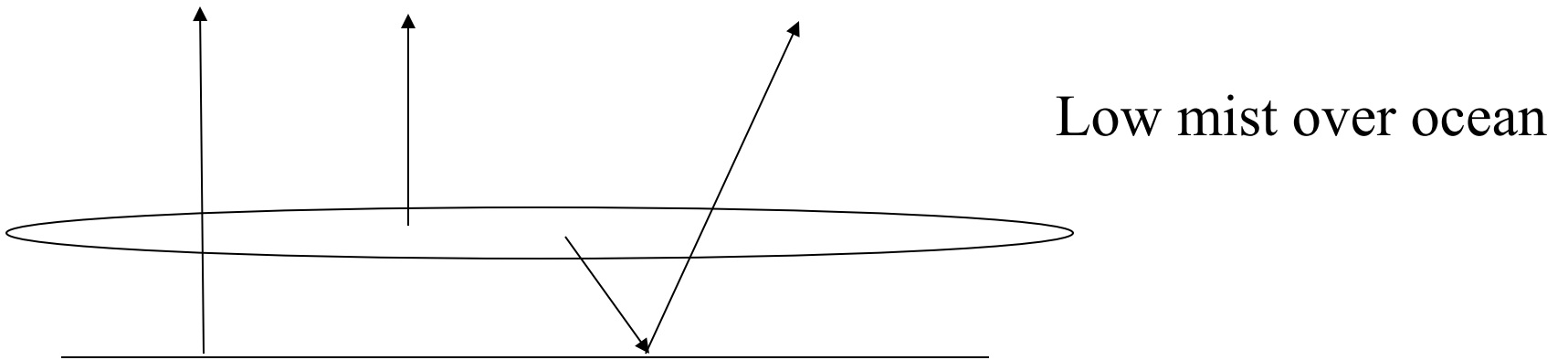
atm Q
warms
BT

31.4
window



50.3
GHz



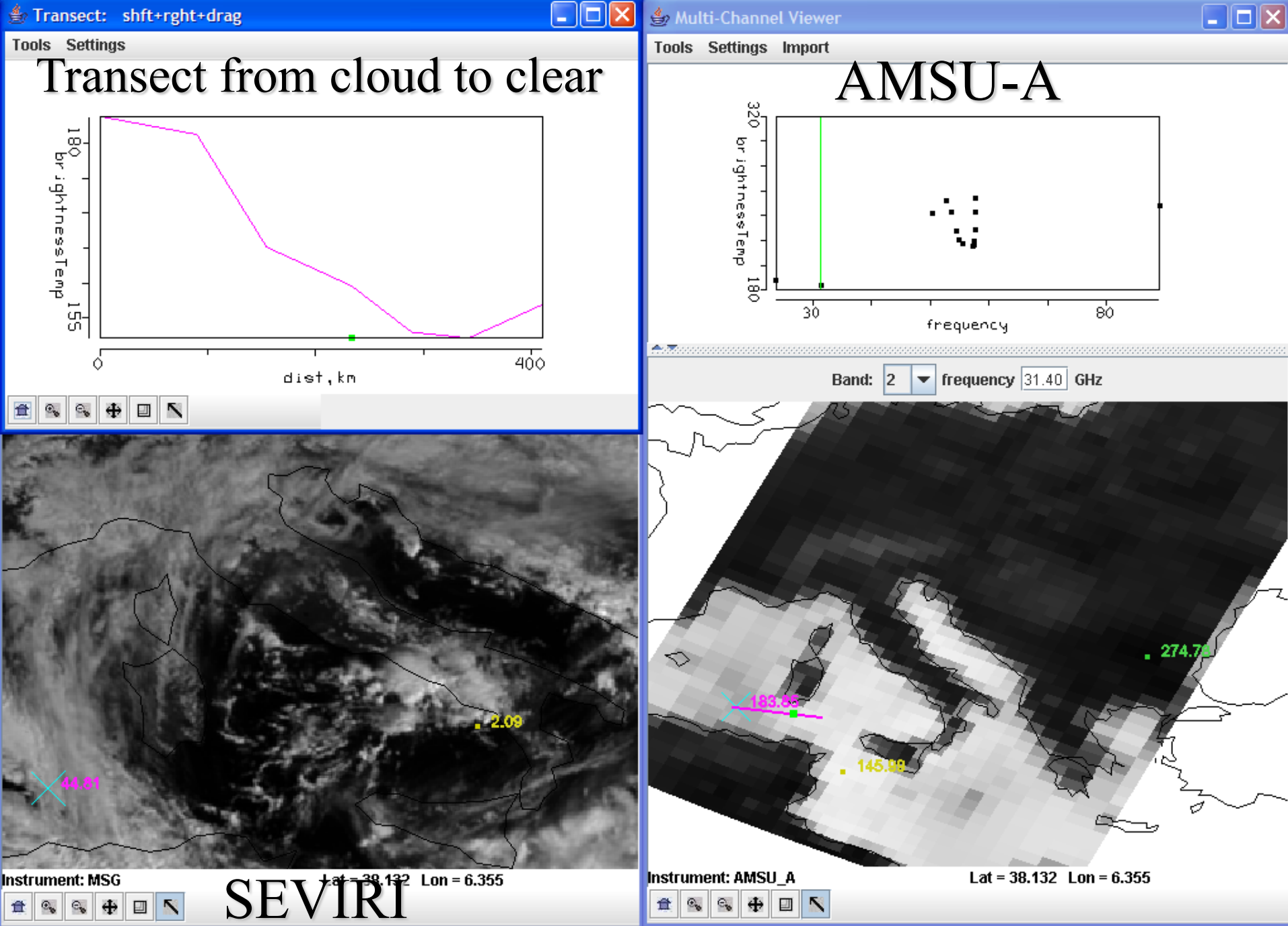


$$T_b = \varepsilon_s T_s (1 - \sigma_m) + \sigma_m T_m + \sigma_m (1 - \varepsilon_s) (1 - \sigma_m) T_m$$

So

$$\Delta T_b = - \varepsilon_s \sigma_m T_s + \sigma_m T_m + \sigma_m (1 - \varepsilon_s) (1 - \sigma_m) T_m$$

For $\varepsilon_s \sim 0.5$ and $T_s \sim T_m$ this is always positive for $0 < \sigma_m < 1$



Accuracy of Satellite Derived Met Parameters

T(p) within 1.5 C of raobs for 1 km layers

SST within 0.5 C of buoys

Q(p) within 15-20% of raobs for 2 km layers

TPW with 3 mm of ground based MW

TO3 within 30 Dobsons of ozone profilers

LI adjusted 3 C lower (for better agreement with raobs)

gradients in space and time more reliable than absolute

AMVs within 7 m/s (upper trop) and 5 m/s (lower trop)

CTPs within 50 hPa of lidar determination

Geopotential heights within 20 to 30 m

for 500 to 300 hPa

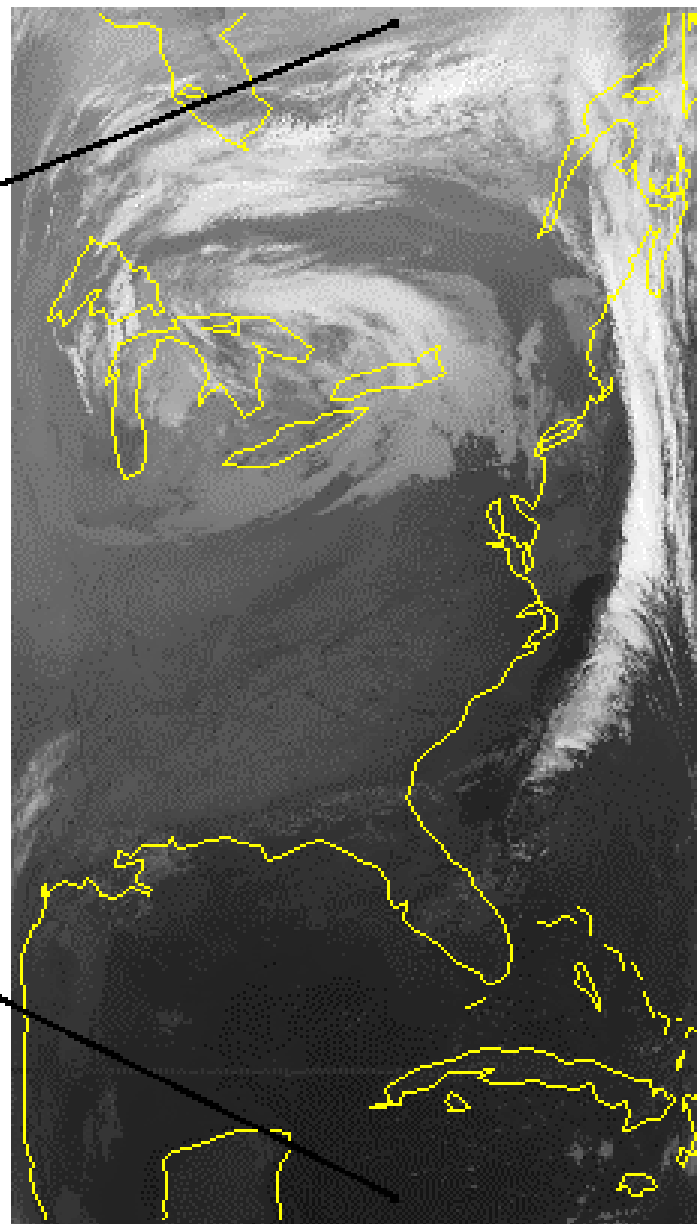
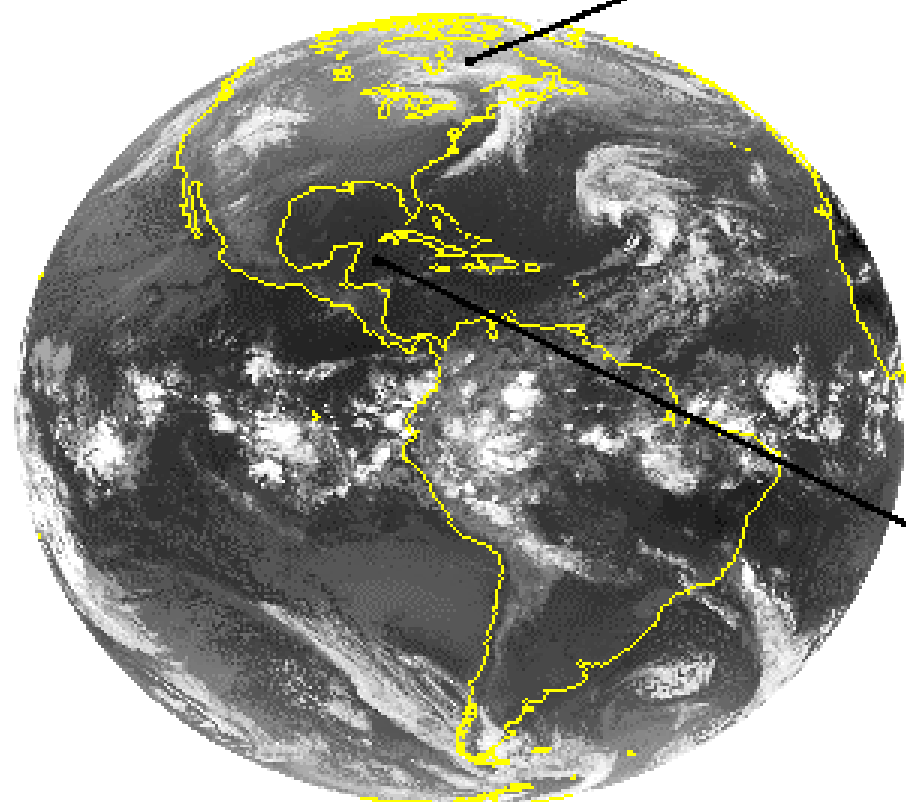
For TC, Psfc within 6 hPa and Vmax within 10 kts

(from MW ΔT250)

Trajectory forecast 72 hour error reduction about 10%



GEO vs LEO

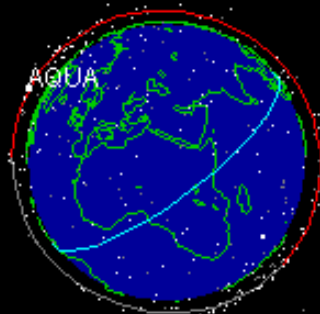


GOES-8 IMAGER 12UTC 02APR98

NOAA-12 AVHRR 12UTC 02APR98

08 Apr 2007 18:52:00 GMH

All
Sats
on
NASA
J-track



Comparison of geostationary (geo) and low earth orbiting (leo) satellite capabilities

Geo

observes process itself
(motion and targets of opportunity)

repeat coverage in minutes
($\Delta t \leq 30$ minutes)

full earth disk only

best viewing of tropics

same viewing angle

differing solar illumination

visible, IR imager
(1, 4 km resolution)

one visible band

IR only sounder
(8 km resolution)

filter radiometer

diffraction more than leo

Leo

observes effects of process

repeat coverage twice daily
($\Delta t = 12$ hours)

global coverage

best viewing of poles

varying viewing angle

same solar illumination

visible, IR imager
(1, 1 km resolution)

multispectral in visible
(veggie index)

IR and microwave sounder
(17, 50 km resolution)

filter radiometer,
interferometer, and
grating spectrometer

diffraction less than geo

HYperspectral viewer for Development of Research Applications - HYDRA

MSG,
GOES



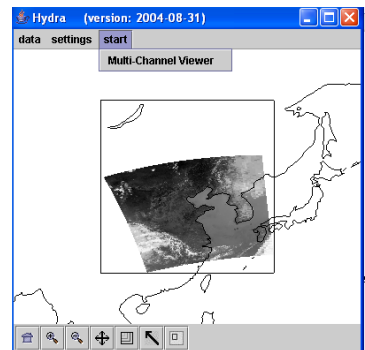
Freely available software
For researchers and educators
Computer platform independent
Extendable to more sensors and applications

Based in VisAD
(Visualization for Algorithm Development)
Uses Jython (Java implementation of Python)

runs on most machines

512MB main memory & 32MB graphics card suggested
on-going development effort

Rink et al, BAMS 2007



MODIS,
AIRS, IASI,
AMSU,
CALIPSO

Developed at CIMSS by
Tom Rink
Tom Whittaker
Kevin Baggett

With guidance from
Paolo Antonelli
Liam Gumley
Paul Menzel
Allen Huang



<http://www.ssec.wisc.edu/hydra/>

For hydra

<http://www.ssec.wisc.edu/hydra/>

For MODIS data and quick browse images

<http://rapidfire.sci.gsfc.nasa/realtim>

For MODIS data orders

<http://ladsweb.nascom.nasa.gov/>

For AIRS data orders

<http://daac.gsfc.nasa.gov/>

Steps in downloading data

- 1) Go to <http://ladsweb.nascom.nasa.gov/>
 - and select data and then search. Make sure that cookies are accepted by your browser (most browsers are set this way already). Under Satellite/Instrument choose either Aqua or Terra
 - 2) Under Group: Choose Aqua Level 1 Products or Terra Level 1 Products (depends on what you chose in step 1).
 - 3) Under Products: Choose either 1km, 500m or 250m L1B Calibrated Radiances or you can choose all 3 if you want.
 - 4) Under Start Date and Time: Use 07/10/2006 00:00:00
 - 5) Under End Date and Time: 07/15/2006 23:59:59
 - 6) In the Spatial Selection section choose: Latitude/Longitude
 - A map should pop up. You can either outline your area of interest by outlining a box on the map, or you can type in the North, South, East and West Limits in the boxes to the right of the images for your area of interest (Sudan). I used 0 South, 20 North, 25 West and 35 East.
 - 7) Under Coverage Selection Choose: If you only want Day granules (will contain channels in the visible wavelengths), then make sure the Night and Both boxes are not checked. I chose to only get Day granules.
 - 8) Click on the Search button at the bottom. This might take a minute or two.
 - 9) Eventually, I received a page that contained 6 pages of granules that met my search criteria. Under the Browse column, I could click on the image to get a quick look view of the granule.
 - 10) I chose to order all of the granules that were returned from my search. I clicked on the Order Files Now button at the bottom of the window.
 - 11) A page appeared that asked for my email address. I typed it in: kathy.strabala@ssec.wisc.edu
 - 12) I chose FTP Pull and clicked on the Order button.
 - 13) It returned a window that told me some of my order is ready (a lot of the data is already online). The rest of the data will be staged and I will be informed via email when it is ready.
 - 14) I received an email that tells me how I can get the data.
-

• Your Order ID is: 500143562

• The data you ordered has been staged, and you can retrieve the data through anonymous FTP using:

• `ftp ladsweb.nascom.nasa.gov`

• `username: anonymous`

• `password: kathy.strabala@ssec.wisc.edu`

• `cd /orders/500143562`

• `binary`

• `prompt`

• `mget *`

High resolution atmospheric absorption spectrum
and comparative blackbody curves.

